REMOTE SENSING TECHNIQUES FOR DETECTING VEGETATION PHENOLOGY

by

Min Li

A Dissertation
Submitted to the
Graduate Faculty
of
George Mason University
in Partial Fulfillment of
The Requirements for the Degree
of
Doctor of Philosophy
Geography and Geoinformation Science

Committee:

Dr. John J. Qu, Dissertation Director

Dr. Daniel B. Carr, Committee Member

Dr. George Taylor, Committee Member

Dr. Ruixin Yang, Committee Member

Dr. Peggy Agouris,
Department Chairperson

Dr. Richard Diecchio, Associate
Dean for Academic and Student
Affairs, College of Science

Dr. Vikas Chandhoke, Dean,
College of Science

Date: 07/27/2010

Summer Semester 2010
George Mason University
Fairfax, VA

Remote Sensing Techniques for Detecting Vegetation Phenology

A dissertation submitted in partial fulfillment of the requirements for the degree of Doctor of Philosophy at George Mason University

By

Min Li
Master of Science
Beijing Normal University, 2003

Director: John J. Qu, Professor
Department of Geography and Geoinformation Science

Summer Semester 2010
George Mason University
Fairfax, VA

DEDICATION

This is dedicated to my loving husband Lisen Xu, and my wonderful parents Xiurong Shang and Daqing Li.

ACKNOWLEDGEMENTS

It is an honor for me to express my sincere gratitude to the many people who have made this happen.

I owe the deepest appreciation to my Ph.D. advisor, Dr. John J. Qu for his supervision, advice and guidance from the very early stages of this research. He created an atmosphere that encouraged innovation and shared his extraordinary experiences throughout the work. Without his unflinching encouragement, it would have been impossible for me to finish this dissertation.

Many thanks go in particular to Dr. Xianjun Hao. I am much indebted to Dr. Hao for his endless patience answering my unintelligent technical questions. He also used his precious time to read my peer-reviewed manuscripts and gave his critical comments.

I am heartily thankful to my committee members, Dr. Daniel B. Carr, Dr. George E. Taylor and Dr. Ruixin Yang. Their invaluable knowledge and constructive suggestions inspired me to explore unexplained problems. They also helped revise this dissertation and improve the presentations.

I gratefully acknowledge all the group members in the Environmental Science and Technology Center (ESTC) and EastFIRE Lab: Drs. Lingli Wang, Wanting Wang, Xie Yong, Sanjeeb Bhoi, and Mr. Di Wu. Their advice and willingness to share their bright thoughts with me were very fruitful for shaping up my ideas and research. I also would like to convey special acknowledgement to Xin Zhang, Jeanne Lee and her family, and Abraham Perez and his family for their indispensable help during my stay in the United States.

Collective and individual acknowledgments are also owed to the professors and staff in the Department of GGS. Many thanks go to Prof. David Wong and Teri Fede for their help dealing with administration and bureaucratic matters during my study at GMU so that I could optimally carry out my research.

My parents deserve special mention for their inseparable support. My Father, Daqing Li, was the first person to encourage the fundamentals of my learning character, showing me the joy of intellectual pursuit ever since I was a child. My Mother, Xiurong Shang, is the one who sincerely raised me with her caring and gentle love.

Words fail me to express my appreciation to my husband Lisen Xu whose dedication, love and persistent confidence in me has taken the load off my shoulders and encouraged me to overcome countless challenges. I owe him for unselfishly letting his intelligence, passions, and ambitions collide with mine. I cannot imagine life as a PhD candidate without his company.

Finally, I would like to thank everybody who was important to the successful realization of this dissertation, and express my apology that I could not mention everyone personally one-by-one.

Table of Contents

LIST OF TABLES

Table Page

LIST OF FIGURES

Figure Page

LIST OF ABBREVIATIONS

AHF	Allegheny Highlands Forests
AMF	Appalachian Mixed Mesophytic Forests
ARF	Appalachian-Blue Ridge Forests
AVHRR	Advanced Very High Resolution Radiometer
BRDF	Bidirectional Reflectance Distribution Function
CD	Chilling Days
CHF	Central U.S. Hardwood Forests
DBF	Deciduous Broadleaf Forest
DEM	Digital Elevation Model
EOS	Earth Observing System
EVI	Enhanced Vegetation Index
GDD	Growing Degree Days
GIMMS	Global Inventory Modeling and Mapping Studies
HDF	Hierarchical Data Format
IGBP	International Geosphere Biosphere Program
IPCC	Intergovernmental Panel on Climate Change
LP DAAC	Land Processes Distributed Active Archive Center
LAI	Leaf Area Index
LST	Land Surface Temperature
MAE	Mean Absolute Error
MACF	Middle Atlantic Coastal Forests
MODIS	Moderate Resolution Imaging Spectroradiometer
NBAR	Nadir BRDF Adjusted Reflectance
NCF	Northeastern Coastal Forests
NDVI	Normalized Difference Vegetation Index
NIR	Near Infrared
NOAA	National Oceanic and Atmospheric Administration
OMF	Ozark Mountain Forests
RMS	Root Mean Square
SMF	Southeastern Mixed Forests
VI	Vegetation Indices

ABSTRACT

REMOTE SENSING TECHNIQUES FOR DETECTING VEGETATION PHENOLOGY

Min Li, Ph. D.

George Mason University, 2010

Dissertation Director: Dr. John J. Qu

Vegetation phenology describing the seasonal cycle of plants is currently one of the main concerns in the study of climate change and carbon balance estimation in ecosystems. In this study, we focus on vegetation phenology observed at landscape level. Phenology at the landscape scale poses challenges to observers because of its complexity, and it often generates confusion among observers because observers may use different approaches. Remote sensing techniques, which can capture canopy reflectance, allow vegetation photosynthetic capacity to be assessed, and provide the potential to move from plant specific observations to complete, continuous expressions of phenological patterns on the landscape. In this study, an improved satellite-based approach for detecting vegetation phenology was developed and the analysis of this satellite-derived phenology expresses an evident spatial pattern along latitude and elevation. Climate regulation of vegetation phenology shows that the vegetation phenological phases can be modeled using the

annual mean Land Surface Temperature (LST). Two types of ecoregion-based models were established to compare the results with satellite-derived greenup onset dates.

Comparing the satellite-based predictions with ground measurements demonstrated that the Normalized Difference Vegetation Index (NDVI) and the Enhanced Vegetation Index (EVI) are efficient at evaluating the greenup onset and dormancy onset respectively. The spatial analysis of satellite-derived phenological phases shows that a greenup wave is progressing northward in latitude and upward in elevation. The rate of change is about two days per degree latitude or per 100-meter elevation. The dormancy begins in the north and at higher elevation and then progresses southward in latitude and downward in elevation. The rate of change is about two days per degree latitude and one day per 100-meter elevation. The interannual variability of vegetation phenology is also identified by satellite measurements. The interannual variability of greenup onset is evident at higher latitudes (45-50^{0}N), while the interannual variability of the dormancy onset is larger at middle (35-45^{0}N) and lower latitudes (30-35^{0}N).

The high goodness of fit (>0.8) indicates that the model based on annual mean LST predicts the average timing of vegetation phenological events successfully. As the annual mean LST rises, the average timing of greenup onset begins earlier, and the growing length is prolonged. The effect of global warming on vegetation greenup onset is evaluated by the thermal-chilling model. The results show that the thermal-chilling models can explain more than 80% of the variation in the Growing Degree-Days (GDD) required for greenup onset. Global warming may advance forest greenup onset when the

chilling requirements are far exceeded and may delay greenup onset when the chilling requirements are nearly exactly sufficient.

Finally, the ecoregion-based models have been established to simulate greenup onset dates and the results are compared with satellite-derived measurements. The greenup onset dates for 90% of the habitat-controlled ecoregions and 80% of temperature-controlled ecoregions are simulated within 10 days of the satellite derived greenup onset.

The satellite-derived vegetation phenology is globally applicable. It is capable of identifying phenological behavior characterized by multiple growth and senescence periods. Remote sensing-based analysis provides a promising approach for the quantification of ecosystem-level response climate change, which is an important complement to species-level studies.

CHAPTER 1

INTRODUCTION

Phenology is the study of recurring biological events in the plants and animals, such as leafing and flowering of plants, maturation of agriculture crops, emergence of insects and migration of birds (Schwartz et al., 2002; Haggerty and Mazer, 2008). Many of these events are sensitive to changes in weather and climate. Vegetation phenology refers to plant life cycle stages, e.g. leaf-on, first flowering, fall leaf coloring, and leaf-off. The changes in vegetation phenology affect the carbon cycle, water cycle and energy fluxes through photosynthesis and evapotranspiration, which are closely related to food security, water resources availability and climate (Xiao et al., 2009). Numerous in situ observations from researchers and volunteers (e.g. gardeners) have documented various phenological phases of plants over years in the United States. In the 1950's, Caprio started what would eventually become the nation's phenological legacy. Caprio sought observers across the Western US who would report to him the local timing of leafing and flowering of the Common Lilac, Syringa vulgaris. Caprio's early success motivated two other researchers to initiate regional phenology networks in Nebraska (W.L.Colville, University of Nebraska) and in the Northeast (R. Hopp, University of Vermont) in the 1960's. Using the same approach as the International Phenological Gardens in Europe,

these two networks recorded observations for a cloned cultivar of Lilac, Syringa chinensis at about 300 sites. Administration of these two networks was juggled for a couple of decades until funding was ultimately lost in 1986, after which University of Wisconsin-Milwaukee climatologist and geography professor Dr. Mark D. Schwartz contacted their volunteer networks to manage the remaining monitoring activities. Recently, the USA National Phenology Network (USA-NPN: http://www.usanpn.org) is currently being designed and organized to engage federal agencies, environmental networks and field stations, educational institutions, and mass participation by scientists. It is a nationwide collaboration among professional and scientists designed to track the progression of the seasons and to relate the timing and duration of phenological events to climate change.

The vegetation phenology can be observed at a variety of scales, ranging from long-distance observations to close-up and detailed views. Scientists are interested in the dates when phenology events occur, their duration and the pace of transition between events and these observations can take place at multiple biological and geographical scales. For example, the dates of first leaf and last leaf can be recorded for an individual plant or percentages of leaf expansion/flowering are recorded by each day or week during the growing period. This can also be done for many individuals of the same species in one population, for multiple populations of a species that occupies different habitats, and for multiple populations of different species that coexist in one habitat.

Vegetation phenological studies performed today are carried out in a wide range of approaches, including in situ observations, climatology modeling, eco-physiological

analysis and satellite-driven remote-sensing. The integration of scientific disciplines makes for particularly powerful studies because the site intensive nature of one tool (e.g., botanical inventories and detailed phenological studies) can complement the geographically extensive information provided by another (e.g., satellites). In this study, we focus on vegetation phenology observed at community level and ecosystem level. Phenology at the landscape scale poses challenge to observers, because of its complexity; and it often generates confusions among observers because observers may use different approaches. Research approaches for vegetation phenology could be roughly grouped into three categories by their observation platforms: climatology modeling, carbon exchange measurements and satellite-based reflectance.

1.1 Approaches for monitoring vegetation phenology

Modeling phenology based on meteorological and climatological variables has a long history and is often incorporated into vegetation models to predict future change of phenology in response to climate change (Hickin and Vittum, 1976; Cannel and Smith, 1983; White et al., 1997; Botta et al., 2000; Kang et al., 2003; Stöckli et al., 2008). Most models are based on the theory that after an arbitrary start date, mean air temperature or soil temperature above an arbitrary threshold is summed until a critical value is exceeded, at which point the prescribed phenological event is predicted to occur. Some models also include chilling requirements in which vegetation must fulfill a chilling condition before warmer temperatures begin to affect springtime growth. The leaf-off event is more related to day length. Photoperiod alone could be used to predict offset of greenness

within a certain temperature range. If the temperature is warm, growth is permitted to continue, while extremely low temperatures will induce offset regardless of photoperiod. Frost-free period is a good indicator for plant growing season length and the growing season can be prolonged by warm temperatures and curtailed by cold temperature.

The carbon exchange approach measures net exchange of CO_2 and water between terrestrial ecosystems and the atmosphere. The approach opened a new frontier in the field of phenology from the ecosystem and landscape perspective. Keeling et al. (1996) suggested that early spring growth, as seen in seasonal atmospheric CO_2 cycles, causes an increase in productivity at northern latitudes. Based on BIOME_BGC ecosystem model, White et al. (1999) indicated that persistent increases in growing season length may lead to long-term increases in carbon storage.

Since the early 1990s, hundreds of eddy flux tower sites have been established and cover all major biome types in the world. Nowadays, there are more than 600 eddy flux tower sites in various biomes of the world; and these CO_2 flux sites formed several networks (e.g. AmeriFlux, ChinaFlux, EuroFlux and AsiaFlux). The networks of CO_2 eddy flux tower sties play an increasing important role in determining whether individual ecosystems are carbon sink or carbon source. Using the eddy covariance technique at the Harvard Forest in central Massachusetts, Goulden et al. (1996) found that even modest change in the length or magnitude of the plant growing season could result in large changes in annual carbon exchange. An analysis of net ecosystem exchange of CO 2 (NEE) between forest ecosystems and the atmosphere during 1991–2000 in Harvard Forest also suggested that weather and seasonal climate (e.g. light, temperature, and

moisture) regulated seasonal and interannual fluctuations of carbon uptake in a temperate deciduous broadleaf forest (Barford et al., 2001).

Vegetation phenology driven from satellite measurements is distinct from observations of individual plants or species, as space-based observations aggregate information on the timing of heterogeneous vegetation development over pixel sized areas. This aggregation often disassociates the response signal of the landscape from that of the individual species, yet is important for representing landscape scale process (e.g., water, energy and carbon fluxes) in biosphere-atmosphere interaction (Reed et al., 2009). The study of vegetation phenology using remote sensing has experienced considerable progress over the past two decades, both in terms of generating the basic satellite data sets that are required for documenting phenology over large areas (Myneni et al., 1997; Shabanov et al., 2002; Tucker et al., 2001; Zhou et al., 2003), and in terms of developing methodologies for creatively working with the data sets to derive metrics that describe the seasonality of vegetation (White et al., 1997; Moulin et al., 1997; Kang et al., 2003; Zhang et al., 2005). Remote sensing provides the potential to move from plant specific observations to complete, continuous expressions of phenological patterns on the landscape (Betancourt et al., 2005), which are important for characterizing large area phenology and for better parameterizing ecological and climate models (i.e., specifying when to change values for seasonally dependent parameters such as albedo, surface roughness, transpiration, etc.).

1.2 Statement of the problem

Many studies have employed various forms of climate data to validate satellite-based measurements of phenology related to canopy duration. These approaches include use of station temperature and precipitation values (Bogaert et al., 2002; Wang et al., 2003; Deng et al., 2007), growing degree-days and other temperature summations (Zhang et al., 2004; de Beurs and Henebry, 2005; Fisher and Mustard, 2007; Fisher et al., 2007), or gridded temperature and precipitation (Zhou et al., 2003; Tateishi and Ebata, 2004). Other studies have used phenology models driven by climate data (Schwartz and Reed, 1999; Schwartz et al., 2002; Kathuroju et al., 2007). A smaller number of studies have compared satellite-derived measures directly to plant phenology, either from multiple locations in a network (Delbart et al., 2005; Studer et al., 2007) or at a few individual sites (Kang et al., 2003; Chen et al., 2005; Ahl et al., 2006; Zhang et al., 2006). While most studies have used some form of climate information to validate satellite-derived measures of phenology and a smaller number used phenological models driven by surface climate data. Direct validation of remote sensing phenology measures with surface phenological information has been limited by a lack of widely distributed surface data sources. Even as more direct observations of phenology become available, a serious impediment to comparing traditional surface phenological measures with satellite-derived measures is scale. The high temporal resolution satellite data record information for areas no smaller than 250 × 250 m, while surface phenological data are recorded for a small number of individual plants. As long as national-level and global surface phenological

data are lacking, there will be an acute need for employing phenological model to validate satellite-derived phenology.

1.3 Objectives of the research

In this study, we integrate the basic concepts of traditional meteorologically based phenology modeling with intensive satellite phenology observations to produce ecoregion-specific phenology models. Potential uses of the models include validation of satellite-derived phenology and regulation of the timing of the growing season in regional scale. The specific objectives are proposed as follows:

(1) To estimate vegetation phenology from satellite products and indentify proper vegetation indices for different phenology events.

(2) To quantify phenological variation at broad geographical scales and investigate the sources of the variation.

(3) To develop ecoregion-based phenology models and compare the model-derived phenology with satellite-derived phenology.

1.4 Dissertation layout

The dissertation consists of six chapters. Chapter 1 presented the background information on phenology and various approaches for monitoring the vegetation phenology. Chapter 2 addressed previous researches on remote sensing of phenology. The following chapters, chapter 3-5 provided research works related to the objectives of this study and the last chapter summarized the dissertation and discussed future work.

Chapter 1 introduced the definition of phenology and the observation of phenology at different scales. Major approaches for monitoring vegetation phenology were presented and the limitations and challenges for validating the phenology derived from remote sensing were addressed, along with the objectives of this study. This chapter also included a list of the data sources and concluded with major findings and contributions of this dissertation.

Chapter 2 presented various approaches for estimating phenology based on satellite data and for validation of satellite-derived phenology. Satellite sensors, spectral channels and various vegetation indices for phenology estimation were summarized. The limitation of the current methods and challenges for validating regional scale phenology were then outlined and discussed. The applications of satellite-derived vegetation phenology were provided at the last session of this chapter.

Chapter 3 adapted the algorithm for monitoring vegetation phenology from Moderate Resolution Imaging Spectroradiometer (MODIS) measurements and investigated the performances of the vegetation indices for estimating different phenological events, e.g. onset of greenness and onset of dormancy. The proper MODIS measurements for different phenological events are determined.

Chapter 4 quantified how phenological events are sensitive to environmental factors, e.g. latitude and elevation. Interannual variability of satellite-derived phenology in deciduous broadleaf forest (DBF) area over 2001 to 2007 was investigated.

Chapter 5 analyzed the variation in phenology due to the influence of the climateological factor, e.g. temperature. The thermal time-chilling model was used to identify how the temperature control onset of greenness.

Chapter 6 developed ecoregion-specific phenology models and compared the model-derived vegetation phenology with satellite-derived vegetation phenology.

Chapter 7 summarized the entire dissertation, discussed the contributions and limitations, and provided future improvements.

1.5 Summary of the datasets

The datasets used in this dissertation consists of satellite data and field observation data. The satellite data include the MODIS Nadir Bidirectional Reflectance Distribution Function (BRDF) Adjusted Reflectance (NBAR) Product (MOD43B4), BRDF Quality Assessment (QA) (MCD43B2), MODIS land cover product (MOD12Q1), and MODIS global Land Surface Temperature (LST) (MOD11A2). The field observation data include North American Yearly First Leaf and First bloom Dates for Lilac Shrubs and Harvard Forest Phenology of Woody Species. Table 1.1 lists the primary datasets and sources. The usages of these datasets in the study are described in details as follows:

(1) MODIS NBAR Product (MOD43B4)

The MODIS Nadir BRDF-Adjusted Reflectance Product (MOD43B4) contains surface reflectance with a 1 km resolution at each 8 day period and adjusted to nadir views (Schaaf et al. 2002). This product was used to derive the Normalized Difference Vegetation Index (NDVI) and Enhanced Vegetation Index (EVI).

(2) MODIS BRDF Quality Assessment (MCD43B2)

Since snow cover can cause non-phenological variations in satellite data, it is necessary to filter snow-covered pixels before determining phenology events. The MODIS BRDF Quality Assessment data were used to identify snow pixels, and the corresponding pixels were filled with the minimum snow-free value in the same year.

(3) MODIS Land Cover Product (MOD12Q1)

The MODIS Land Cover Product at 1-kilometer resolution (MOD 12Q1) was used to identify DBF) areas. The primary land-cover types in this product include 17 land-cover classes following the International Geosphere-Biosphere Program (IGBP) scheme (Friedl et al., 2002). In this study, both deciduous broadleaf forest and mixed forest were treated as DBF.

(4) MODIS global Land Surface Temperature (LST) (MOD11A2)

The MODIS LST product provides estimates of land surface skin temperature, and is calculated using satellite thermal-infrared measurements for clear-sky pixels with a spatial resolution of 1 km. The LST product provides surface temperature for 8 day time periods by averaging the daily LST measurements (Wan et al., 2002).

(5) North American Yearly First Leaf and First bloom Dates for Lilac Shrubs

The NOAA Paleoclimatology Program distributes archives of North American phenology data: Yearly First Leaf and First Bloom Dates for Lilac Shrubs (Syringa chinensis and Syringa vulgaris) at 1126 locations in the United States and Canada (Schwartz and Caprio, 2003). In this study, the stations located in the United Sates and identified as DBF by MODIS landcover product were selected

Table 1.1 Data and Sources

Data	Data Source
MODIS NBAR Product (MOD43B4)	USGS EOS Data Gateway
MODIS BRDF Quality Assessment (QA) (MCD43B2)	USGS EOS Data Gateway
MODIS Land Cover Product (MOD12Q1)	USGS EOS Data Gateway
MODIS global Land Surface Temperature (LST) (MOD11A2)	USGS EOS Data Gateway
North American Yearly First Leaf and First bloom Dates for Lilac Shrubs	The NOAA Paleoclimatology Program
Harvard Forest Phenology of Woody Species	Harvard Forest Data Archive
Global Land One-kilometer Base Elevation (GLOBE)	National Geophysical Data Center
World Wildlife Fund Ecoregions	World Wildlife Fund Website

(6) Harvard Forest Phenology of Woody Species

The spring and fall phenology data were recorded on Harvard Forest, which covers latitude from 42.53^0N to 42.54^0N and longitude from 72.19^0W to 72.18^0W. The observations are used to compare with both greenup onset and dormancy onset derived from MODIS.

(7) Global Land One-kilometer Base Elevation (GLOBE) data

GLOBE is an internationally designed, developed, and independently peer-reviewed global digital elevation model (DEM), at a latitude-longitude grid spacing of 30 arc-seconds (30") (GLOBE Task Team and others, eds., 1999). The DEM maps covering the continental U.S. was downloaded, mosaicked and reprojected to Sinusoidal projection.

(8) World Wildlife Fund Ecoregions

Ecoregions defined by the World Wildlife Fund (Olson et al., 2001) were used to analyze

the variation of phenology. The ecoregions are built on the foundations of classical biogeography and reflect extensive collaboration with over 1000 biogeographers, taxonomists, conservation biologists, and ecologists from around the world.

1.6 Principal results

This dissertation studied satellite remote sensing of vegetation phenology of DBF in eastern United States. The principal results of this study include an improved method for detecting vegetation phenology transition dates by using MODIS measurements, two qualified patterns of phenological phases regulated by geographical and climate factors respectively, and two types of ecoregion-based model for predicting greenup onset date.

The satellite-based approach for detecting vegetation phenology has identified that NDVI is suitable for greenup onset detection and EVI is more proper for dormancy onset detection.

After reviewing the series of satellite-derived vegetation phenology, a greenup wave is progressing northward in latitude and upward in elevation, and in reverse, a dormancy wave is progressing southward in latitude and downward in elevation. The presence of growing length is longer in the south and higher elevation. The rate of change is about 2 days per degree latitude or per 100-meter elevation for greenup onset. For dormancy onset, the rate of change is about 2 days per degree latitude and 1 day per 100-meter elevation. The interannual variability of greenup onset is evident at higher latitudes (45-50^0N), while the interannual variability of the dormancy onset is larger at middle (35-45^0N) and lower latitudes (30-35^0N). The extent of interannual variability of growing

length is smaller than that of greenup onset and dormancy onset. There is a presence of slightly longer growing length in the seven years from 2001 to 2007, especially at higher latitudes, which is mainly contributed by the early greenup onset.

As a representative of climate effect, the annual mean LST is associated with vegetation phenological phases. When the annual mean LST rise, the average timing of greenup onset begins earlier, the dormancy onset begins later and the growing length is prolonged. The high goodness of fit (>0.8) indicates that the model based on annual mean LST predict the average timing of vegetation phenological events successfully. The thermal-chilling model is applied to satellite-derived greenup onset date. The results show that the thermal-chilling models can explain more than 80% of the variation in the GDD required for greenup onset. Global warming may advance forest greenup onset when the chilling requirements are far exceeded and may delay greenup onset when the chilling requirements are nearly exactly sufficient.

The eight ecoregions in DBF have been divided into two groups according to the effect of environmental factors on greenup onset. The habitat-controlled group is sensitive to the habitat conditions (latitude and elevation) and the temperature-controlled group is influenced mainly by the temperature. Model 1 combining the latitude and elevation with LST is used to simulate greenup onset for habitat-controlled group. Model 2 based on growing degree days (GDD) and chilling days (CD) is used to simulate greenup onset for temperature-controlled group. The models simulate greenup onset dates for each ecoregion realistically. The greenup onset dates for 90% of the habitat-controlled ecoregions are simulated within 10 days of the satellite derived greenup onset dates and

85% of temperature-controlled ecoregions are simulated within 20 days of the satellite derived greenup onset dates.

CHAPTER 2

LITERATURE REVIEW: METHODS FOR MONITORING VEGETATION PHENOLOGY FROM SATELLITES

A number of approaches using a variety of satellite remote sensing products have been used to derive metrics related to the timing of phenology events. The advantages of utilizing remote sensing for phenology are the ability to capture the continuous expression of phenology patterns across the landscape and the ability to retrospectively observe phenology from archived satellite data. Numerous satellite-based sensors with a variety of spectral, spatial, and temporal characteristics have been utilized for vegetation phenology studies, each providing certain advantages and disadvantages (Table 2.1).

The Advanced Very High Resolution Radiometer (AVHRR) has been providing data for land surface studies since the 1980s. A variety of AVHRR collections are available for vegetation phenology studies. For example, global, twice monthly data (15-day composites) at 8 km resolution are available for the post-1982 period (Global Inventory Modeling and Mapping Studies – GIMMS; Tucker et al. 2004); conterminous United States coverage is available at biweekly intervals (14-day composites) at 1 km resolution since 1989 (Eidenshink 1992). One of the primary advantages of AVHRR is its relatively long-term continuity; there are data since the 1980s and current plans call for this sensor

family to continue into the 2020s with the National Oceanic and Atmospheric Administration (NOAA) and the European Organization for the Exploitation of Meteorological Satellites (EUMETSAT) sharing operations.

Table 2.1 Satellite sensors and data sets utilized for vegetation phenology studies

Satellite	Sensor	Operation	Resolution	Frequency
Landsat	MSS	1973–1985	79 m	18 days
Landsat	TM	1984–present	30 m	16 days
Landsat	ETM+	1999–present	30 m	16 days
SPOT	Vegetation	1999–present	1 km	1–2 days
NOAA	AVHRR	1982–present	8 km	15 days
NOAA	AVHRR	1989–present	1 km	14 days
Terra	MODIS	2000–present	250 m, 500 m, 1 km	1–2 days
Aqua	MODIS	2002–present	250 m, 500 m, 1 km	1–2 days
Envisat	MERIS	2002–present	300 m	1–3 days

The Landsat series of satellites offers two primary advantages; a 30 m spatial resolution that is appropriate for landscape characterization and a data archive that extends back to the 1970s. However, Landsat's 16-day repeat cycle does not readily support the frequent observations that are necessary during rapidly changing phenological stages. But Landsat availability is undergoing an important change that promises to rapidly advance multitemporal satellite analysis studies (Woodcock et al. 2008). The availability of web enabled, free-of-charge data through the U.S. Geological Survey (USGS) make Landsat imagery accessible to all researchers, who have the opportunity to develop new methodologies that can potentially overcome the shortcomings of this satellite series.

The newer generation of sensors that are well suited for phenological studies includes the Moderate Resolution Imaging Spectroradiometer (MODIS) and Medium Resolution Imaging Spectrometer (MERIS) sensors. They each have additional spectral bands that are utilized for a variety of applications, and importantly for phenological studies, maintain bands in the visible and near infrared wavelengths. There are currently MODIS sensors aboard two satellites, Terra and Aqua, collecting data in 36 spectral bands at 250 m, 500 m, or 1,000 m resolution. MODIS data are processed into a suite of data products, including surface reflectance, vegetation indices, land surface temperature, and others (Justice et al. 2002).

Alternative approaches to vegetation phenology studies may involve non-optical sensors, such as Advanced Microwave Scanning Radiometer (AMSR-E) or other radar sensors, which can be used to detect moisture conditions of the land surface including vegetation and soil (Doubková and Henebry, 2006). An issue of concern to vegetation phenology studies is the long-term continuity of sensors that are best suited for such studies. Even though the AVHRR series of sensors has been operating since the 1980s, there are issues with continuity between sensors as they have differing overpass times (morning vs. afternoon) with varying illumination conditions, and different spectral band response characteristics. The current generation of satellites (MODIS and MERIS) have spatial resolutions that are better suited for vegetation studies, but the value of the data would be significantly increased if a connection to past sensors, such as the AVHRR, and to future sensors, such as the Visible Infrared Imager/Radiometer Suite (VIIRS) can be made (Murphy et al., 2001).

2.1 Physical principles for deriving phenology from satellite measurements

A number of spectral transformations are commonly utilized to prepare sensor data for monitoring vegetation phenology. The transformations are designed to enhance spectral reflectance and emissive characteristics of vegetation or environmental conditions that are related to phenological development. These conditions include changing leaf area, soil moisture, and vegetation water content. The set of transforms collectively referred to as vegetation indices utilize the reflective characteristics of vegetation in the red and near infrared wavelengths. Plants generally absorb energy in the 0.6–0.7μm wavelengths of the electromagnetic spectrum (chlorophyll absorption of red energy) and reflect very strongly in the near infrared (NIR). Satellite sensors that are designed for land surface analysis applications usually collect data in discrete bands that approximate the red and near infrared wavelengths in order to differentiate and highlight varying land surface conditions. Vegetation indices utilize the reflective characteristics of vegetation often by some kind of ratio and/or differencing of the red and NIR reflectance bands or utilize other reflective wavelengths for reducing the effects of atmospheric aerosols or soil background (blue reflectance) and for highlighting leaf water content (shortwave infrared).

The Normalized Difference Vegetation Index (NDVI) is a commonly used index for vegetation studies (Loveland et al. 1991; Townshend et al. 1994). The NDVI is strongly coupled to red reflectance, which is related to the photosynthetic capacity of vegetation and biophysical variables such as the fraction of photosynthetically active radiation

(fPAR) and fractional green cover (Huete et al. 1997). Other indices have been developed to reduce canopy background effects and atmospheric contamination, including the Soil Adjusted Vegetation Index (SAVI, Huete 1988) and the Soil and Atmospherically Resistant Vegetation Index (SARVI, Kaufman and Tanré 1992). The SAVI and SARVI are more tightly linked to near infrared reflectance and to structural parameters such as leaf area index (LAI) and biomass. The Enhanced Vegetation Index (EVI) is an extension of the progress made in reducing soil and atmospheric effects (Huete et al. 2002) designed to improve sensitivity in high biomass regions and to reduce the canopy background signal and atmospheric influences. The EVI includes the blue reflectance band to correct the influence of atmospheric aerosols on red reflectance.

2.2 Approaches for monitoring vegetation phenology from satellite measurements

Many satellite phenology detection approaches have been addressed since early 90s. (Table 2.1). The threshold for NDVI has been applied for phenological classification of terrestrial vegetation (Lloyd, 1990), modeling seasonal variation of vegetation (Fischer, 1994) and detecting characteristic of vegetation phenology (Markon et al., 1995). They assume that a single threshold is applicable across landcovers. However, variation in background reflectances of different vegetation types makes this a tenuous assumption (Huete et al., 1992). Therefore, it is not possible to establish a single, meaningful threshold that signifies the onset (or end) of vegetative activity for the wide variety of cover types that occur in the continental United States. Reed et al. (1994) developed an

automated, quantitative approach to derive phenological measures from multitemporal AVHRR NDVI observations. To identify the onset of the growing seasons, an auto-regressive moving average of previous smoothed nine NDVI biweekly composite values was compared to the smoothed NDVI value. Selecting the moving average time interval (the number of NDVI composite periods used to calculate the moving average) is a critical issue; a large time interval may miss natural vegetation changes, while a small interval may result in extremely noisy NDVI curves. White et al. (1997) provided a methodology which determined the start and the end of growing season by the threshold of the normalized NDVI ratio. Instead of original NDVI values, they normalized the NDVI to 0-1 by its maximum and minimum value. A new smoothed NDVI ratio curve was developed based on the method of Reed et al. (1994), and then the NDVI ratio threshold of 0.5 was used to identify growing season length. Similar to NDVI threshold method, the normalized NDVI ratio threshold is somewhat arbitrary. They only used it in the northeastern DBF, and similar canopy conditions may or may not exist at other land cover types. Moulin et al. (1997) used time derivative of NDVI to detect three transition dates of vegetation cycle: beginning, maximum and end. The time derivative before beginning date should be zero and after beginning date should be positive; the end date was calculated similarly to the beginning date. The algorithm is sensitive of the weight of the derivative term. If the weight is too large, the detection may be confused by short-term signal variations due to residual noise (e.g., soil color, directional effects). If the weight is too small, the algorithm may fail for pixels, which remain partly green during the year. Therefore, the weights are empirically. Duchemin et al. (1999) revealed that the

Table 2.2 Summary of approaches for satellite-derived phenology

Approach	Reference	Advantage	Disadvantage
NDVI threshold	Lloyd (1990); Fischer (1994); Markon et al. (1995)	Easy to apply	Not applicable across landcovers
Moving average of smoothed NDVI	Reed et al. (1994)	Independent of landcover types	Hard to determine the moving average time interval
Normalized NDVI ratio	White et al. (1997)	Ecologically meaningful	Dependent of landcovers
Derivative of NDVI	Moulin et al. (1997)	Independent of landcover	Sensitive to the weight of the derivative term
Linear segments of NDVI time series	Duchemin et al. (1999)	Easy to apply	sensitive to a change in the rate of NDVI variation
Curvature-change rate for vegetation indices	Zhang et al. (2003)	For multiple growth cycle Independent of landcovers	Hard to determine the single growth and senescence periods

temporal variation of NDVI during budburst and senescence was nearly linear. A line segment model was used to fit the effect of budburst and senescence. The method was sensitive to a change in the rate of NDVI variation, resulting, for instance, from a spring frost during budburst, or from a severe drought in summer accelerating the senescence. Zhang et al. (2003) identified phenological transition dates based on the curvature-change rate of a logistic model for time series of MODIS vegetation indices. This method has been applied in many researches (Zhang et al., 2004; Ahl et al., 2006; Peckham et al., 2008) because it is able to handle multiple growth cycle and is not tied to a specific calendar period (e.g., January to December). The challenge for this method is to identify

a single sustained increase and decrease period before the MODIS measurements could be fit to the logistic model.

2.3 Validation effects

The link between phenology estimated from remote sensing and ground observations is often weaker. Badeck et al. (2004) hypothesized that this is caused by qualitative differences between the observations, as well as the heterogeneity of pixel composition in satellite scenes. They state that the modest correlations between ground and satellite observations should be expected and that a key to resolving these problems lies with improved spatial interpolation of ground observation data. The two scales of observation should be thought of as complementary, with scaling studies a rich area of prospective research.

Climate-based model is a popular method to validate satellite-derived phenology. The Spring Index (SI) models (developed from cloned lilac and honeysuckle data) have a demonstrated potential to represent seasonally integrated changes in temperature for selected plant species (Schwartz et al. 2006). These models are most applicable to temperature responsive forest trees and shrubs and agricultural crops planted in temperate regions with adequate rainfall. Other validations strategies include general comparisons to land cover types in different locations (Hoare and Frost 2004; Bradley et al. 2007), and use of contiguous uniform (pixel-level) land cover sites (White et al. 1997). Many early or methodological studies essentially used no validation at all (Lloyd 1990; Reed et al. 1994; Slayback et al. 2003; Cao et al. 2004). One recent study made comparisons to

various surface radiation-derived measures, such as Photosynthetically Active Radiation (PAR) and Plant Area Index (PAI; Ahl et al., 2006). Two others employed ground-level imagery, either along transects (Fisher et al., 2006) or from a fixed location atop a flux tower (Richardson et al. 2007). A promising development in validating satellite-derived phenology is the use of inexpensive downward- or outward-looking cameras to record phenological development around eddy covariance monitoring sites where the instrument towers afford an above-canopy view (Richardson et al., 2007). Widespread adoption of these devices will greatly increase the data available to improve understanding of the general relationships among surface phenology and various satellite-derived measures.

2.4 Applications of satellite-derived vegetation phenology

A variety of applications demonstrate the utility of satellite derived phenology estimates. Westerling et al. (2006) relate early spring (defined by hydrological estimates) to increased forest wildfire activity in the western US. Increased spring and summer temperatures, along with earlier snowmelt produce a relatively large increase in cumulative moisture deficit by midsummer and subsequent increased fire danger. Incorporating ground and satellite-derived phenology information into further study of fire severity and possible early warning of fire is a logical next step for such studies. Brown et al. (2008) include start of season anomalies (derived from AVHRR) as a key input to a vegetation drought response index (VegDRI). The VegDRI incorporates climate-based drought indicators with satellite-derived vegetation metrics and other biophysical data to identify drought conditions in near-real time. The phenology

component of their model helps to distinguish a delayed growing season from one that is experiencing stressful growing conditions.

More needs to be known about growing season length as a limiting factor of productivity and carbon flux, and better parameterizing models for changing surface conditions, such as albedo or surface roughness are necessary. Increased knowledge in these areas would lead to improvement in models that change the value of certain parameters at pre-determined times of the year. Improving our understanding of the issues underlying these questions can be achieved by analysis of multiple, simultaneously collected data at intensive phenology observation sites (Betancourt et al., 2005). These can be instrumented research sites, such as Ameriflux or Long Term Ecological Research stations where observations of weather, biogeochemistry, satellite imagery, and plant phenology can be collected. While some of these efforts are underway (Richardson et al. 2007), the USA-NPN plans to facilitate more such studies.

Changes in land surface phenology have been used as an indicator of land use change. De Beurs and Henebry (2004) used 8 km AVHRR data to identify agricultural land cover change in Kazakhstan. They state that institutional change was manifested as land cover change, principally as an increase in fallow land (and pioneering weedy species) that was reflected in changing land surface phenology. Similarly, Reed (2006) identified agricultural practices in Saskatchewan, Canada as a source of changing land surface phenology using a similar 8 km AVHRR data set. White et al. (2002) used satellite based start of season estimates in a study of the urban heat island effect on seasonality of deciduous broadleaf forest. Urbanization was associated with an expansion of the

growing season by 7.6 days during the 1990s. Most of this effect was caused by an earlier start of the growing season. In a similar study using MODIS data from 2001, Zhang et al. (2004) identified an increase in the growing season of about 15 days in urban areas relative to adjacent unaffected rural areas. They saw an urbanization influence on the length of the growing season up to 10 km beyond the edge of the urban areas.

Zhang et al. (2007) utilize AVHRR global vegetation index data (GVI) to characterize a diverse response of vegetation phenology to a warming climate. They identify a latitudinal transition zone where the landscape changes from an earlier to a later trend in the time of greenup from north to south due to differential fulfillment of chilling requirements. This latitudinal transition zone appears to be shifting northward at a rate of 0.1º of latitude per year. Bunn and Goetz (2006) used a 22-year record (1982–2003) of satellite observations from AVHRR to identify trends in circumpolar photosynthetic activity. They report disparate seasonality trends over this period between tundra areas (greening) and boreal forests (browning). They speculate that the boreal forest may be responding to climate change in unexpected ways, thus necessitating an expanded observation network and revisiting ecosystem process models. Reed (2006) identified similar patterns in Alaska, but suggests that the boreal forest "browning" may, in part, be due to insect and/or fire disturbance. Regardless of the cause, it is apparent that continued observation and investigation in this northern biome are warranted.

Real time monitoring and short-term forecasting of vegetation phenology can contribute significantly to land management, human health, and other applications (White and Nemani 2006). Phenology forecasts, based on remote sensing data, coupled with

uncertainty estimates could be used for estimating future crop conditions, fire danger, and potentially contribute to early warning of drought conditions. Kathuroju et al. (2007) used vegetation phenolgy derived from AVHRR to develop prognostic phenology models and tested these models against climatological phenology values from AVHRR. The prognostic model did not perform any better than using a mean date model for most of their model runs. The authors state that other, more advanced sensors or the addition of snow and atmospheric information may produce better results. They also suggest that species-specific models coupled with vegetation phenology may be more appropriate approach.

CHAPTER 3

DETECTION OF VEGETATION PHENOLOGICAL PHASES FROM MODIS MEASUREMENTS

This study focused on Deciduous Broadleaf Forest (DBF) regions in the continental United States. DBF is adapted to a seasonal climate in mid-latitudes. Timing of phenological events, such as first leaf appearance, offset of greenness and growing length can be influenced by various local and genetic factors, permitting vegetation to serve as effective indicators of climate change. MODIS Land Cover Product at 1-kilometer resolution (MOD 12Q1) was used to identify DBF areas. The primary land-cover types in this product include 17 land-cover classes following the International Geosphere-Biosphere Program (IGBP) scheme (Friedl et al., 2002). In this study, both deciduous broadleaf forest and mixed forest were treated as DBF.

3.1 Satellite data

MODIS measurements were used to identify phenological transition dates in DBF over the continental United States. MODIS is a key instrument aboard the Terra (EOS AM) and Aqua (EOS PM) satellites. Terra's orbit around the Earth is timed so that it passes from north to south across the equator in the morning, while Aqua passes south to north

over the equator in the afternoon. Terra MODIS and Aqua MODIS are viewing the entire Earth's surface every 1 to 2 days, acquiring data in 36 spectral bands. The Land Processes Distributed Active Archive Center (LP DAAC) processes, archives, and distributes land data and products derived from the MODIS. The MODIS land data products incorporate enhanced atmospheric correction, cloud detection, improved georeferencing and enhanced ability to monitor vegetation (Justice et al. 1997). In this study, two vegetation indices, i.e. MODIS NDVI and EVI were used to determine forest phenology. NDVI and EVI were calculated using the MODIS Nadir Bidirectional Reflectance Distribution Function (BRDF) Adjusted Reflectance (NBAR) product at 1km resolution (MCD43B4, version 5).

$$NDVI = \frac{r_2 - r_1}{r_2 + r_1} \tag{3.1}$$

$$EVI = G\frac{r_2 - r_1}{r_2 + C_1 r_1 - C_2 r_3 + L} \tag{3.2}$$

where r_1, r_2 and r_3 represent surface reflectance of MODIS band 1 (620-670 nm), band 2 (871-876 nm), and band 3 (459-479 nm), respectively. L (=1) is the coefficient for canopy background adjustment, C_1 (=6) and C_2 (=7.5) are aerosol resistance coefficients and G (=2.5) is a gain factor (Huete et al., 2002).

3.2 MODIS data processing

MODIS land data products, i.e. NBAR (MCD43B4), BRDF Quality Assessment (QA) (MCD43B2), Landcover (MOD 12Q1) for the continental United States from year 2001 to 2007 were collected through the LP DAAC at the U. S. Geological Survey Earth

Resources Observation and Science (EROS) Data Center (EDC). These data products are archived in equal area tiles of 1200 by 1200 pixels in a Sinusoidal projection (SIN) at 1km spatial resolution, and released in Hierarchical Data Format – Earth Observing System (HDF - EOS). The continental United States is covered by 21 tiles including 7 horizontal tiles (h7-h13) and 3 vertical tiles (v4-v6). A series of preprocessing steps were performed to MODIS land data products using MATLAB before onset dates were identified (Fig. 3.1):

(1) Mosaic

For every 8-day period from year 2001 to 2007, 21 tiles of MODIS NBAR, BRDF Quality Assessment, and LAI data products for the continental United States were mosaicked together to one matrix of 8400 by 3600. MODIS land cover data products were mosaicked similarly year by year.

(2) NDVI and EVI calculation

NDVI and EVI were calculated from mosaic NBAR data using equation (3.1) and (3.2), respectively.

(3) Data Quality Control

Since snow cover can cause non-phenological variations in NDVI and EVI values, it is necessary to filter snow-covered pixels before determining onset days of vegetation. MODIS NBAR Quality Assessment data were used to identify snow pixels and the corresponding NDVI and EVI values were filled with the minimum snow-free value in the same year.

(4) DBF mask

Finally, DBF mask was derived from MODIS landcover product, and was applied to produce snow-free NDVI and EVI data for DBF in the continental U.S.

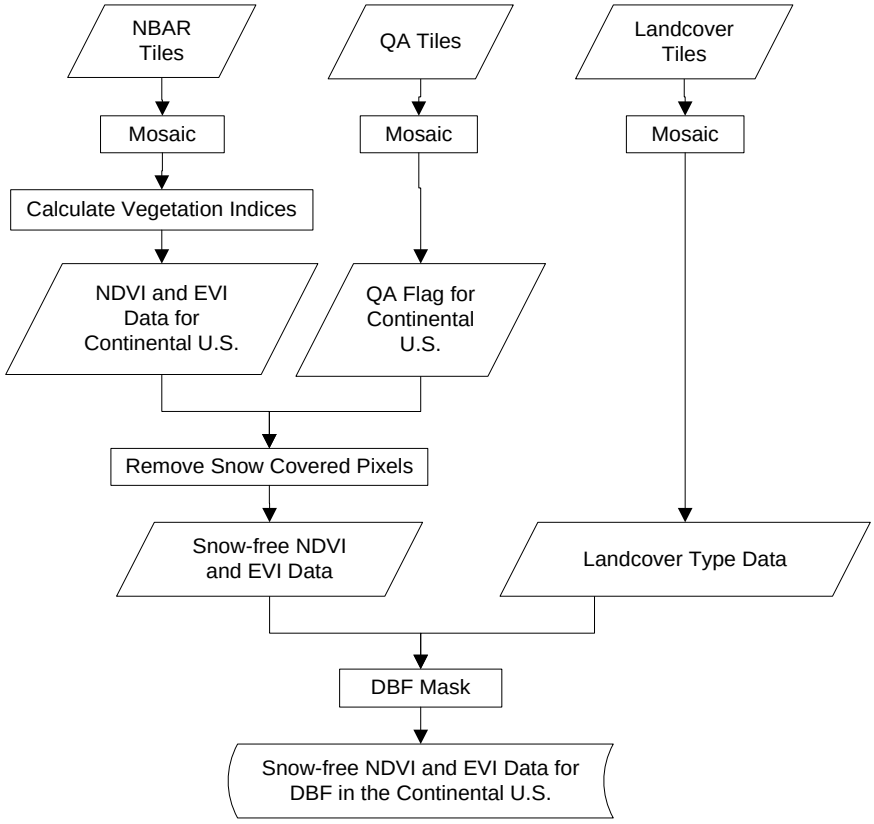

Fig. 3.1 Flowchart of data processing

3.3 Satellite-derived forest canopy phenology

Zhang et al. (200) suggested a logistic model to simulate vegetation phenology. Every single ascending (growth) or descending (senescence) period can be simulated by the logistic model. In this study, instead of the moving average window used in Zhang (2003), the Fourier series is used to decompose the periodic VIs of the seven years (2001-2007) into a sum of simple oscillating function as showed in Eq. (3.3),

$$y = a + b\cos(\omega x) + c\sin(\omega x) \tag{3.3}$$

where a, b and c are fitting parameters, ω is the angular frequency which is equal to $2 \times \pi/T$, and T is period time of the growth cycle. For instance, the T for the single growth cycle is the number of data samples for one year. For multiple growth cycle, T equals to the number of data samples divided by the number of cycles for one year. The other parameters are solved by least square fitting. Local maximum and minimum points of the simulated data divided original data into a series of sustained increasing and decreasing trends (Fig. 3.2). The advantages of using Fourier series to identify the single growth or senescence period are the independence of temporal resolution of datasets. There is no need to set any parameters empirically, and so this method is somewhat objectively.

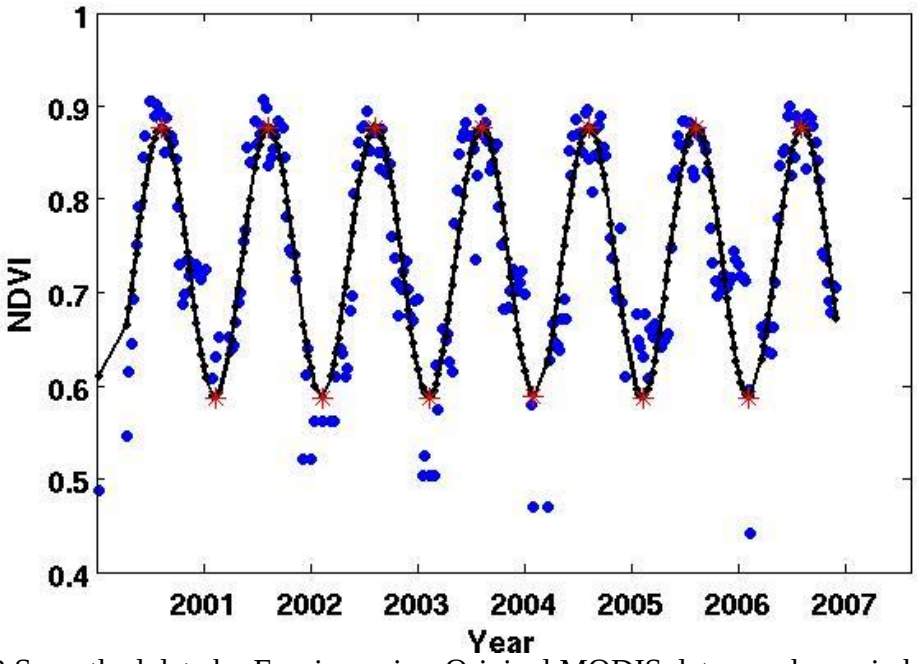

Fig. 3.2 Smoothed data by Fourier series. Original MODIS data are shown in blue points and simulated data in black solid line. The red star marks are local maximum and local minimum.

The logistic model (Zhang et al., 2002) used to simulate a single growth and senescence cycle is in the following form:

$$y(t) = \frac{c}{1+e^{a+bt}} + d \tag{3.4}$$

where t is time in days, y(t) is the vegetation indices (VI) value at time t, a and b are fitting parameters, c+d is the maximum VI value, and d is the initial background VI value. For each of the VIs (NDVI and EVI), the corresponding model parameters a and b were determined using least square fitting, the parameter d was set to minimum VI and the parameter c was determined with d and maximum VI.

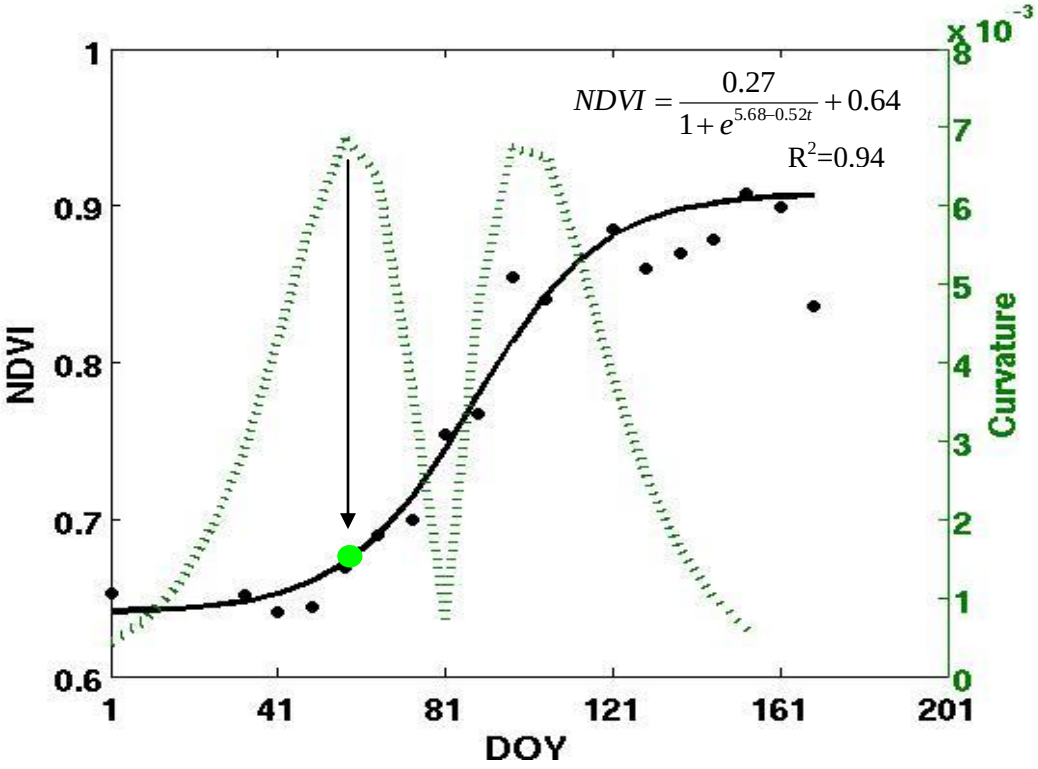

Fig. 3.3 Identification of onset date. The solid line is fitted logistic model and the dashed line is the curvature of the NDVI time series. The green point indicates the greenup onset.

To identify transition dates of forest canopy phenology, the curvature of the fitted logistic models has to be determined. The first point with largest curvature in increasing period corresponds to the greenup onset and the second point with largest curvature in decreasing period corresponds to the dormancy onset (Fig. 3.3, Fig 3.4). The accuracy of the logical model depends on the number of observations. The more observations, the more accurate of the estimates is. In this study, we use onset value threshold, i.e. 0.3 and the coefficient of determination R-squared i.e. 0.7 to ensure that the model produces at least 70% of the variability of the observed signal and a reasonable onset value. .

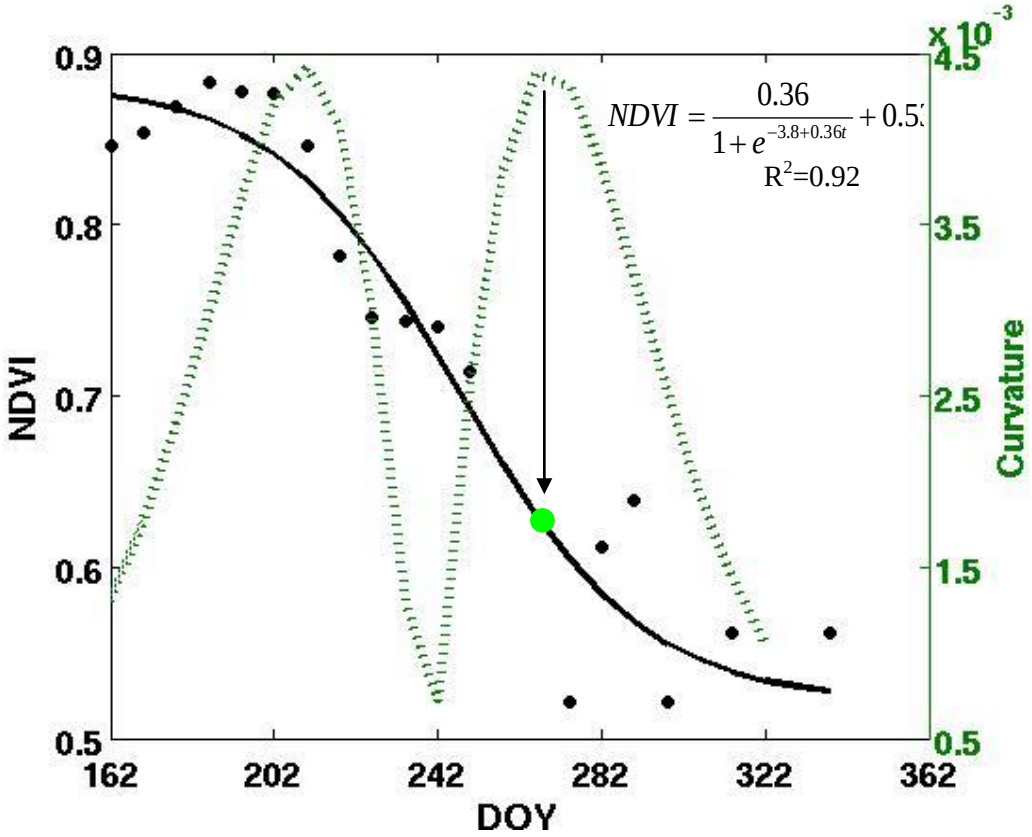

Fig. 3.4 Identification of offset date. The solid line is fitted logistic model and the dashed line is the curvature of the NDVI time series. The green point indicates the dormancy onset.

3.4 Validation of satellite-derived phenological transition dates

3.4.1 Comparison with Harvard forests

Researchers at Harvard Forest, which covers latitude from 42.53^0N to 42.54^0N and longitude from 72.19^0W to 72.18^0W, have observed the timing of woody vegetation development during the growing season since the spring of 1990 (O'Keefe, 2000). All species are located within 1.5 km of the Harvard Forest headquarters at elevations between 335m and 365m, in habitats ranging from closed forest, through forest-swamp margins, to dry, open field. Data were collected for 33 understory and overstory species at 3-7 day intervals from April through June. Budburst and leaf development (percentage of total leaf size) are recorded for spring phenology. They have also observed fourteen species for fall phenology since 1991. Weekly observations of percent leaf coloration and percent leaf fall begin in September and continue through leaf fall. The observations are used to validate both greenup onset and dormancy onset derived from MODIS.

Greenup onsets derived from NDVI and EVI are very close. But they are both two or three weeks earlier than the average dates on which leaves are 10% of final leaf size observed in Harvard Forest. The logistic model (Eq. 3.4) fits the MODIS NDVI and EVI very well. The coefficient of determination (R-squared) achieves 0.89 in average. The differences between greenup onset dates derived from NDVI and EVI are within 10 days. The average onset dates for 7 years (2001-2007) are 113 and 111 determined by NDVI and EVI, respectively, while the average date that leaves grow to 10% of final size is 131 in Harvard Forest (Table 3.1).

Table 3.1 Satellite-derived greenup onset and ground observations.

Year	10% of final leaf size	Greenup onset from NDVI	Greenup onset date from EVI
2001	127	119(-8)	109(-18)
2002	128	111 (-17)	105(-23)
2003	132	117(-15)	121(-12)
2004	129	105(-24)	105(-24)
2005	135	121(-14)	117(-18)
2006	132	105(-27)	111(-21)
2007	132	-	111(-21)
Average	131	113(-18)	111(-20)

For additional insight, the developmental stage of sampled species given as the percentages of final size is plotted together with NDVI and fitted logistical model (Fig. 3.5). The developmental stage can vary greatly by species. Even on the same day, some species have approached the final leaf size, while other species are only 10% of final leaf size. The average greenup speed from 1% of final leaf size to 100% of final leaf size observed in Harvard Forest is 30 to 40 days. MODIS NDVI and EVI may only provided 4 to 5 8-day composited observations during this period. However, 10 or more MODIS observations are needed to develop the logistical model. The average greenup speed from onset of greenness to the maturity determined by NDVI and EVI is 70 to 80 days. Although the onset of growth differs from field observations and satellite observations, the timing of maturity is close in the both observations. The logistical model stops ascending when the average percentage of final leaf size is 90%. The earlier satellite-derived onset of greenness is likely contributed to 1) the understory component; Ahl et al. (2006) found that understory components greened earlier than canopy in DBF. This

explains in part why the satellite-derived onset is earlier than field observations. At the beginning, satellite-based vegetation indices capture understory reflectance. Subsequently, overstory components greenup and become the main contributor to the vegetation indices; 2) the compositing method of satellite products; NDVI and EVI are computed from 8-day composited NBAR products. The individual specie greenup may occur in 10 to 20 days, which means that satellite-derived onset could underestimate or overestimate the spring phenology signal; 3) spatial scales; the spatial resolution of satellite measurements is 1 km. So the satellite-derived onset dates are representative of canopy phenology. The average of field observations may be too simple to represent developmental stage of canopy.

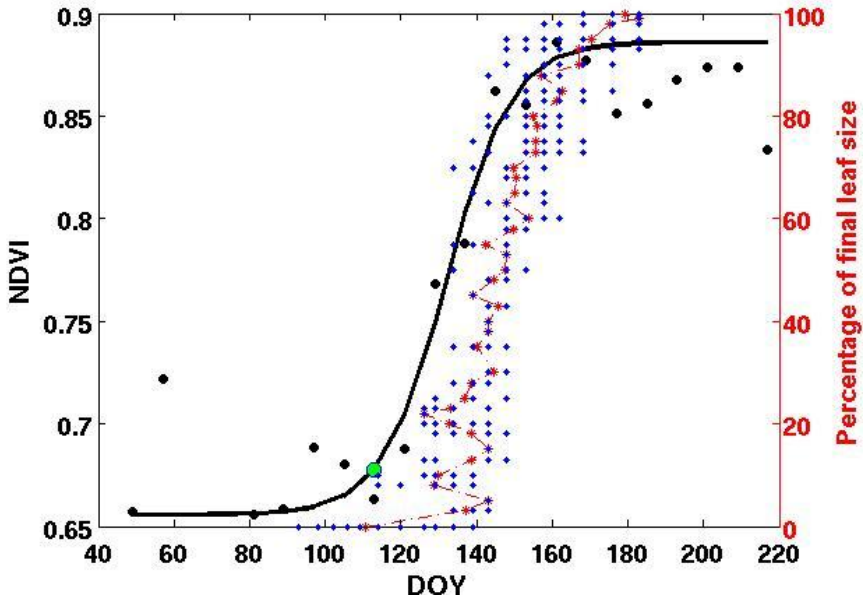

Fig. 3.5 Comparison of Harvard Forest observations and satellite observations in spring of year 2002. The black dots are NDVI value during growing season. The solid line is fitted logistic model for NDVI. The blue dots are the developmental stage of sampled species given as the percentages of final size. The red dash-dot line with star makers is the average percentage of final size. The green spot is the greenup onset derived from NDVI.

The dormancy onset derived by EVI match the field data much better than that derived by NDVI. Although considerable variability exists, results suggest that dormancy onset based on EVI corresponds to a ground stage of 70% leaves drop in the fall. The average results of 7 years (2001-2007) indicate that there is only 2-day difference between field records of 70% leaves fall and EVI-derived dormancy onset. While the dormancy onset based on NDVI is far behind the stage of 70% leaves fall and even later than 90% leaves fall (Table 3.2). Whereas the NDVI is chlorophyll sensitive, the EVI is more responsive to canopy structural variations, including leaf area index, canopy type and architecture. (Huete et al., 2002). Another explanation for inaccurate estimates of NDVI on fall phenology is the saturation problem of NDVI over densely vegetated area where LAI exceeds 2 or 3. Since the sensitivity of vegetation index is crucial for the efficiency of the logistical model, it is reasonable that EVI is better than NDVI on estimates of fall phenology.

Table 3.2 Satellite-derived dormancy onset and ground observations

Year	70% leaves fall	Dormancy onset from EVI	90% leaves fall	Dormancy onset from NDVI
2001	284	287 (3)	305	-
2002	300	307 (7)	310	323 (13)
2003	294	287 (7)	297	329 (32)
2004	281	299 (18)	294	353 (39)
2005	289	291 (2)	299	329 (30)
2006	285	281 (-4)	304	-
2007	299	295 (-4)	304	341 (37)
Average	290	292 (2)	301	335 (34)

Figure 3.6 presents the falling stage of sampled species given as the percentages of leaves fall together with EVI and fitted logistical model. Similar to the developmental stage, the falling stage can vary greatly by species. Though the logistical model does not exactly match the stage of leaves fall, it is comparable to the general stages of fall phenology in Harvard Forest. The falling stage observed from field records spans the descending period of EVI model.

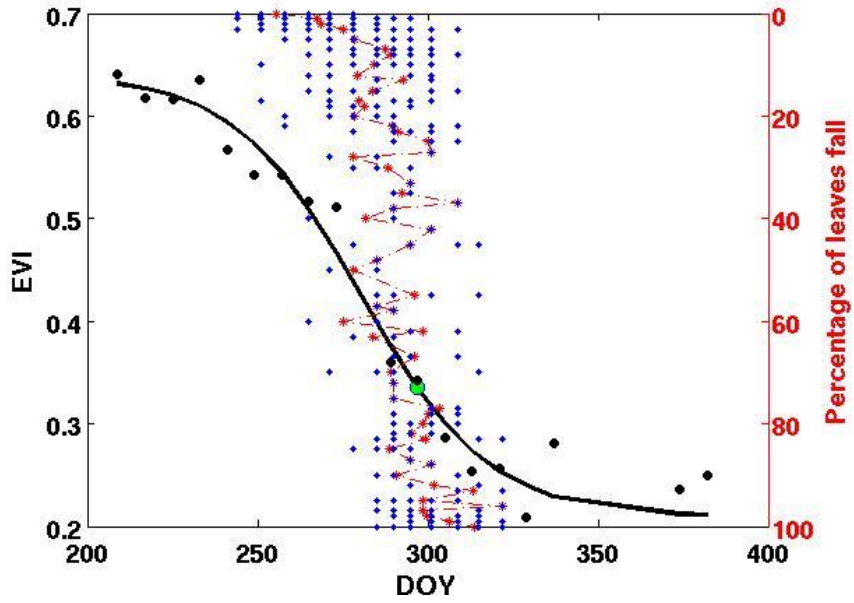

Fig. 3.6 Comparison of Harvard Forest observations and satellite observations in fall of year 2002. The black dots are EVI value during senescence phase. The solid line is fitted logistic model for EVI. The blue dots are percentage of leaves that have fallen from sample trees. The red dash-dot line with star makers is the average percentage of fallen leaves of all sample trees. The green spot is the dormancy onset derived from EVI.

3.4.2 Comparison with North American first leaf Lilac phenology data

The NOAA Paleoclimatology Program distributes archives of North American phenology data: yearly first leaf and first bloom dates for lilac shrubs (Syringa chinensis and Syringa

vulgaris) at 1126 locations in the United States and Canada (Schwartz and Caprio, 2003). In this study, the stations located in the United Sates and identified as DBF by MODIS landcover product were selected (Table 3.3). Although the station 13 is located in the province of Nova Scotia, Canada, it is close to the state of Maine and the observations from the station is also selected. All of the 16 stations are in the Northeastern United Sates (Fig 3.7) and possess humid continental climate. Summers are often warm and humid and winters can be very cold with frequent snowfall and persistent snow cover. First leaf dates for lilac shrubs of the 16 stations from 2000 to 2003 are analyzed to validate the greenup onset derived from MODIS measurements.

Table 3.3 Yearly dates of first leaf at 16 stations in DBF area.

Station ID	Station Name	State	Latitude	Longitude	First leaf dates			
					Year 2000	Year 2001	Year 2002	Year 2003
1	BUFFUMVILLE LAKE	MA	42.12	-71.90	84	100	101	97
2	LANCASTER	NH	44.48	-71.57	115	-	-	-
3	BRIDGEHAMPTON	NY	40.95	-72.30	68	92	89	105
4	CANTON	NY	44.58	-75.17	104	-	-	-
5	CHAZY	NY	44.88	-73.47	108	110	105	104
6	EVERETT	PA	40.00	-78.38	66	98	97	91
7	CAVENDISH	VT	43.38	-72.6	107	111	96	108
8	ESSEX JUNCTION	VT	44.52	-73.12	97	110	98	106
9	NORFOLK 2 SW	CT	41.97	-73.22	94	104	97	108
10	BIRCH HILL DAM	MA	42.63	-72.12	105	120	107	-
11	ORONO	ME	44.93	-68.70	122	-	-	-
12	DURHAM	NH	43.13	-70.93	105	115	114	119
*13	ASPEN RR2	NS	45.30	-62.05	109	-	126	124
14	GRAFTON	NY	42.78	-73.47	117	119	85	-
15	UNION VILLAGE DAM	VT	43.80	-72.27	110	114	102	111
16	UWM FIELD STATION	WI	43.39	-88.02	87	109	102	105

* Station 13 is located in the province of Nova Scotia, Canada.

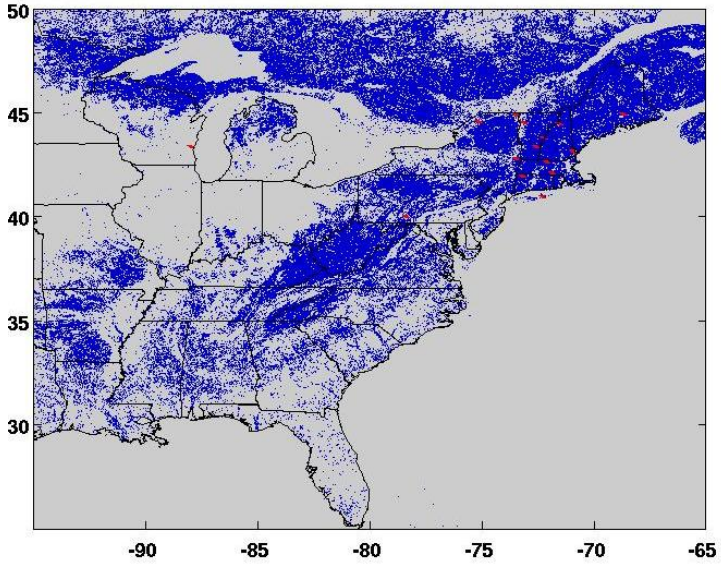

Fig. 3.7 DBF distribution map (blue area) of the continental United States and station locations of North American First Leaf Lilac Phenology Data (red dots).

Since the dormancy onset is not available in the NOAA dataset, greenup onset dates derived by MODIS NDVI and EVI were compared with yearly first leaf dates for lilac. Statistic results are summarized in Table. 3.4. Mean absolute error (MAE), mean error (bias) and standard error are used to evaluate the predictions. Since NBAR data is a 8-day product, NDVI MAE (8.51) and EVI MAE (9.58) show that they both have good predictions. But the smaller bias indicates that NDVI predicts more reasonable greenup onset dates than EVI. The histogram of difference between ground measurements and NDVI and EVI predictions is illustrated in Fig 3.8 and Fig 3.9 respectively. The difference represents ground measurements minus VI predictions. Most of the NDVI predictions are within 5 days of ground measurements. While EVI predictions have more observations in 5 days earlier or later than ground observations.

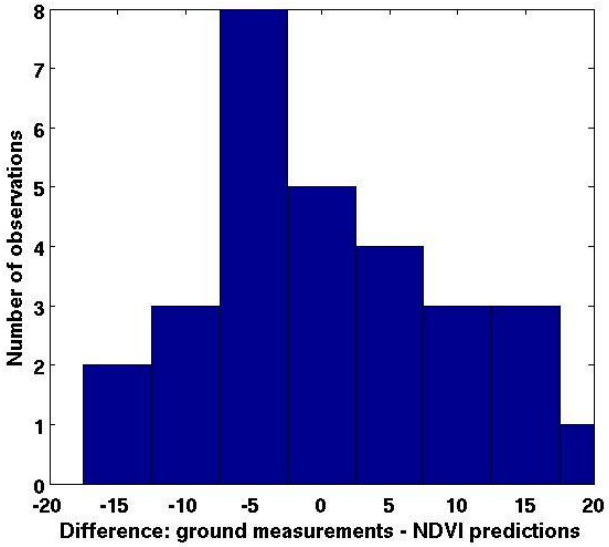

Fig. 3.8 Ground measurements minus NDVI predictions

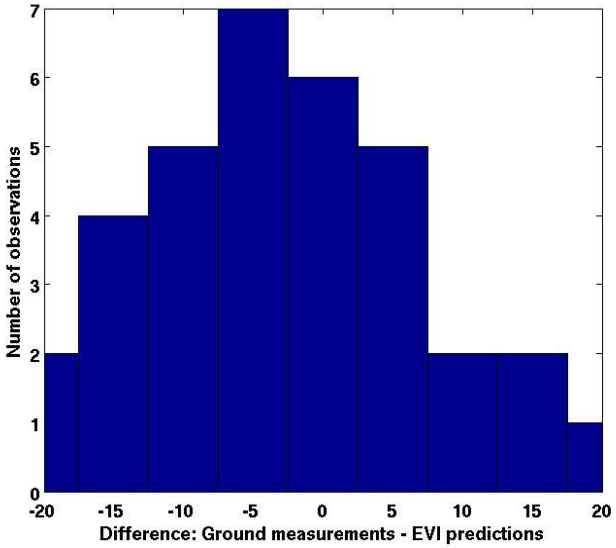

Fig. 3.9 Ground measurements minus EVI predictions

Table 3.4 Statistic summary of onset dates prediction

MODIS data	MAE	Bias	Standard Error
NDVI (n*=31)	8.51	-1.10	11.06
EVI (n*=36)	9.58	-4.81	12.21

*n is the number of field observations

3.5 Summary

The field observations from the Harvard Forests and NOAA phenology network are used to validate satellite-derived phenology events. These data, while limited to northeastern DBF and thus certainly not a complete validation, are extremely valuable and suggest that (1) Satellite measurements tend to predict earlier greenup onset than filed observations. (2) NDVI predicts more reasonable greenup onset dates than EVI. (3) EVI-derived dormancy onset dates match the field observations better than NDVI, which correspond to a ground stage of 70% leaves drop in the fall within 2 days.

The accuracy of greenup and dormancy onset derived by satellite measurements is dependent on the temporal resolution of MODIS NBAR products. MCD43B4 reflectance represents that best characterization of the surface possible from the inputs available over a 16-day period. The compositing method likely contributed to the uncertainty of estimates of onset dates. For phenology studies aimed at detecting the effects of climate change, it may be more meaningful if the MODIS product contained information on the dates from which the product was developed or weighted most heavily. The increase of temporal resolution of NBAR data is critical to the accuracy of phenological retrievals. The continuity of NBAR data can also influence the estimates for onset of greenness. The missing data during vegetation growth period could underestimate or overestimate the actual spring canopy phenology signal. Furthermore, since the spatial resolution of NBAR products is 1 km, the onset dates identified in this paper are representative of canopy phenology, rather than individual species.

CHAPTER 4

APPLICATION OF SATELLITE-DERIVED VEGETATION PHENOLOGY

The detection of phenological patterns across broad geographic scales plays an important role in our understanding of global environmental changes. The satellite-derived vegetation phenology has enabled the integration of historically disparate phenological events and have helped to develop a stronger understanding of how environmental conditions, affect phenological patterns among broad scales. Greenup onset and dormancy onset determined by NDVI and EVI and the growing length determined by combined NDVI and EVI in DBF areas over the continental U.S. in the year of 2003 are presented in Fig 4.1, Fig 4.2 and Fig 4.3 respectively. These figures show obvious spatial patterns of greenup onset, dormancy onset and growing length in latitude. Some questions emerged about how phenological events are sensitive to environmental factors, e.g. latitude and elevatioin; whether there is interannual variability existing in these phenological events. These questions will be discussed in the following sessions.

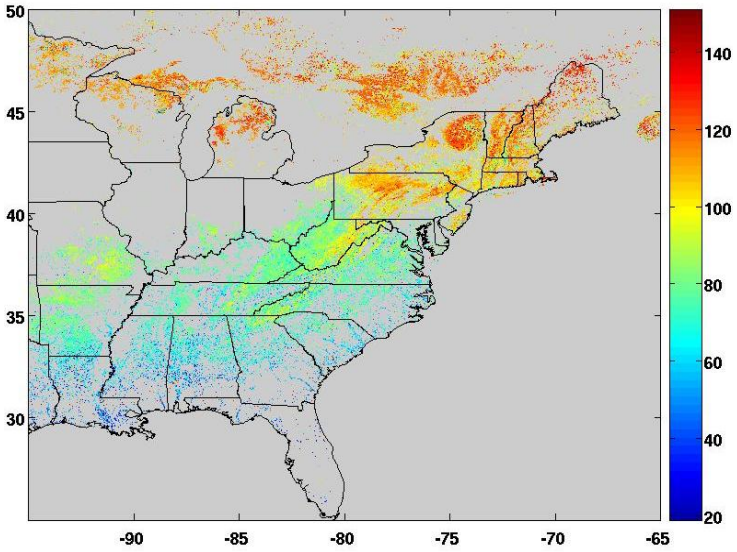

Fig. 4.1 Greenup onset estimated by NDVI in DBF over the continental U. S. in 2003. The color legend indicates the day of year.

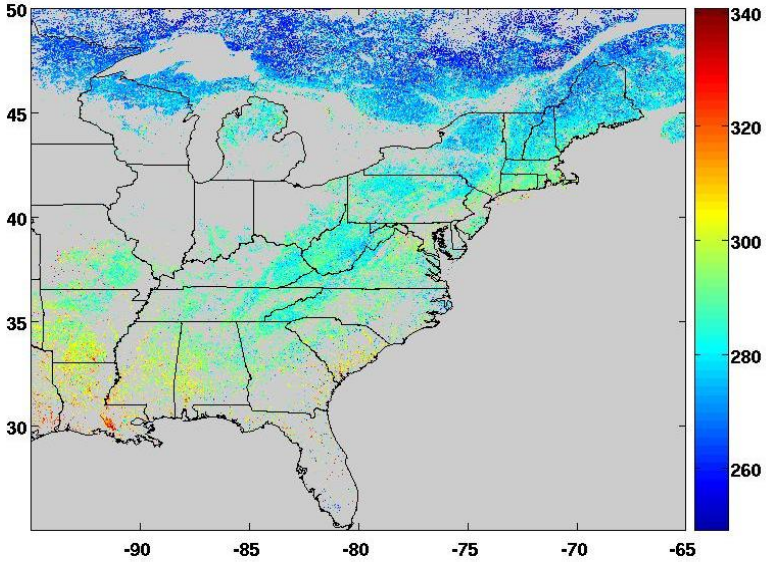

Fig. 4.2 Dormancy onset estimated by EVI in DBF over the continental U. S. in 2003. The color legend indicates the day of year.

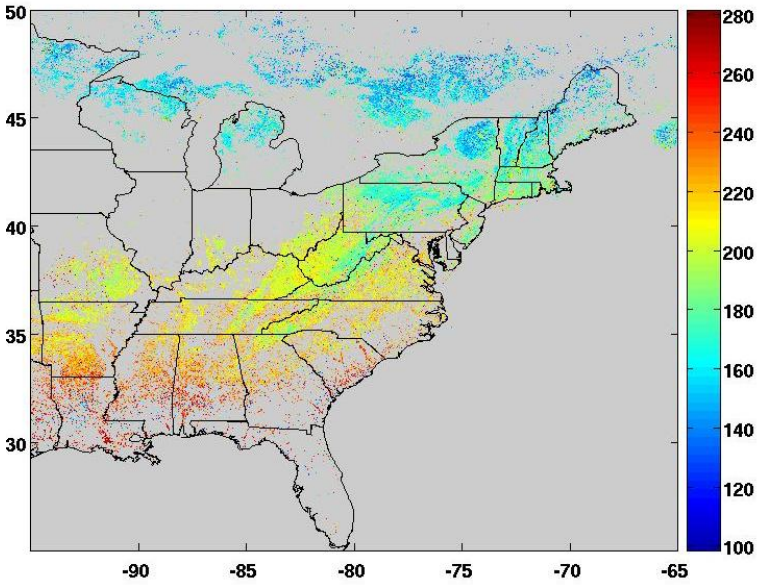

Fig. 4.3 Growing length estimated by combined NDVI and EVI in DBF over the continental U. S. in 2003. The color legend indicates the day of year.

4.1 Variation of vegetation phenology in latitude

Figure 4.4 presents the timing of satellite-derived phenological events versus latitude in DBF areas over the continental U.S. The result shows an obvious pattern dependent on latitude, in which greenup onset dates are gradually late from low latitudes to high latitudes, whereas dormancy onset dates are gradually early from low latitudes to high latitudes. As a result, the growing length is longer in low latitudes than in high latitudes. The linear regression models are established to estimate the rate of change in greenup and dormancy onset dates as a function of latitudes. The regression model for greenup onset is

$$Greenup\_onset = 0.0378 + 2.3266 \times Latitude \quad (4.1)$$

with the goodness of fit of 0.72 and strongly significant (P<0.0001). The regression model for dormancy onset is

$$Dormancy\_onset = 373.3130 - 2.0887 \times Latitude \quad (4.2)$$

with the goodness of fit of 0.78 and strongly significant (P<0.0001). The rate of change is about 2 days per degree of latitude and the greenup onset changes a little greater than the dormancy onset. The greenup onset tends to have more variances than the dormancy onset, especially at latitudes higher than 42^0N.

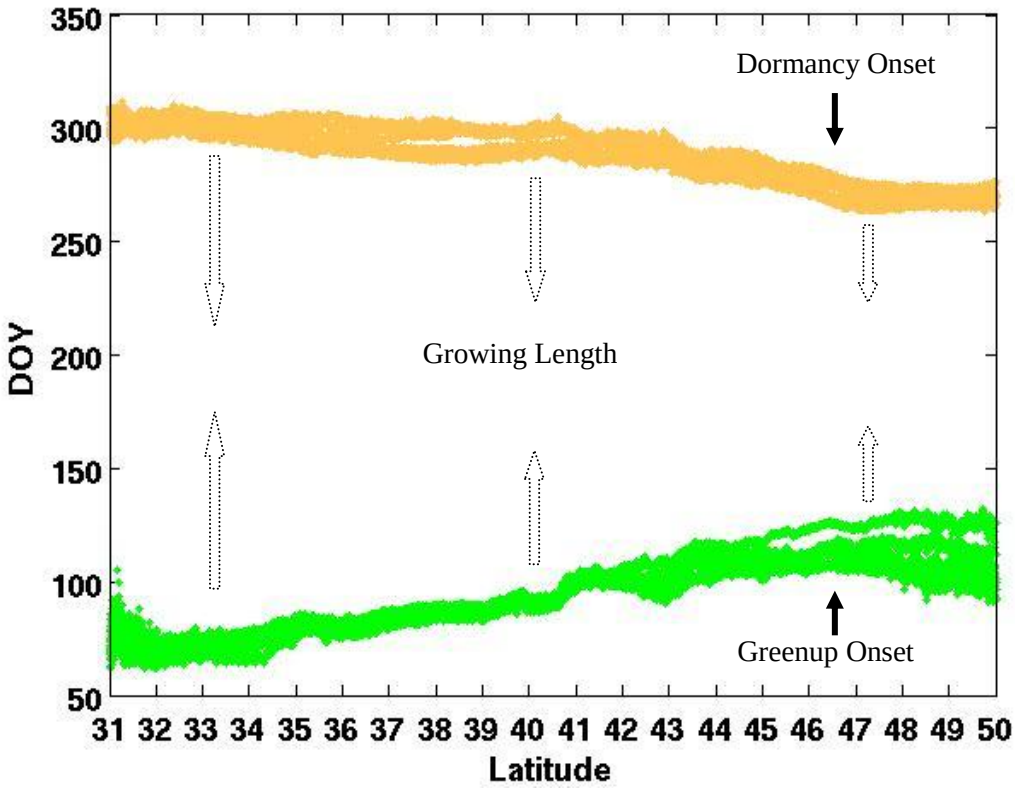

Fig. 4.4 DBF phenology variation along latitudes over Continental U.S.

4.2 Variation of vegetation phenology in elevation

To investigate the elevation impacts, Global Land One-kilometer Base Elevation (GLOBE) data set was used in this study. GLOBE is an internationally designed, developed, and independently peer-reviewed global Digital Elevation Model (DEM), at a

latitude-longitude grid spacing of 30 arc-seconds (30") (GLOBE Task Team and others, eds., 1999). The technical descriptions and DEM map are available at the Web site: http://www.ngdc.noaa.gov/mgg/topo/gltiles.html. The DEM maps covering the continental U.S. was downloaded, mosaicked and reprojected to Sinusoidal projection (Fig. 4.5). The highest elevations of DBF in the eastern continental U.S. are no more than 2000 meters and are located between 35^0N and 40^0N. The most part of DBF are less than 1000 meters.

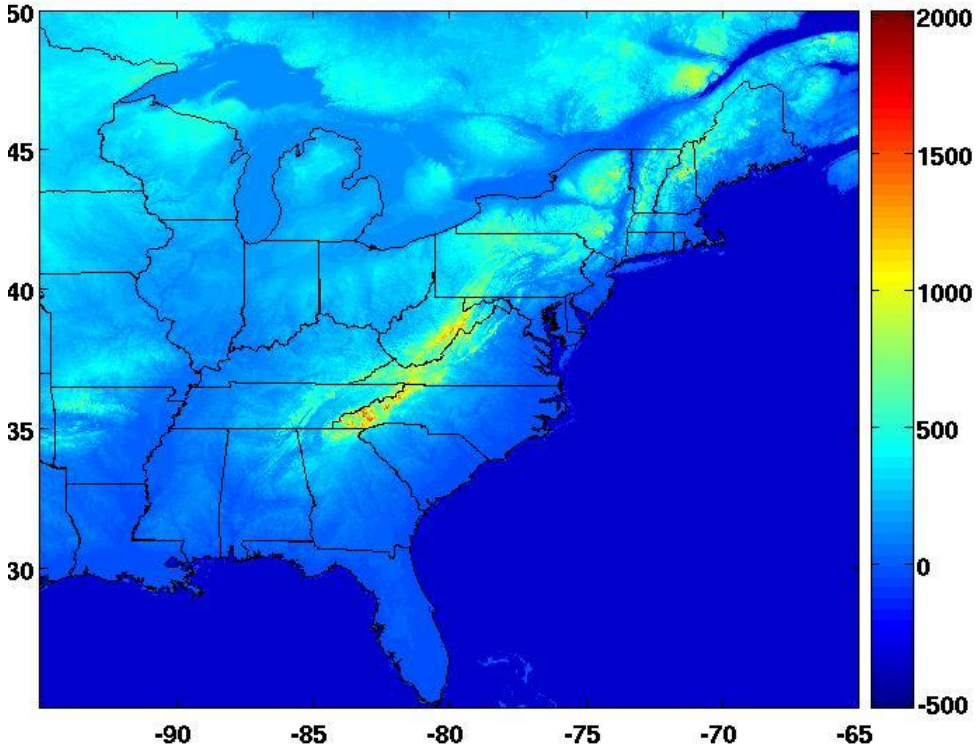

Fig. 4.5 DEM map for DBF area in the U.S.. The color legend indicates elevation in meter.

The average phenological events timing, i.e. greenup onset, dormancy onset and growing length in different elevations from the year of 2001 to 2007 is presented in Fig. 4.6. These three phenological events present an evident pattern dependent on elevation below

500 m. The greenup onset starts earlier at lower elevations and progresses upward in elevation. The dormancy onset appears earlier at higher elevations and progress downward in elevations. The presence of growing length is longer at lower elevations and gradually shorter upward in elevations. However, these trends are not identified in elevations higher than 500 m. Furthermore, there is large variance in vegetation phenology as elevations higher than 1250 m.

To identify the potential reason, the average latitude with standard deviations versus elevation is showed in Fig. 4.7. The average latitude is southward as the elevation increases below 500 m, while the average latitude is northward as the elevation increases higher than 500 m. The standard deviation of latitude is high as the elevation below 1250 m. The highest elevation mostly appears in the latitude near 36^0N and 44^0N. As southward in latitude, the greenup onset should be earlier; the dormancy onset should be later; and the growing length should be longer. However, in the elevation below 500 meters, these patterns are not identified and even in reverse. It is suggested that in eastern DBF, in lower elevation, the vegetation phenology is influenced by elevation rather than latitude. The elevation dependent pattern in vegetation phenology is more obvious than the latitude dependent pattern. As the elevation higher than 500m, the latitude dependent pattern and elevation dependent pattern are not such obvious. Though the average latitude is northward as the elevation increases, the high standard deviation indicates that a wide spread of elevations from 500 m to 1250 m in eastern DBF area. If the latitudinal and altitudinal regulation of vegetation phenology are consistent, e.g. the higher elevation in the north or the lower elevation in the south, obvious elevation dependent pattern will be

identified. Whereas the latitudinal and altitudinal regulation of vegetation phenology are inconsistent, e.g. the lower elevation in the north or the higher elevation in the south, the effect of elevation in vegetation phenology will be counteracted by the effect of latitude.

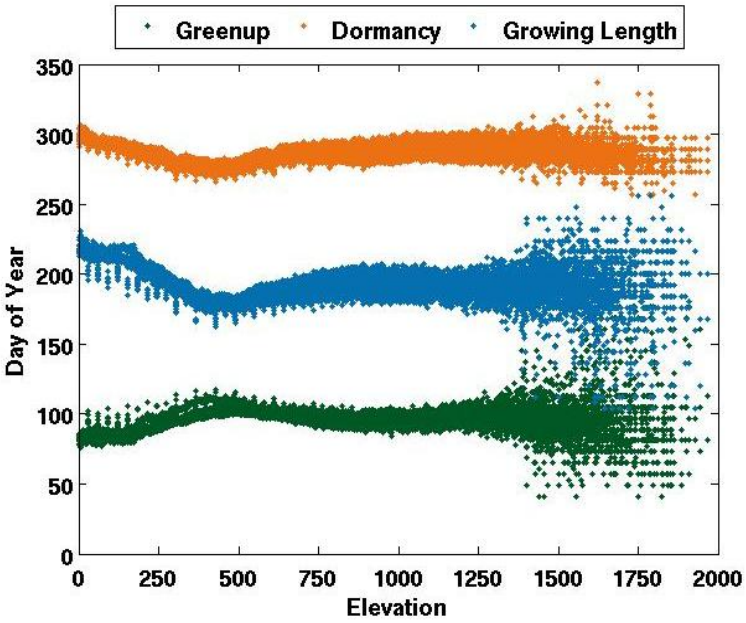

Fig. 4.6 Phenological phases versus elevation (m).

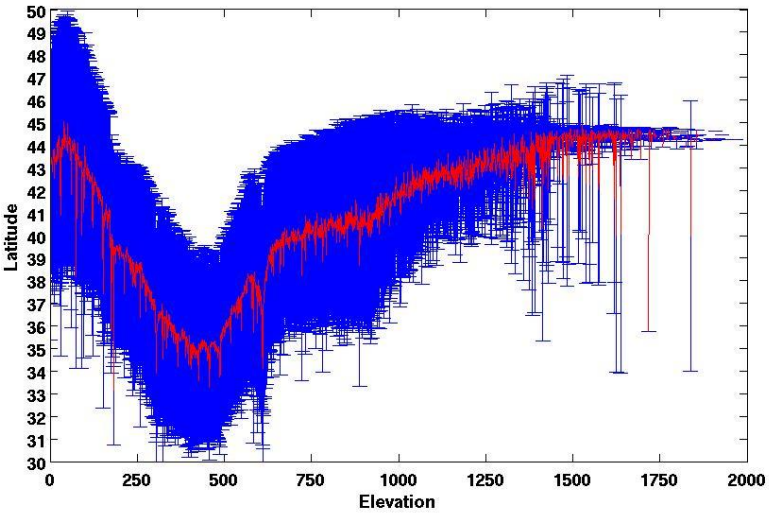

Fig. 4.7 Elevation distribution in latitude. The red line is the average elevation and the blue lines are the standard deviation of elevations in latitudes.

To quantify the effect of elevation in vegetation phenology, the variability of vegetation phenology in elevation in one degree of latitude (35^0N and 40^0N) is investigated (Fig 4.8). The linear regression models are established to estimate the rate of change in greenup and dormancy onset dates as a function of elevation. In the latitude of 35^0N, the regression model for greenup onset is

$$Greenup\_onset = 71.8619 + 0.0212 \times Elevation \quad (4.3)$$

the regression model for dormancy onset is

$$Dormancy\_onset = 300.6569 - 0.006 \times Elevation \quad (4.4)$$

and the regression model for growing length is

$$GrowingLength = 229.0341 - 0.0247 \times Elevation \quad (4.5)$$

In the latitude of 40^0N, the regression model for greenup onset is

$$Greenup\_onset = 81.7673 + 0.0231 \times Elevation \quad (4.6)$$

the regression model for dormancy onset is

$$Dormancy\_onset = 299.2586 - 0.0138 \times Elevation \quad (4.7)$$

and the regression model for growing length is

$$GrowingLength = 217.4970 - 0.0360 \times Elevation \quad (4.8)$$

These models have goodness of fit above 0.65 and strongly significant ($P<0.0001$).

The rate of change for greenup onset is about 2 days per 100 meters in elevations and the rate of change for dormancy onset is about 1 day or less than 1 day per 100 meters in elevation and so the rate of change for growing length is about 2 or 3 days per 100 meters. So the effect of elevation in vegetation phenology is more evident in greenup onset than dormancy onset.

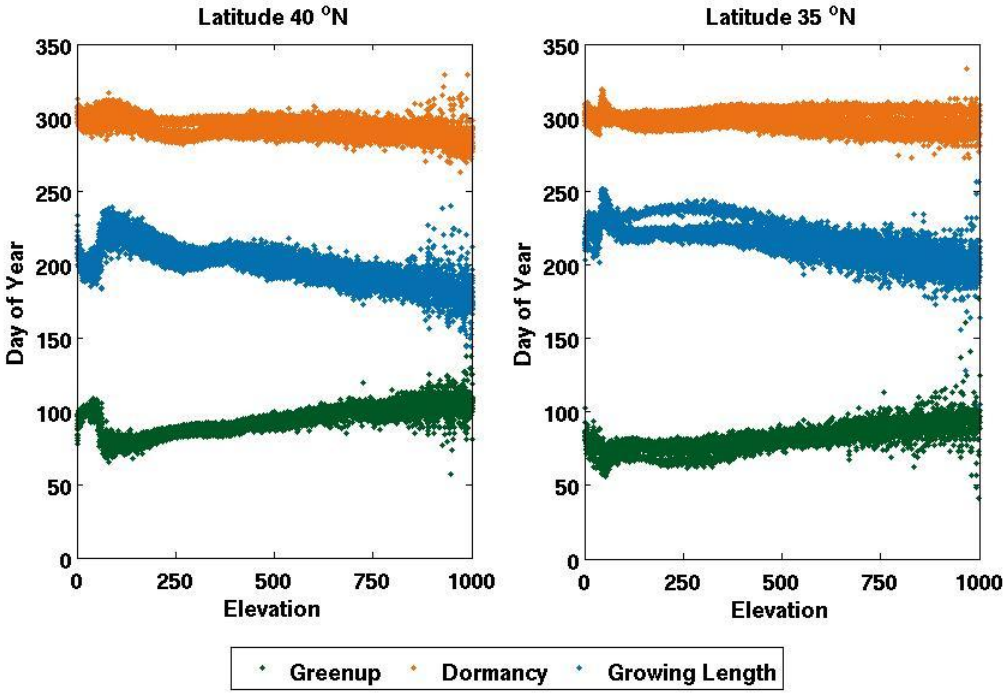

Fig. 4.8 Phenological events timing versus elevation at different latitudes.

4.3 Interannual change of vegetation phenology

Extensive interannual variability in vegetation phenological events is evident in DBF at different latitudes from 2001 to 2007. The greenup onset is temporally variable at higher latitudes (45-50^{0}N) and relatively consistent at middle (35-45^{0}N) and lower latitudes (30-35^{0}N) (Fig. 4.9). An obvious trend of early greenup onset is identified at higher latidudes, especially after the year of 2002. The extent of interannual variability of the dormancy onset is larger at middle and lower latitudes than higher latitudes (Fig. 4.10). The similar interannual trend of the dormancy onset is identified at higher and middle latitudes. For instances, the dormancy onset is relatively late in 2002 and 2005 and relatively early in 2006. The extent of interannual variability of growing length is smaller than that of greenup onset and dormancy onset. There is a presence of slightly longer growing length

in the seven years, especially at higher latitudes (Fig. 4.11). Considering there is no evident prolonged dormancy onset at higher latitude, the longer growing length is mainly contributed by the early greenup onset. While the interannual variability of growing length at middle and lower latitudes are somewhat consistent and similar to the variability trend of dormancy onset.

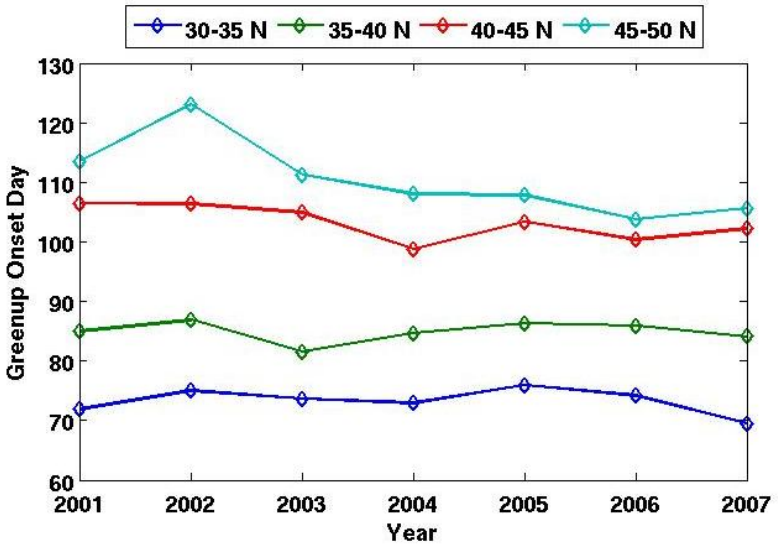

Fig. 4.9 Interannual variability of satellite-derived greeunp onset.

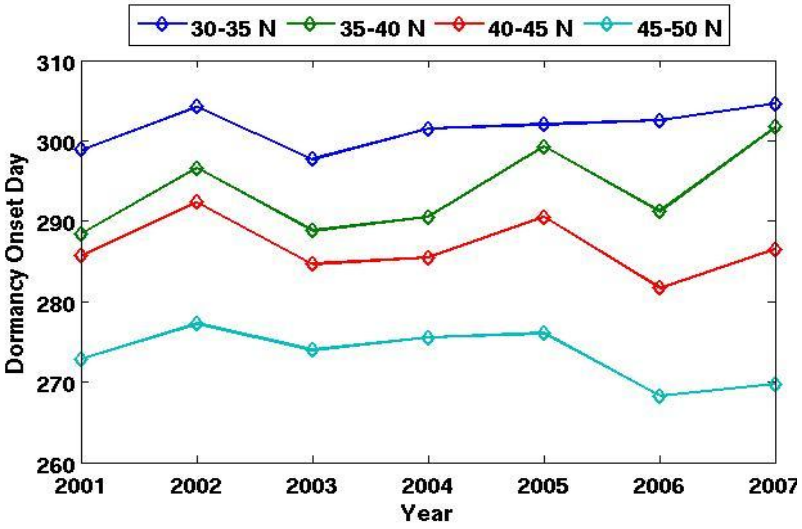

Fig. 4.10 Interannual variability of satellite-derived dormancy onset.

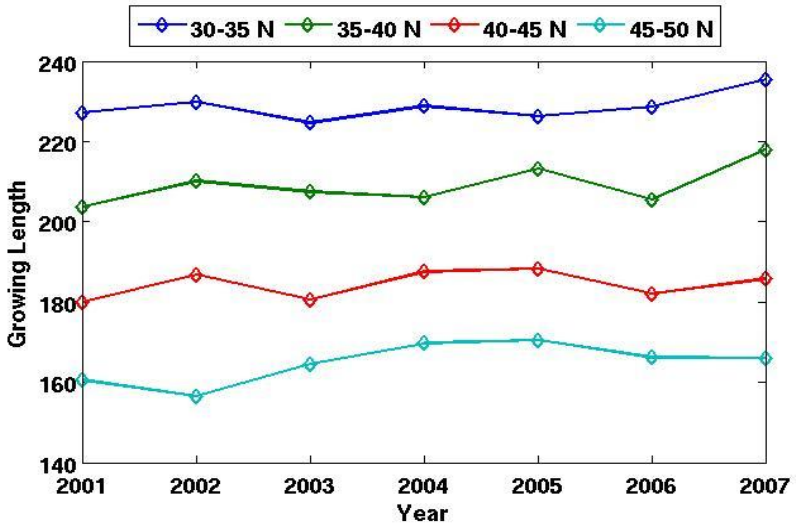

Fig. 4.11 Interannual variability of satellite-derived growing length.

4.4 Summary

The satellite-derived vegetation phenology shows obvious spatial variability and interannual variability. Of course the intricate vegetation phenology depend on the topography of the land as well as many physical, chemical, and biological factors, but the broad geographic patterns are remarkable: When reviewing the series of satellite-derived vegetation phenology, it appears as though that a greenup wave is progressing northward in latitude and upward in elevation, and in reverse, a dormancy wave is progressing southward in latitude and downward in elevation. The presence of growing length is longer in the south and higher elevation. The rate of change is about 2 days per degree latitude or 100 meters elevation for greenup onset. For dormancy onset, the rate of change is about 2 days per degree latitude and 1 day per 100 meters elevation. It is a little different with the Hopkin's Law that the date of first leaf (and other phenophases) is

delayed by approximately 4 days per degree latitude or 120 meters elevation. While the vegetation phenology reflects the sensitivity of phenophases to environmental factors, genetic factors also regulate the timing of phenophases and that the patterns we see in nature are largely the result of interactions between environmental and genetic factors.

The interannual variability of greenup onset is evident at higher latitudes (45-50^{0}N), while the interannual variability of the dormancy onset is larger at middle (35-45^{0}N) and lower latitudes (30-35^{0}N). The extent of interannual variability of growing length is smaller than that of greenup onset and dormancy onset. There is a presence of slightly longer growing length in the seven years, especially at higher latitudes, which is mainly contributed by the early greenup onset.

CHAPTER 5

ASSESSING CLIMATE IMPACTS ON THE VARIATION OF VEGETATION PHENOLOGY

There are two major aspects of phenological variation that are illustrated in Chapter 4, i.e. latitude trend and elevation trend. These phenological changes with latitude and elevation represent strong direct climate regulation of biological activities, typically by temperature. Several facts about changes in temperature have been documented in the 2007 Assessment Report of the Intergovernmental Panel on Climate Change (IPCC - http://www.ipcc.ch/). For instance, global average surface temperatures have increased by 0.74˚C (1.33˚F) during the last 100 years; this is the largest and fastest warming trend in the last millennium. The rate of warming has increased in recent decades. The most recent 50 years have warmed at nearly twice the rate seen in the previous 50 years, and 11 of the last 12 years have been the hottest in recorded history (since 1850). Land surfaces have warmed slightly faster than ocean surfaces, and the greatest rates of surface warming are continually found in mid- to high-latitude continental regions of the Northern Hemisphere. These changes, and many others that are not described here, are largely attributable to the emission of greenhouse gasses into the atmosphere and their continued accumulation, including carbon dioxide (CO_2), methane (CH_4), nitrous oxide

(N_2O), and fluorinated gasses (e.g., hydrofluorocarbons, perfluorocarbons, and sulfur hexafluoride). There is no doubt in the scientific community that human activities such as industrialization, burning of fossil fuels, and deforestation have contributed to increased concentrations of greenhouse gasses and therefore to global climate change.

One direct consequence of global warming is the earlier onset of spring temperatures. Across the entire Northern Hemisphere, spring is arriving earlier at a pace of approximately 1.2 days per decade (Mynenl et al., 1997). Land surfaces are also retaining more heat during the summer, leading to persistent summer temperatures that linger into the fall. Thus, with regard to the temperatures that permit plants to grow, an earlier spring and a persisting summer means that the growing season is expanding (whether plants will receive enough rainfall to take advantage of these warmer temperatures is an unresolved question of great concern). Across Europe, for example, the growing season expanded 10.8 days during the period 1960-1999 (6 days toward an earlier spring, 4.8 days toward a longer-lasting summer) (Menzel and Fabian).

On a spatial scale, many species of plants have expanded their geographic ranges poleward in latitude (northward in the northern hemisphere; southward in the southern hemisphere) and upward in elevation over the last century, following shifting temperatures. As higher elevations experience more mild winters, for example, species from lower elevations may expand their range towards higher elevations because they can now tolerate the winters there. The same may be true across latitudes; species from lower latitudes (i.e., closer to the equator) may expand their range toward higher, or poleward, latitudes. On a temporal scale, at any given location, living plants respond to the

expanding or shifting growing season by changing their phenological schedules. Thousands of biological records spanning both the globe and the 20th century indicate a nearly ubiquitous shift in spring phenology toward earlier calendar dates. Plants are tracking an earlier start to the growing season by developing new leaves and stems earlier. Not surprisingly, similar delays in autumn phenology are occurring due to a persistent summer—deciduous trees are shedding their leaves later than expected.

5.1 Temperature pattern in latitude and elevation over DBF

5.1.1 Satellite temperature data set

MODIS global Land Surface Temperature (LST) (MOD11A2) provides estimates of land surface skin temperature, and is calculated using satellite thermal-infrared measurements for clear-sky pixels with a spatial resolution of 1 km. The LST product provides surface temperature for 8 day time periods by averaging the daily LST measurements (Wan et al., 2002), which is consistent with temporal resolution of the NBAR data. The quality assessment (QA) information from the LST product is used to control the accuracy of LST within 1 ^{o}C. These LST data calculated from MODIS observations are standard and comparable, although they are not equivalent to the near surface air temperature (Huband & Monteith, 1986). MOD11A2 is comprised of day time and night time LSTs. The average of day time and night time LST is used to represent the daily mean temperature. Fig 5.1 illustrates the distribution of mean LST for seven years from 2001 to 2007 for DBF area in the continental U.S.

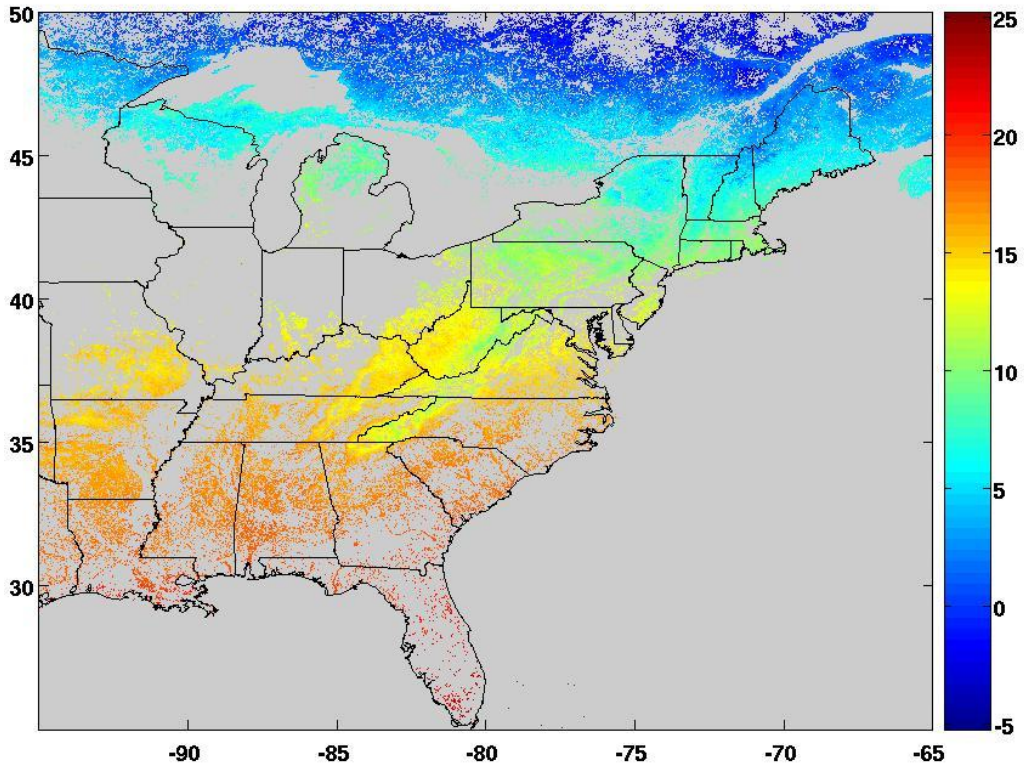

Fig. 5.1 mean LST map for DBF in U.S.. The color legend indicates LST in Celsius.

5.1.2 Variability of temperature in latitude

Solar radiation and duration of day length are important in influencing the distribution of temperature on land surface. The latitude of the location determines how much solar radiation is received and influences the angle of incidence and duration of daylength. Fig 5.1 illustrates the annual mean LST distribution patterns in latitude for DBF from 2001 to 2007. The spatial variations of LST for these seven years have latitudinal patterns. The annual mean LST decrease northward in latitude. The latitude dependent pattern for temperature indicates a potential reason for the spatial pattern of vegetation phenological events. The vegetation phenology has an evident latitude-dependent pattern because of the influence of latitude on temperature. The rate of change in annual mean LST as a

function of latitude indicates that the annual mean LST vary by about 0.95 ^{0}C per degree of latitude.

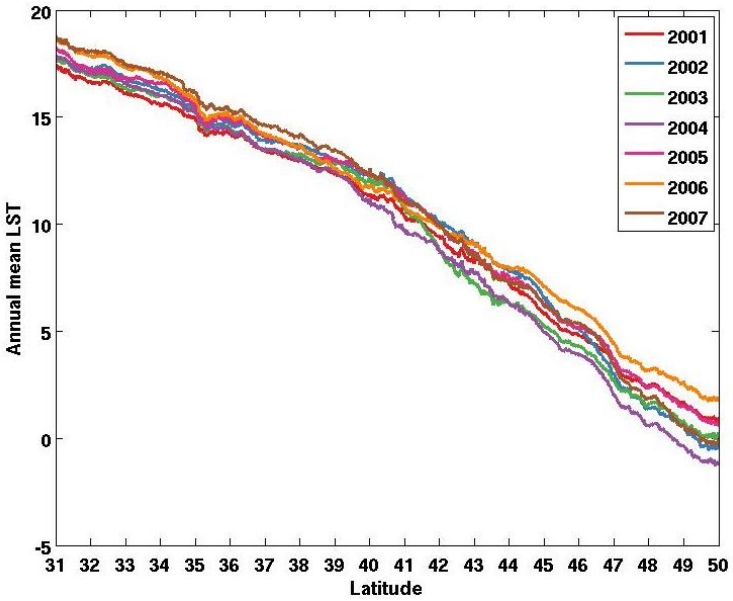

Fig. 5.2 The annual mean LST (^{o}C) in latitude

5.1.3 Variability of temperature in elevation

Fig 5.5 illustrates the annual mean LST distribution patterns in elevation for DBF from 2001 to 2007. The variations of annual mean LST are in two different directions in blow 400 m and higher than 400 m. In the elevation below 400 m, the annual mean LST decrease about 4 ^{0}C per 100 meters, while the annual mean LST increase about 0.8 ^{0}C per 100 meters in elevation higher than 400 m. The more variances appear in annual mean LST, the higher elevation rise than 400 m. It provides the source for the large variances in vegetation phenology in higher elevations as we discussed in Chapter 4. The land surface is strongly heated by solar radiation. The surrounding ambient atmosphere in high elevation is relatively cool because, in the free atmosphere, the temperature decreases by approximately 6.5 ^{0}C per kilometer (the so-called moist adiabatic lapse rate) from the

temperature of the warmed, near-sea level surface. The warm land surface, in contact with the cold atmosphere, transfers sensible heat to the atmosphere, thereby cooling the land surface. That is reason for the drop in LST in elevation lower than 400 m. However, many other factors can contribute to land surface temperature changes. As we discussed in 5.2.2, the annual mean LST drop about1.6 ^{o}C for one degree rise in latitude. So if the rate of change in elevation is smaller than the rate of change in latitude, the LST in higher elevation and lower latitude can be higher than the LST in lower elevation and higher latitude. The urban island effect may be another potential reason for LST rise in elevation higher than 400 m. Zhang et al. (2004) pointed that the mean annual temperature in urban areas is about 1-3 higher relative to rural areas. Fig 4.5 and fig 4.7 illustrated that the high elevation in DBF mostly spread out in the middle of eastern United States. The middle part of eastern Unites Sates contains larger urban area than the northern.

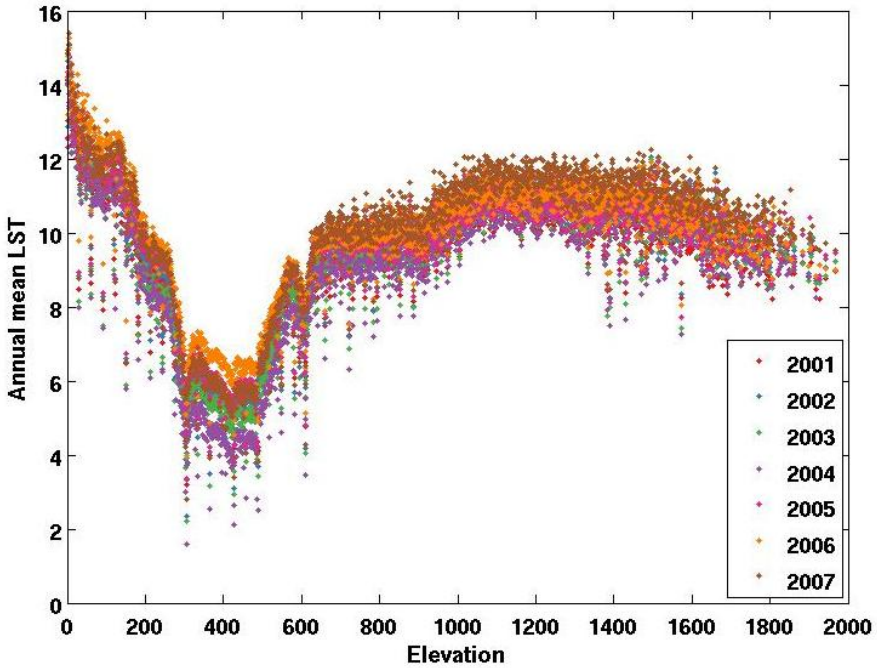

Fig. 5.3 The annual mean LST (^{o}C) in elevation (m)

5.2 Vegetation phenology response to LST change

5.2.1 Dependence of vegetation phenology on LST

The relationship between phenological events and LST is investigated by computing the average timing of the three phenological events, e.g. greenup onset, dormancy onset and growing length, in different annual mean LST. The annual mean LST for DBF over the continental U.S. range from -5 ^{o}C to 25 ^{o}C. The average timing of the greenup onset, dormancy onset and growing length are calculated for each 1 ^{o}C respectively. Fig 5.4, Fig 5.5 and Fig 5.6 illustrate the variation of the average timing of greenup onset, dormancy onset and growing length versus annual mean LST in 1 ^{o}C respectively from 2001 to 2007. The evident LST dependent pattern exists in all these three phenological events for the 7 years. As the annual mean LST rise, the average timing of greenup onset begins earlier, the dormancy onset is delayed and the growing length is prolonged. The average greenup onset progresses from about day 120 in -5 ^{o}C to day 70 in 25 ^{o}C. The dormancy onset regresses from about day 280 in -5 ^{o}C to day to day 310 in 25 ^{o}C. The growing length is prolonged from about 170 days to 300 days. The standard deviation indicates that within 1 ^{o}C, there are about 10-days variation in greenup onset, about 20-days variation in dormancy onset and about 25-days variation in growing length. The smaller standard deviation in greenup onset indicates that the climate regulation implement stronger in greenup onset than dormancy onset.

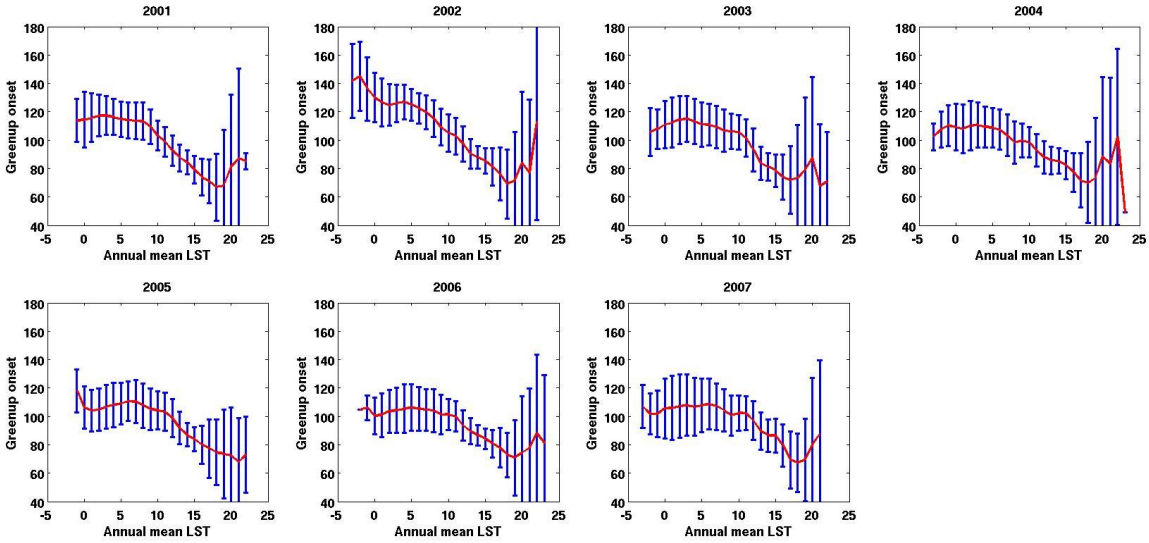

Fig. 5.4 Average greenup onset with standard deviation versus annual mean LST for DBF from 2001 to 2007. The red line is the average greenup onset and the blue bar is the deviation above and below the average.

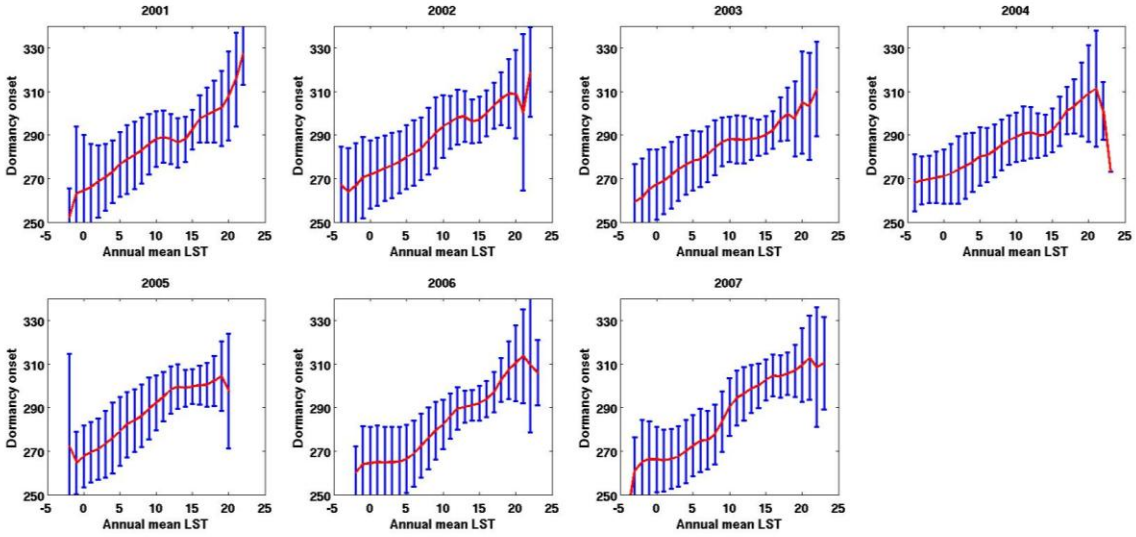

Fig. 5.5 Average dormancy onset with standard deviation versus annual mean LST for DBF from 2001 to 2007. The red line is the average greenup onset and the blue bar is the deviation above and below the average.

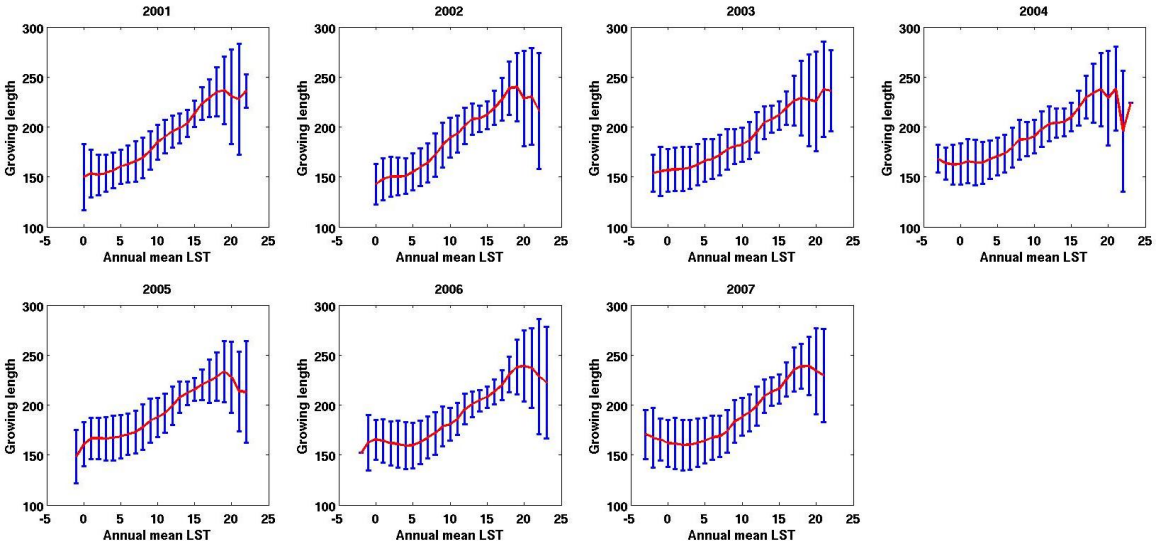

Fig. 5.6 Average growing length with standard deviation versus annual mean LST for DBF from 2001 to 2007. The red line is the average greenup onset and the blue bar is the deviation above and below the average.

5.2.2 Vegetation phenology Models for DBF

The model for greenup onset based on annual mean LST is in the formula (5.1) and the model for dormancy onset and growing length is in the formula (5.2)

$$y(T) = \frac{c}{1 + e^{a+bT}} + d \tag{5.1}$$

$$y(T) = a * x + b \tag{5.2}$$

where the T is the annual mean LST in Celsius, y(T) is the average timing of phenological events, i.e. day of year for greenup onset, dormancy onset and number of days for growing length. The a, b and c are the parameters determined using nonlinear least square fitting.

Fig 5.7, Fig 5.8 and Fig 5.9 illustrate the model simulated results for greenup onset,

dormancy onset and growing length respectively. Table 5.1, Table 5.2 and Table 5.3 list the models in the formula with parameters and the goodness of fit. The high goodness of fit (>0.8) indicates that these models predict the average timing of vegetation phenological events successfully. The greenup onset model suggests that the average greenup onset changes rapidly as the annual mean LST rise up from 10 ^{o}C to 20 ^{o}C. There is an excellent fit of the greenup onset model to satellite observed greenup onset as the annual mean LST lower than 15 ^{o}C. When the annual mean LST is higher than 15 ^{o}C, the capability of greenup onset model is limited because of the high variance in the observed data. The greenup onset model furthermore indicates the interanuual variability of greenup onset under same temperature conditions. The linear model for dormancy onset and growing length indicates that the influence of annual mean LST on these two phenological events is relatively simple. The dormancy onset and growing length shift quickly as the annual mean LST rise up. Interannual variability of average timing of vegetation phenological events under same temperature conditions, suggests that only use of the annual mean LST may not be powerful enough to predict the greenup onset. The average greenup onset, for instance, is close to day 110 in LST of 10 ^{o}C in 2003, but that is about day 100 in 2006. More environmental factors such as latitude, elevation and other biotic factors could be included together to improve the model.

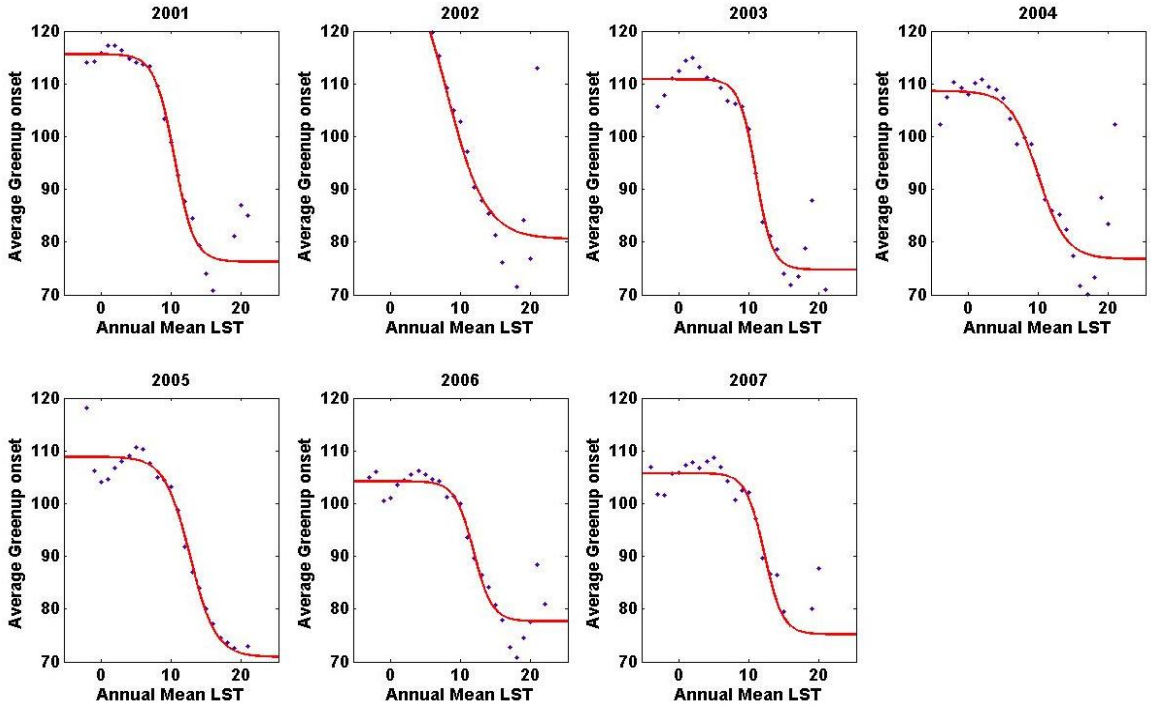

Fig. 5.7 Model simulation of greenup onset. The blue dots are the average greenup onset observed from satellite and the red line represents simulated greenup onset from the model (5.1).

Table 5.1 Greenup onset model based on annual mean LST

Year	Greenup onset Model	Goodness of fit (R-square)
2001	y=39.36/(1+exp(-7.42+0.71*x))+76.25	0.9296
2002	y=55.23/(1+exp(-2.95+0.36*x))+80.54	0.8708
2003	y=36.08/(1+exp(-9.26+0.84*x))+74.76	0.9459
2004	y=31.86/(1+exp(-5.01+0.50*x))+76.78	0.7259
2005	y=37.95/(1+exp(-6.93+0.55*x))+70.91	0.9680
2006	y=26.53/(1+exp(-8.97+0.76*x))+77.67	0.9295
2007	y=30.54/(1+exp(-9.34+0.77*x))+75.21	0.8969

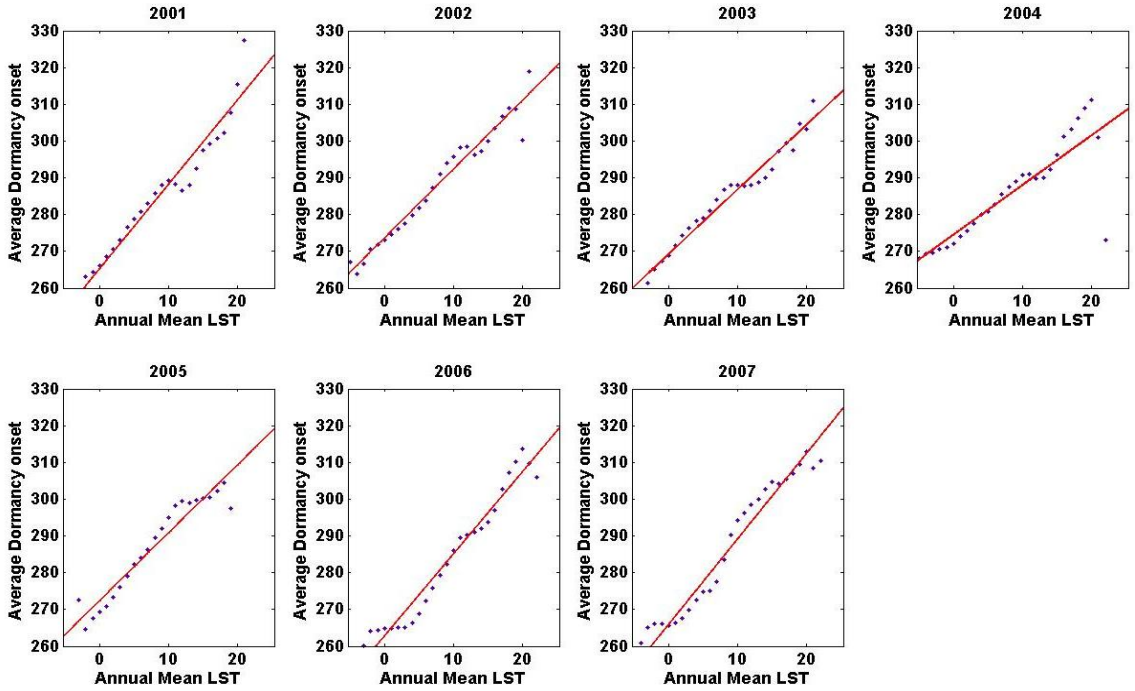

Fig. 5.8 Model simulation of dormancy onset. The blue dots are the average dormancy onset observed from satellite and the red line represents simulated dormancy onset from the model (5.2).

Table 5.2 Dormancy onset model based on annual mean LST

Year	Dormancy onset Model	Goodness of fit (R-square)
2001	y=2.30*x+265.15	0.9385
2002	y=1.87*x+273.58	0.9592
2003	y=1.76*x+269.23	0.9695
2004	y=1.35*x+274.52	0.7172
2005	y=1.85*x+272.30	0.9214
2006	y=2.23*x+262.70	0.9594
2007	y=2.33*x+265.79	0.9464

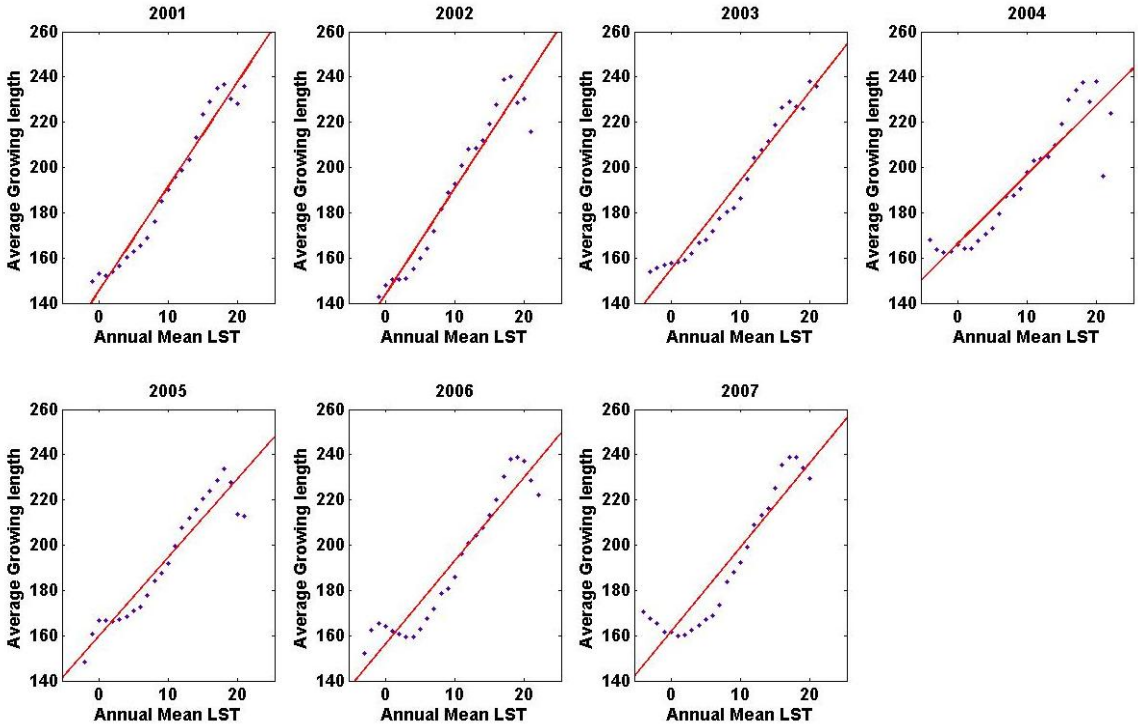

Fig. 5.9 Model simulation of growing length. The blue dots are the average growing length observed from satellite and the red line represents simulated growing length from the model (5.2).

Table 5.3 Growing length model based on annual mean LST

Year	Growing length Model	Goodness of fit (R-square)
2001	y=4.63*x+145.24	0.9600
2002	y=4.71*x+143.64	0.9315
2003	y=3.93*x+154.84	0.9635
2004	y=3.07*x+166.25	0.8471
2005	y=3.48*x+159.63	0.9055
2006	y=3.69*x+156.09	0.9070
2007	y=3.73*x+161.63	0.8677

5.3 Thermal - chilling model

To investigate how global warming might influence dates of vegetation greenup onset in DBF over continental U.S., the thermal-chilling model is applied to satellite-derived greenup onset date. For individual species, various models are available for predicting vegetation greenup. Commonly used models include those based on spring warming, sequential chilling (chilling triggered), thermal-chilling, and photothermal (light triggered) criteria (Sarvas, 1974; Cannell and Smith, 1983; Hunter and Lechowicz, 1992; Kramer, 1994; Linkosalo, 2000). In the thermal-chilling model, vegetation is assumed to respond to increased duration of previous chilling by decreasing the requirements of temperature forcing to initiate spring greenup. This model is appropriate for investigating vegetation greenup at continental scales (Botta et al., 2000). In this framework, growing degree-days (GDD) to greenup onset (budburst) can be expressed as an exponential function of the chilling duration (Cannell & Smith, 1983; Cannell et al.),

$$GDD = \alpha + \beta e^{\gamma CD} \tag{5.3}$$

where GDD is the degree days from a specific date to greenup onset, CD is the chill days counted as the number of days from a given date to the date of greenup onset when the daily temperature is equal to or below the base temperature. α, β, and γ are coefficients estimated using the Levenberg-Marquardt method.

The correct starting date and an appropriate threshold or base temperature for calculating GDD and CD are critical to this model. The starting date is usually chosen in late autumn after leaf senescence, so November 1 is often used to calculate CD and February 1 is commonly used for GDD (e.g. Cannell and Smith, 1983; Hunter and Lechowicz, 1992).

Choosing a temperature threshold between 0 ^{o}C and 5 ^{o}C has little effect on the accuracy of DD calculations (Spano et al., 1999), so 0 ^{o}C is used in this study to calculate the GDD in the following form:

$$\mathrm{GDD(t)} = \sum_{\mathrm{Feb1}}^{\mathrm{t}} \mathrm{Max(T, 0)} \tag{5.4}$$

where t is the greenup onset date, T is the daily LST on those days. Chill days are counted as the number of days from November 1 to the date of greenup onset when the daily LST is equal to or below 0 ^{o}C. The LST is an 8-day composite product, the degree days and chill day will be multiply by 8 when one LST meets the requirements. The results show that the thermal-chilling models can explain more than 80% of the variation in the GDD required for greenup onset (Fig. 5.10; Table 5.4).

According to established thermal-chilling models, the duration of chilling should decrease as a result of climate warming, and in turn, the thermal time required for greenup onset should increase. Thus, global warming may act to delay or advance forest greenup onset, depending on the extent to which the chilling and thermal time requirements are currently met. The established models show that the minimum requirement for GDD in DBF is 130 ^{o}C. When CD is larger than about 60 days, GDD mainly fluctuates within 130 ± 20 ^{o}C. In these regions, chilling requirements are far exceeded. Therefore, any decrease in chilling days caused by global warming will have little or no effect on GDD, and greenup onset should advance with climate warming. In contrast, in the regions where GDD decreases rapidly with increasing CD, the chilling requirements are nearly exactly sufficient at present and slight reductions in CD may

result in a large increase in thermal time requirements. Climate warming should therefore cause an increase in GDD requirements, so that advances in greenup onset will be limited or even inverted. This type of pattern is similar to the species level results described by Cannell & Smith (1986) in the Scottish uplands. Moreover, this finding is also supported by observed trends in the onset of spring in recent decades inferred from Bowen ratio data in the Eastern United States (Fitzjarrald et al., 2001). Specifically, the results described by Fitzjarrald et al. (2001) show that spring dates advanced by 6–8 days in northeastern areas, and that the amount of change decreased towards the south where spring actually occurred later in southern areas of Virginia and the Carolinas.

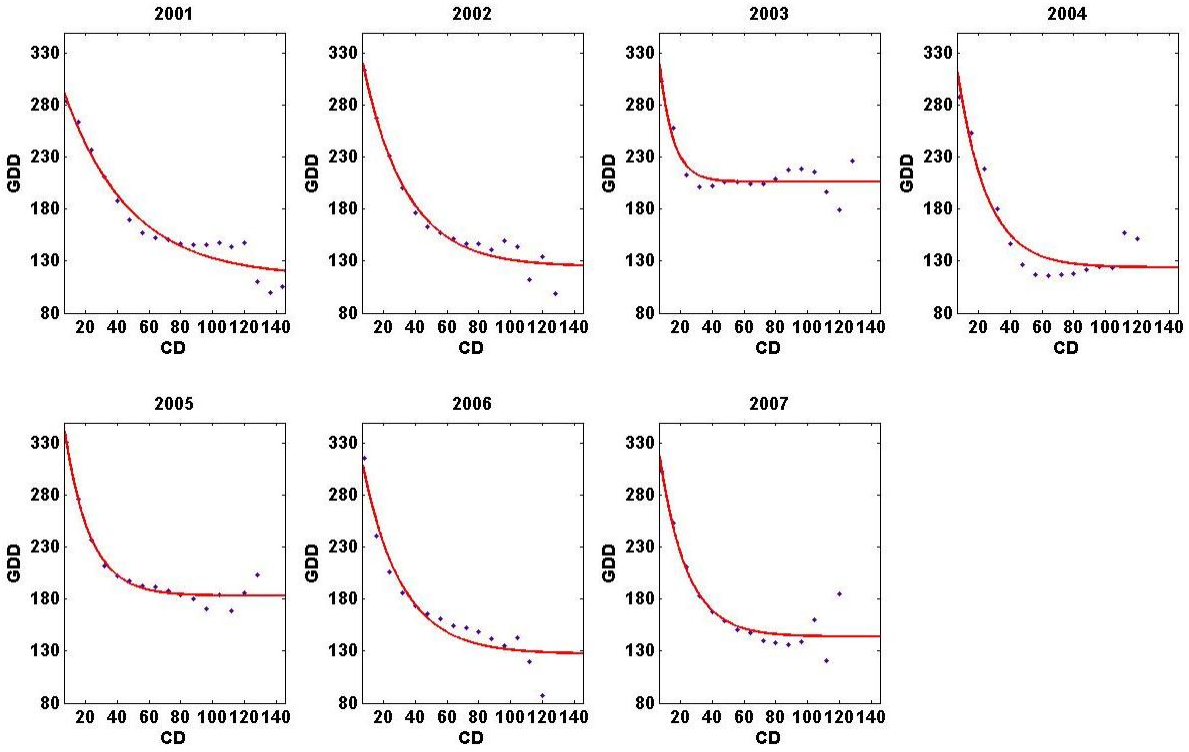

Fig. 5.10 Relationship between the number of chill days with daily LST < 0 ^{o}C from November 1 to the greenup onset date and growing degree days > 0 ^{o}C from February 1 to the greenup onset for DBF over the continental U.S. from 2001 to 2007. The fitted line (red) is described by equation (5.3) and the parameters and the goodness of fit are given in Table 5.4

Table 5.4 The thermal-Chilling model

Year	Thermal - Chilling Model	Goodness of fit (R-square)
2001	GDD=114.73+210.54*exp(-0.02*CD))	0.9445
2002	GDD =124.54+252.97*exp(-0.04* CD))	0.9627
2003	GDD =206.42+257.03*exp(-0.12* CD))	0.8339
2004	GDD =123.91+275.06*exp(-0.05* CD))	0.9040
2005	GDD =194.15+263.90*exp(-0.08* CD))	0.9677
2006	GDD =127.22+242.72*exp(-0.04* CD))	0.9247
2007	GDD =143.93+261.15*exp(-0.06* CD))	0.9184

5.4 Summary

This chapter investigates the climate influence on vegetation phenological process. The climate regulation of vegetation phenology is expressed as following:

(1) The annual mean LST decrease northward in latitude provide a potential reason for the latitude-dependent pattern of phenological events. The rate of change in annual mean LST as a function of latitude indicates that the annual mean LST vary by about 0.95 ^{0}C per degree of latitude.

(2) The variations of annual mean LST are in two different directions in blow 400 m and higher than 400 m. In the elevation below 400 m, the annual mean LST decrease about 4 ^{0}C per 100 meters, while the annual mean LST increase about 0.8 ^{0}C per 100 meters in elevation higher than 400 m.

(3) As the annual mean LST rise, the average timing of greenup onset begins earlier, the dormancy onset is delayed and the growing length is prolonged. The high goodness of fit (>0.8) indicates that the model based on annual mean LST predict the average timing of

vegetation phenological events successfully. The greenup onset model suggests that the average greenup onset changes rapidly as the annual mean LST rise up from 10 ^{o}C to 20 ^{o}C. The average dormancy onset shifts quickly as the annual mean LST rise. The growing length is also ensitive to annual mean LST.

(4) To investigate how global warming might influence dates of vegetation greenup onset in DBF over continental U.S., the thermal-chilling model is applied to satellite-derived greenup onset date. The results show that the thermal-chilling models can explain more than 80% of the variation in the GDD required for greenup onset. Global warming may advance forest greenup onset when the chilling requirements are far exceeded and may delay greenup onset when the chilling requirements are nearly exactly sufficient.

CHAPTER 6

COMPARING SATELLITE-BASED VEGETATION PHENOLOGY WITH ECOREGION MODEL SIMULATIONS

The variability of vegetation phenological phases and its relationship to latitude, elevation and climate factors has been documented in chapter 4 and 5. As the previous discussion, the latitude, elevation-dependent pattern and climate regulation are evident in vegetation phenological variability, there is although variance in some regions. Environmental factors are important in controlling the vegetation growth. However, biotic factors cannot be ignored. The same biota can spread out large areas which may cover several degrees of latitude and hundreds meters of elevation. The temperature condition in the same biota can vary greatly. But the genes inherited by the same biota tend to have similar response to the environmental change. The vegetation phenological variability is often determined by interactions between the genes that affect the phenological trait and the environment in which they are expressed. Unfortunately, at large scales, biotic factors would be very difficult to model. One alternative way is to use the ecoregion to represent the biotic trait. An ecoregion is an ecologically and geographically defined area that contains characteristic, geographically distinct

assemblages of natural species. The biodiversity of flora, fauna and ecosystems that characterize an ecoregion tends to be distinct from that of other ecoregions.

Despite being geographically small regions of the United Sates, the DBF possess variety of ecoregions. Rainfall varies from over 50 inches annually in some coastal areas, to 32 inches in the western part of Pennsylvania and New York. Snowfall can range from over 100 inches per year in Upstate New York to only a foot or so in the coastal areas of southern New Jersey (MacDonald, 2002). In this study, we use Ecoregions defined by the World Wildlife Fund (WWF) (Olson et al., 2001). The ecoregions, representing distinct biotas, are nested within the biomes and realms and together, these provide a framework for comparisons among units and the identification of representative habitats and species assemblages. The ecoregions are built on the foundations of classical biogeography and reflect extensive collaboration with over 1000 biogeographers, taxonomists, conservation biologists, and ecologists from around the world. The sources for the ecoregions, technical descriptions and digital data are available at the Web site: http://www.worldwildlife.org/science. The map was downloaded in GIS database and reprojected to the Sinusoidal projection and matched to MODIS products using MATLAB. DBF was spatially partitioned according to the ecoregions map and eight ecoregions were identified. The WWF ECO_ID that we use throughout this study consists of five numbers: one number for real code + two numbers for biome code + two numbers for specific ecoregion code. These ecoregions (Fig 6.1) occur in one realm: Nearctic (code = 5) and two biomes: temperate broadleaf and mixed forest (code = 04) and temperate conifer forest (code = 05). The eight ecoregions are: Allegheny Highlands

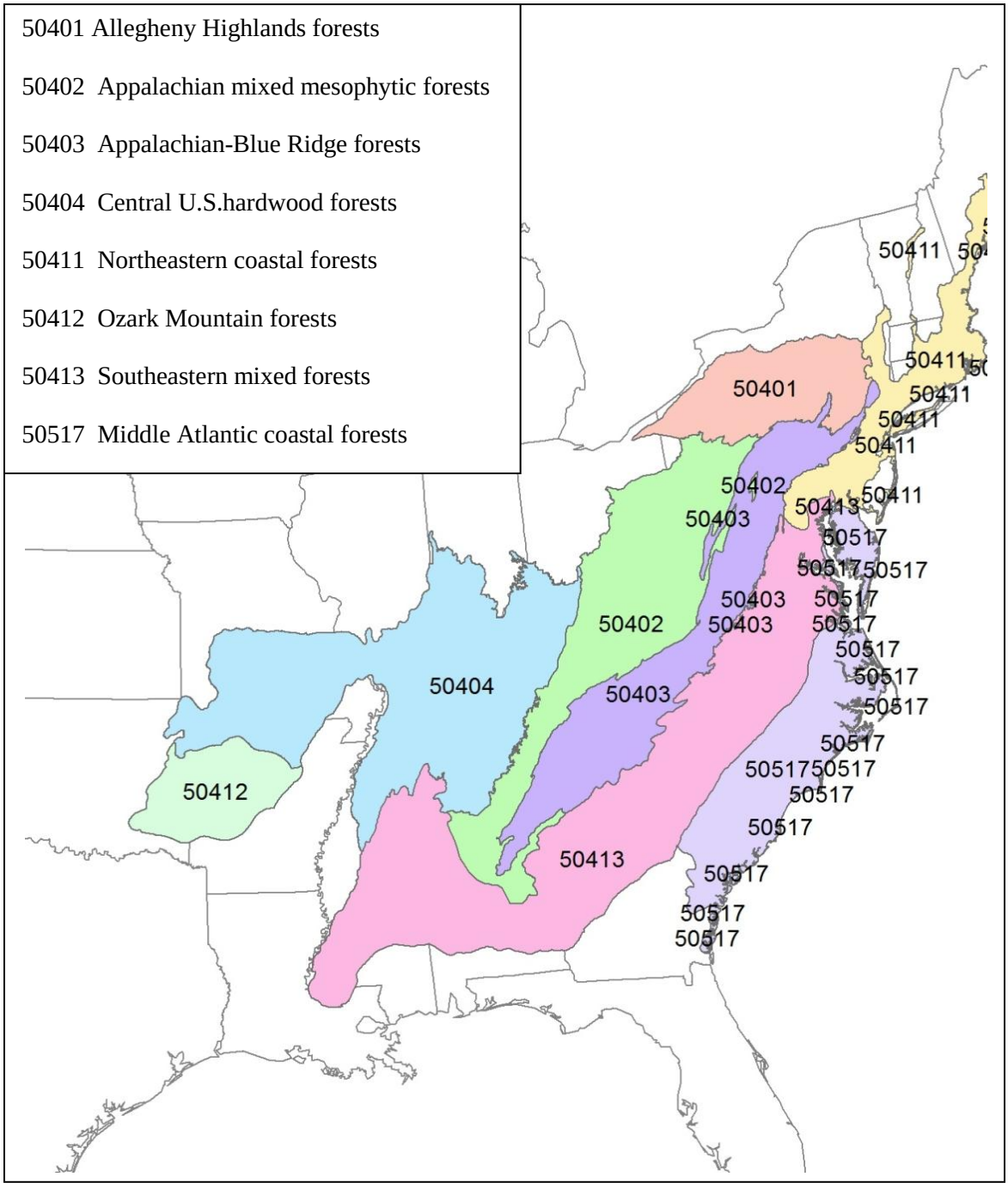

Fig. 6.1. The map of ecoregions in DBF

forests (AHF, code = 01, ECO_ID = 50401), Appalachian mixed mesophytic forests (AMF, code = 02, ECO_ID = 50402), Appalachian-Blue Ridge forests (ARF, code = 03, ECO_ID = 50403), Central U.S. hardwood forests (CHF, code = 04, ECO_ID = 50404), Northeastern coastal forests (NCF, code = 11, ECO_ID = 50411), Ozark Mountain forests (OMF, code = 12, ECO_ID = 50412), Southeastern mixed forests (SMF, code = 13, ECO_ID = 50413), and Middle Atlantic coastal forests (MACF, code = 17, ECO_ID = 50517). Among the vegetation phenological phases, greenup onset is most sensitive to the biotic factors. So in this study, models for greenup onset are established for these ecoregions.

6.1 Variability of greenup onset in ecoregions

For each ecoregion in DBF, we calculated the average greenup onset day from year 2001 to 2007 (Fig.6.2). According to the sequence of greenup onset, these eight ecoregions can be divided into three groups. The first group is the early greenup onset group, which include SMF 50413, MACF 50517, OMF 50412 and CHF 50404. For most years, the average greenup onset day for these four ecoregions is no later than day 85. Following the first group, the greenup onset occurs in the second group which includes AMF 50402 and ARF 50403. The average greenup onset is between day 85 and day 95 for most years. The last group consists of NCF 50411 and AHF 50401. The average greenup onset for the last group is later than day 95 for most years. We notice that the ecoregions in the same group are not geographically related and the latitude range of the ecoregions is vary

greatly, Therefore, in somewhat degree, the obvious sequence of greenup onset in different ecoregions reflects the controlling of the biotic factors on phenological process.

To further investigate the trait of ecoregions, the greenup onset averaged by seven years for these ecoregions in latitude is illustrated in Fig 6.3. The northward progressing pattern exists in these ecoregions, except AHF 5040. The latitude range of each ecoregion is visible in Fig 6.3. Except NCF 50411 and AHF 5040, other six ecoregions coexist between the latitude of 34^0N and 39^0N. The greenup onset is still progressing from the first group to the second group in this range of latitude. It demonstrated again that the biotic trait of the second group is distinguished from the first group. In the first group, there is no stable sequence in greenup onset among the ecoregions. In the second group, the greenup onset of ARF 50403 is earlier than AMF 50402 in most latitude. Considering the same environmental conditions in ARF 50403 and AMF 50402, the different phenological phases are caused by biotic factors. In higher latitude, NCF 50411 in the third group tends to greenup earlier than the second group. Since NCF 50411 distributes in higher latitude than the second group, it is indicated that the late greenup of NCF 50411 showed in Fig 6.2 is contributed mostly by environmental factors. In the third group, the greenup onset of AHF 50401 always occur latter than NCF 50411. The abnormally northward progressing pattern in AHF 50401 suggested that the trait of AHF 50401 should be distinct from other ecoregions. In a summary, the ecoregion effect on phenological process is demonstrated by the relatively stable sequence of greenup onset in different years and the different sequence of greenup onset in same latitude.

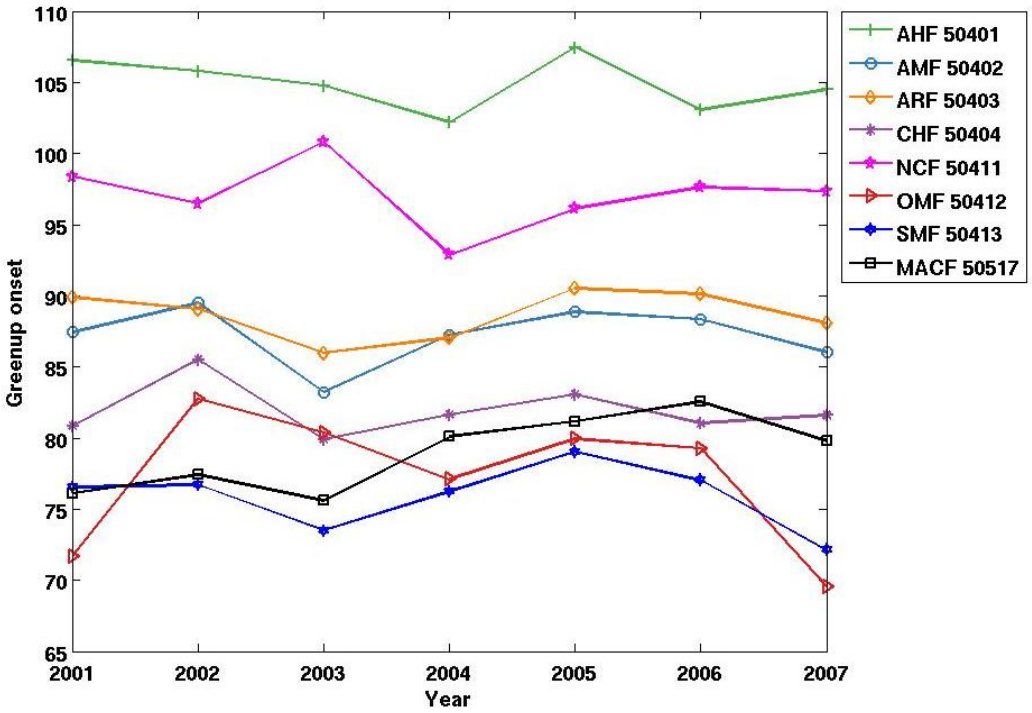

Fig. 6.2 The Greenup onset day for eight ecoregions from year 2001 to 2007

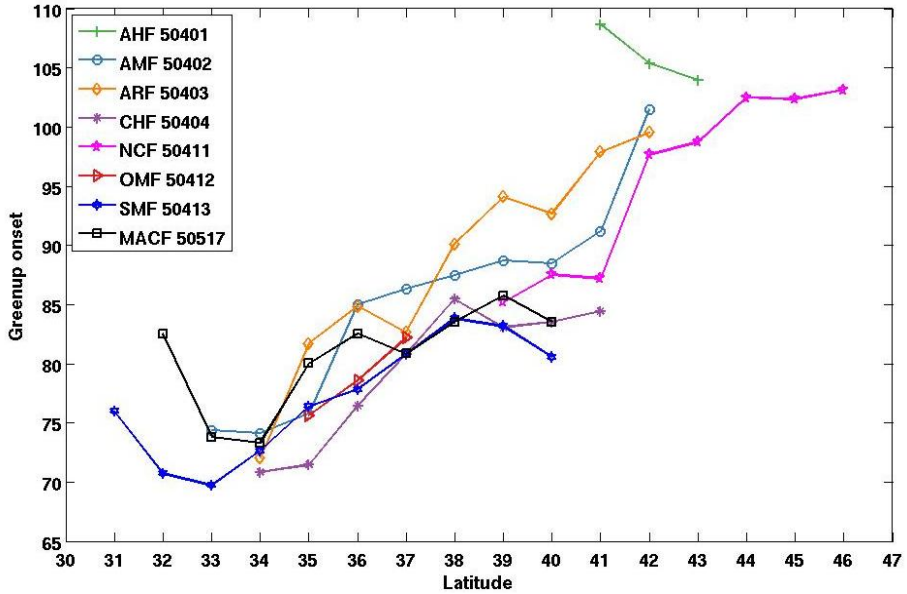

Fig. 6.3 The average greenup onset for ecoregions in latitude

6.2 The environmental conditions in ecoregions

The environmental condition of each region is introduced by the interaction between latitude and elevation. The interaction results in the variability of temperature and further controls the vegetation phenological phases. Fig 6.4, Fig 6.5 and Fig 6.6 illustrates the elevation, annual mean LST and average greenup onset in latitude in each ecoregion respectively. As we discussed before, the late greenup onset associates with the increasing in latitude, the rising in elevation, and the decreasing in LST. The early greenup onset associates with the decreasing in latitude, the drop in elevation and the increasing in LST. So the increasing in latitude, the rising in elevation, and the decreasing in LST is defined as "deferred effect". The decreasing in latitude, the drop in elevation, and the increasing in LST is defined as "advanced effect". For each ecoregion, the interaction between deferred effect and advanced effect on greenup onset would be investigated as following.

The AHF 50401, across latitude from 41^0N to 43^0N, covers a relatively small area. The greenup onset moves earlier with latitude increasing from 41^0N to 43^0N. However, there is a deferred effected in latitude and annual mean LST. The only advanced effect appears in elevation with latitude increasing from 42^0N to 43^0N. So the environmental factors will not be included in the greenup onset model for AHF 50401.

The AMF 50402 has a large range from the latitude of 32^0N to 42^0N. The greenup onset moves late with latitude increasing from 32^0N to 42^0N. It is the result of deferred effects in latitude, elevation and LST together. The advanced effect only appears in elevation with latitude from 37^0N to 39^0N, so the greenup onset are relatively invariable in that

region. The environmental factors should be considered in modeling greenup onset of AMF 50402.

The ARF 50403 covers similar latitude range with the AMF 50402. The greenup onset moves gradually late with latitude increasing from 33^0N to 42^0N. This trend is consistent with the function of the deferred effects in latitude, elevation and annual mean LST. However, the advanced effect of elevation with the latitude from 38^0N to 42^0N makes the rate of change very small in that area. So the environmental factors would be included in the model of ARF 50403 for greenup onset.

The range of the CHF 50404 is from the latitude of 34^0N to 40^0N. The trend of the greenup onset is more consistent with the effect of elevation. As the elevation rise, the greenup onset is deferred and as the elevation drop, the greenup onset is advanced. The effect of annual mean LST is not obvious in the variability of greenup onset. The elevation and latitude factors should be concerned in modeling greenup onset for the CHF 50404.

The NCF 50411 is located in the north coastal area across the latitude from 39^0N to 45^0N. The greenup onset progresses northward in latitude. There is no evident deferred or advanced effect in elevation and annual mean LST. The environmental factors are not important to model the greenup onset for the NCF 50411.

The OMF 50412 is another small ecoregion across latitude from 34^0N to 36^0N. The variation of greenup onset along latitude is almost same with the variation of elevation along latitude. The potential reason is that in the small region, the extent of elevation change is much greater than that of latitude change. So elevation becomes the dominant

factor controlling the phenological phases, the environmental factors will be used to model greenup onset for the OMF 50412.

The SMF 50413 is located in the southeast across latitude from 30^0N to 40^0N. The greenup onset progresses northward in this ecoregion. This is the result of the deferred effect in latitude and elevation. Although there is an advanced effect in elevation with latitude from 36^0N to 38^0N, the extent of elevation change is relatively small. So the effect is not obvious on greenup onset. The environmental factors will not be concerned in modeling greenup onset for the SMF 50413.

The MACF 50517 is located in the middle coastal area and in a different biome from other ecoregions. Other ecoregions are all in the biome of temperate broadleaf and mixed forest and only the MACF 50517 is in the biome of temperate conifer forest. There is no obvious latitude-dependent pattern in the greenup onset and no any effect is observed in elevation and annual mean LST. The environmental factors are not very important roles in modeling greenup onset for the MACF 50517.

In a summary, the eight ecoregions can be divided into two groups according to the effect of environmental factors on greenup onset. The first group, defined as "habitat-controlled group", includes AMF 50402, ARF 50403, CHF 50404, and OMF 50412, in which the environmental factors (latitude and elevation) have an evident effect on greenup onset. The second group, defined as "temperature-controlled group", includes AHF 50401, NCF 50411, SMF 50413, and MACF 50517, in which the effect of environmental factors cannot be identified distinctly and the greenup onset is influenced mainly by the temperature.

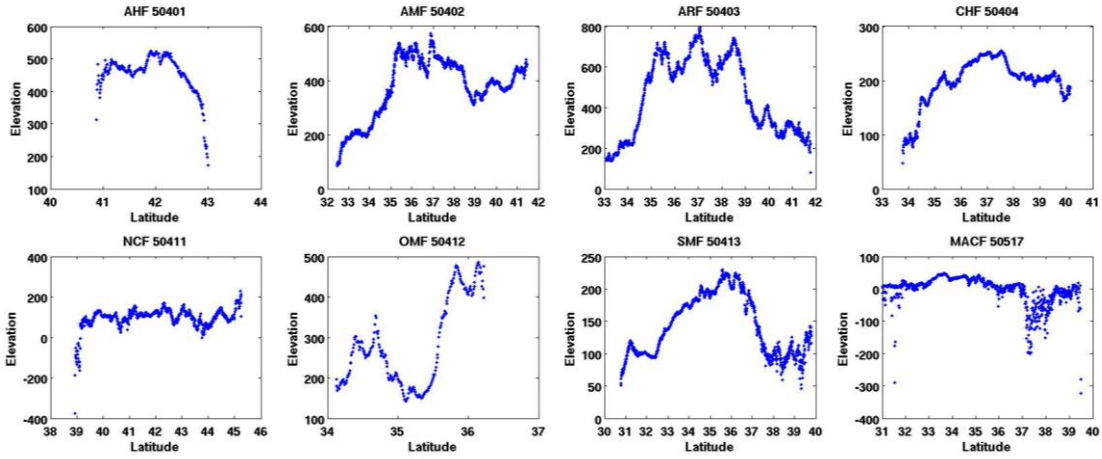

Fig. 6.4 The average elevation in latitude in each ecoregion

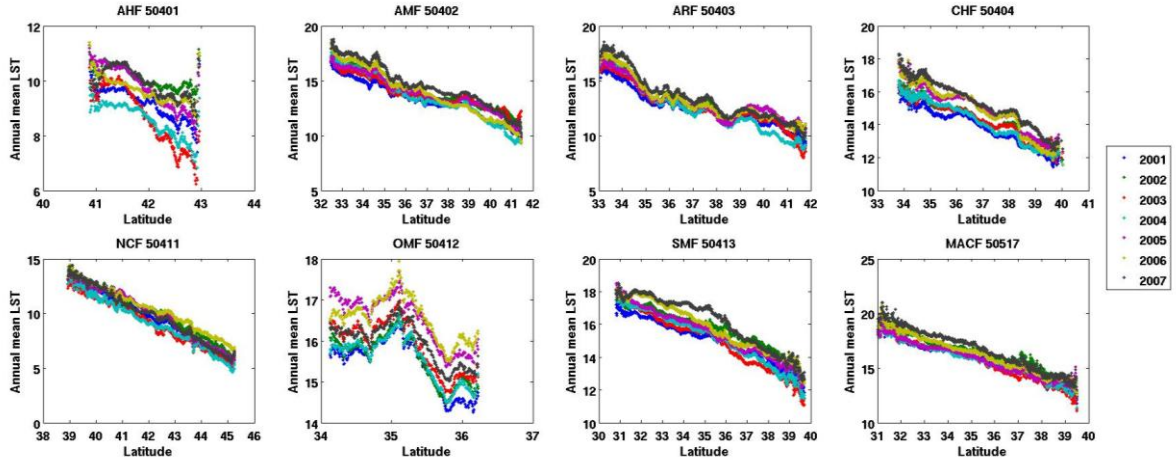

Fig. 6.5 The annual mean LST in latitude in each ecoregion

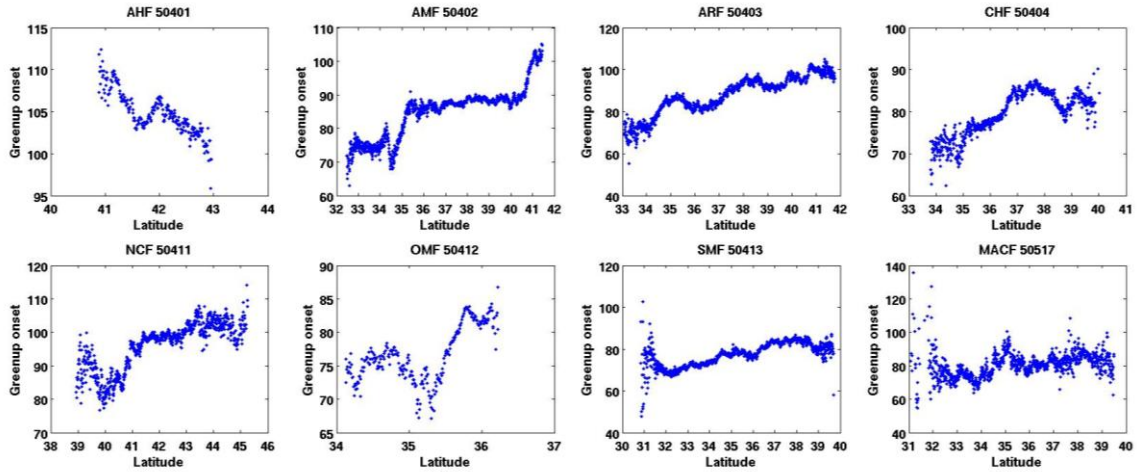

Fig. 6.6 The average greenup onset in latitude in each ecoregion

6.3 Ecoregion-based models

The physiological processes involved in triggering greenup onset are still not fully understood. Models ordinary use one of two approaches. A few studies have compute greenup onset based on the optimization of resources (Kindermann et al., 1993; Kikuzawa, 1995), but most adopt an empirical approach using bioclimatic factors to define the climate factors that limit greenup onset (e.g. drought, light, or frost). We follow the second approach as being the more common in the literature. The first step is the identification of limiting factors for greenup onset for each ecoregion. Temperate deciduous forest is the most studied biome. Several models of greenup onset date based on temperature have been developed. Earlier works have assumed that the parameters controlling bud development are related linearly to temperature. For instance, leaf onset occurs when the sum of average daily temperature above a given threshold, accumulated from a starting date reaches a prescribed value. Later experiments have identified the need to incorporate other factors such as light and chilling conditions, which influence the temperature dependency of greenup onset (Vegis 1964; Garber 1983). Some models have determined the thermal control on greenup onset using the duration of the photoperiod, since longer days promote the onset of vegetation (Nizinski and Saugier, 1988), and different strategies have been developed to introduce chilling requirements (Cannell and Smith 1986; Hari and Häkkinen 1991; Häkkinen 1994).when applied in a range of sites, however, more sophisticated models do not necessary produce better results (Hunter and Lechowicz 1992).

Very few studies have been carried out on greenup onset at ecoregion levels. Since the unique characteristics of each ecoregion, the models for entire temperate deciduous forest should be adapted according to the trait of each ecoregion. Overall, we have established two models to apply to the different ecoregions. Model 1 is suitable for the "habitat-controlled group" and model 2 is for the "temperature-controlled group".

Model 1: The effect of temperature on greenup onset is estimated using "growing degree days" (GDD). We sum the daily mean LST above an arbitrary threshold (Tth = -5 ^{o}C or 0 ^{o}C, according to the ecoregion) for a fixed period of time (N = 30 or 40 days). Greenup onset occurs when GDD reaches a critical value (GDD_c). In this model, GDD_c varies with the latitude and elevation. The parameters (a and b) are determined with the following equations:

$$GDD(t) = \sum_{t-N}^{t} Max(T - T_{th}, 0) \text{ and } GDD(t) \geq GDD_c \quad (6.1)$$

$$GDD_c = a * Latitude + b * Elevation + c \quad (6.2)$$

Model 2: This model combines heat and chill requirements assuming that an increase in chilling days reduces the plant's GDD demand (Cannell and Smith 1986; Murray et al., 1989). A chilling day has a daily mean temperature below a particular threshold (T_{th} = 0 ^{o}C or 5 ^{o}C depending on the ecoregion). We use the method of Murray et al. (1989), starting summation from fixed dates: November for the number of chilling days (CD_{Nov}) to cover the major part of the dormant period, and January 1 for growing degree days (GDD_{Jan}). In this study, the cool ecoregions are limited in the high latitude, the use of fixed dates is then possible. The greenup onset occurs when the observed GDD_{Jan} exceeds

a critical value, which is an exponential function of CD_{Nov}. We thus have to determine three parameters (a, b, and c), according to the following equations:

$$GDD_{Jan}(t) = \sum_{Jan1}^{t} Max(T - T_{th}, 0) \quad (6.3)$$

and $GDD_{Jan}(t) \geq a + b * e^{(c*CD_{Nov}(t))}$ with c < 0 (6.4)

For each ecoregion, we used satellite leaf onset dates and LST data to retrieve the observed spatial distribution of the model parameters. We plot the variables for all pixels belonging to the ecoregion, and apply a least-square fit regression. We reject the model if r-square is lower than 0.5, to ensure that the relationship reproduces at least 50% of the variability of the observed signal.

6.4 Results

6.4.1 The Model for each ecoregion

The parameters are determined by running the model for each ecoregion from 2001 to 2003. Distinct ecoregions may have identical parameterizations. Table 6.1 shows the T_{th} and the average GDD_c plus/minus standard deviation in model 1 for the ecoregions: AMF 50402, ARF 50403, CHF 50404, and OMF 50412. Model 1 appears to predict the greenup onset date using arbitrary thresholds of -5 ^{0}C for AMF 50402 and ARF 50403, and 0 ^{0}C for CHF 50404 and OMF 50412. The thresholds for GDD vary more than 100 degree days in the same ecoregion. The GDD_c for CHF 50404 and OMF 50412 is relatively larger than AMF 50402 and ARF 50403. It indicates that the thermal requirements of CHF 50404 and OMF 50412 are higher than AMF 50402 and ARF

50403. The parameters for model 2 are showed in table 6.2. The thermal threshold for AHF 50401 and NCF 50411 is lower than SMF 50413 and MACF 50517. The parameters a, b, and c are showed as the average value plus/minus standard deviation. The greenup onset date for each pixel in the ecoregion is determined by the exponential model with these parameters.

Table 6.1 The value for model 1

Ecoregion	T_{th} (^{0}C)	GDD_c (degree days)
AMF 50402	-5	242 ± 128
ARF 50403	-5	255 ± 140
CHF 50404	0	286 ± 130
OMF 50412	0	392 ± 152

Table 6.2 The value for model 2

Ecoregion	T_{th} (^{0}C)	a	b	c
AHF 50401	0	126 ± 20	126 ±17	-0.02 ± 0.01
NCF 50411	0	247 ± 50	249 ± 43	-0.03 ± 0.02
SMF 50413	5	243 ± 38	282 ± 33	-0.01 ± 0.009
MACF 50517	5	194 ± 60	108 ± 44	-0.01 ± 0.01

6.4.2 Spatial goodness of fit of the models

The quality of the fit is determined after running the different model in each ecoregion for the year of 2007. Two statistical criteria correlation coefficient (ρ) and root mean square (RMS) between satellite-observed and model simulated greenup onset are used to evaluate the results. The percentage of pixels (PP) which are successfully simulated by

model in each ecoregion is also illustrated (Table 6.3). In general, model 1 has lower RMS than model2. The vegetation greenup onset date of habitat-controlled ecoregions is simulated by model 1 between 8 to 9 days, compared with 7 to 17 days for temperature-controlled ecoregions simulated by model 2. However, ρ can be equally high in both models. Figure 6.7 illustrates this apparent paradox, by showing satellite observed vs. model simulated greenup onset dates for each ecoregion. The range of greenup onset in MACF 50517 is clearly much larger than the range of greenup onset in AMF 50402. Thus, MACF 50517 can show a higher ρ despite a quite large RMS. Therefore, ρ is not a good estimator of model reliability for ecoregions like AMF 50402, which have a narrow range of greenup onset. Furthermore, the distributions around 1:1 line indicate that the models tend to underestimate the late greenup onset date, especially in the ecoregions of AHF 50401, AMF 50402, ARF 50403, and MACF 50517.

Table 6.3 Results of model simulation

Model	Ecoregion	ρ	RMS	PP (%)
Model 1	AMF 50402	0.75	8.13	78
	ARF 50403	0.77	8.42	84
	CHF 50404	0.81	9.14	77
	OMF 50412	0.81	9.66	76
Model 2	AHF 50401	0.76	7.76	65
	NCF 50411	0.82	10.88	77
	SMF 50413	0.83	9.11	61
	MACF 50517	0.81	17.34	52

In general, the models simulate greenup onset dates for each ecoregion realistically. The primary spatial gradients, including the latitude gradient and the elevation gradient are well presented (Fig 6.8). Fig. 6.9 exhibits the difference between the model simulated and the satellite retrieved greenup onset dates. The difference is not computed where the model is unable to simulate the greenup onset date. As shown in Table 6.3, the percentage of pixels (70%-80%) simulated by model 1 is higher, compared to the 50%-70% of pixels simulated by model 2. The model 2 fails to simulate nearly half pixels in the MACF 50517 and the ARF 50403 has the most successful model simulated pixels. The results for each ecoregion depend on the scatter of fitted parameters and the nonlinearity models. For example, CHF 50404, OMF 50412, and SMF 50413 are well represented, in which the differences of most areas are near zero compared to the satellite observations. Areas below the 1:1 line in Fig 6.7 have an early simulated greenup onset date with respect to the satellite observations, and areas above the 1:1 line have a late simulated greenup onset date. The early simulated greenup onset dates appear more in the south region of AMF 50402 and ARF 50403. The late simulated greenup onset dates in the south of SMF 50413, and the north of AHF 50401.

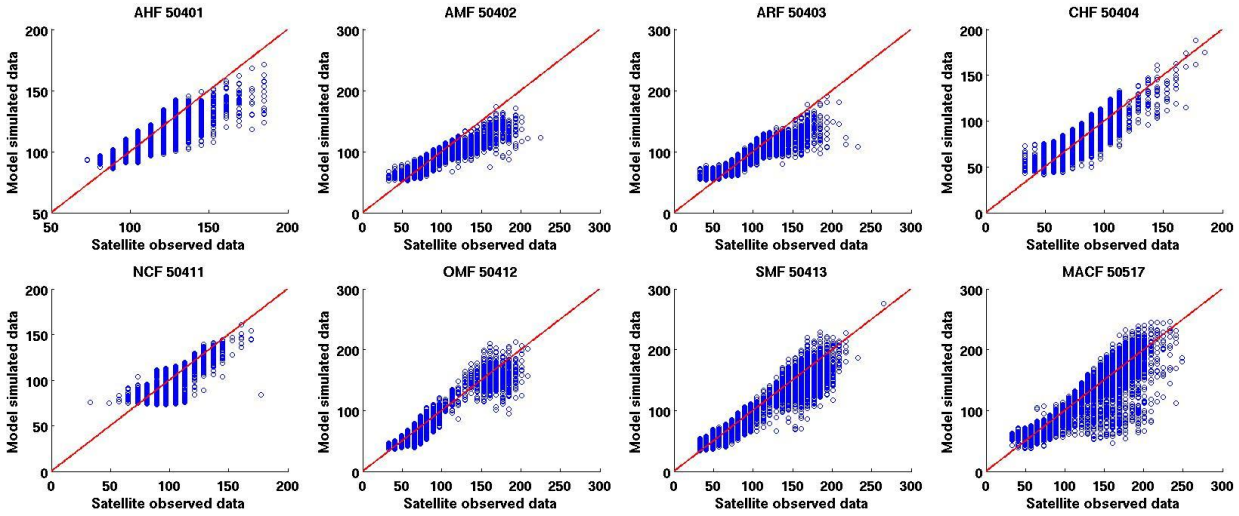

Fig. 6.7 Satellite observed vs. model simulated greenup onset dates for eight ecoregions. The red line is the 1:1 line

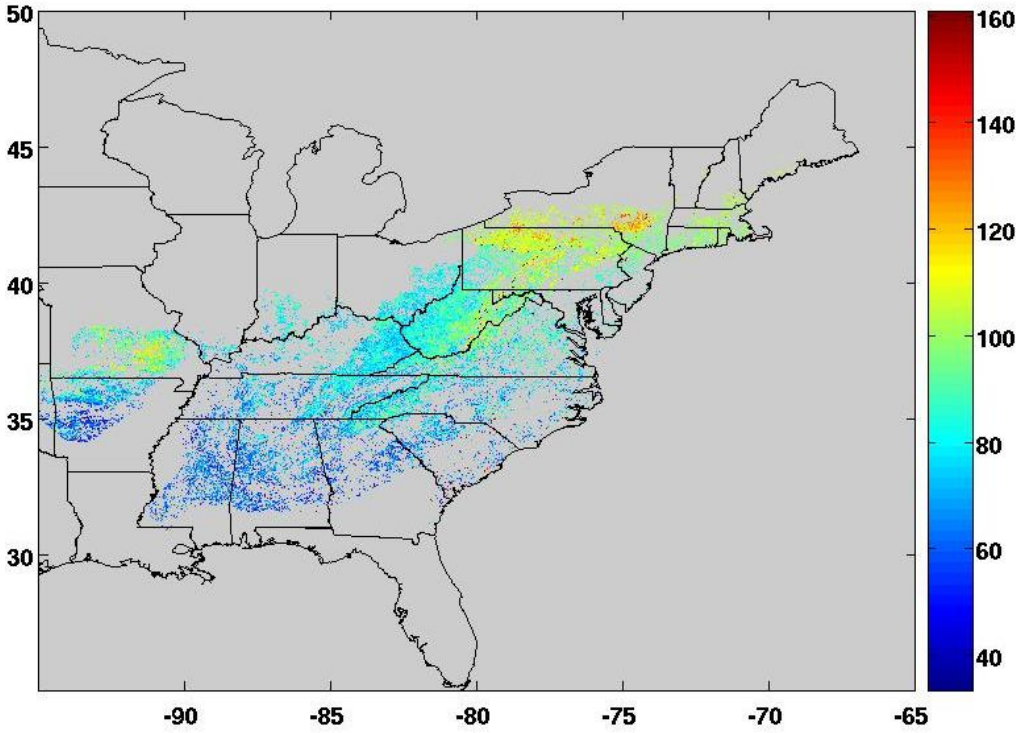

Fig. 6.8 Greenup onset simulated by model.

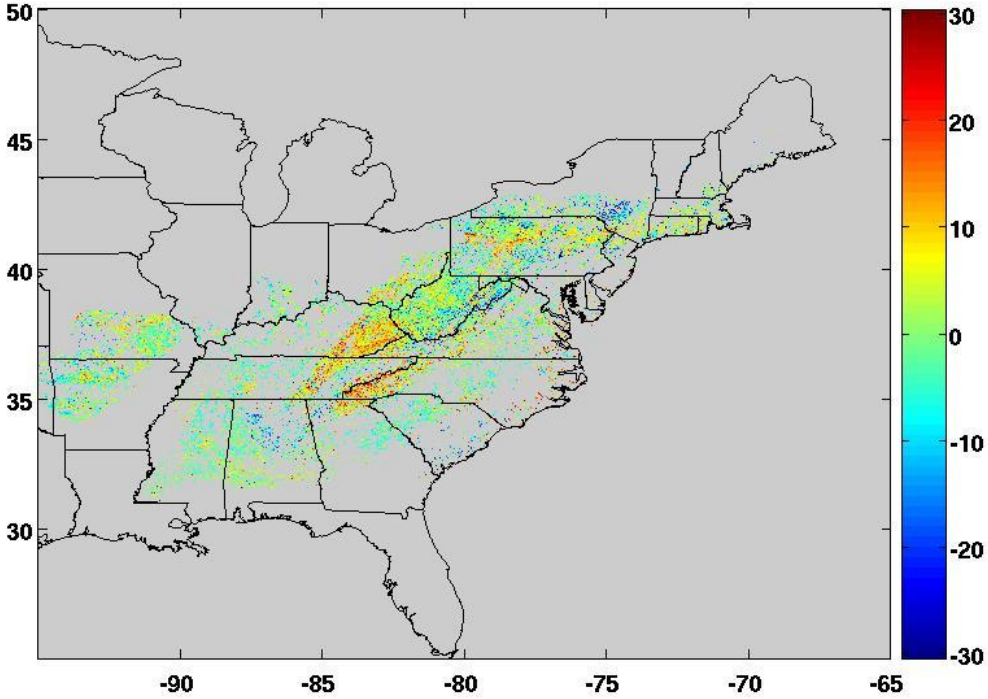

Fig. 6.9 Spatial distribution of satellite observed minus model simulated greenup onset.

The study shows that the ecoregion based models successfully predict the vegetation greenup onset for deciduous broadleaf forest. Our model reproduces the greenup onset date for 90% of the habitat-controlled ecoregions and 80% of temperature-controlled ecoregions within 10 days of the satellite derived greenup onset date (Fig 6.10). The temperature-controlled ecoregions have relatively lower accuracy. The 90% of the temperature-controlled ecoregions are achieved within 70 days of the satellite derived greenup onset. The potential reason is the temporal limit of the LST products. The 8-day composite LST product can only provide about four observations for one month. So the GDD and CD are calculated based on the 8-day period and the results tend to be underestimated or overestimated. To adequately simulate the temperature-controlled ecoregions greenup onset dates, it may essential to apply the high temporal LST products.

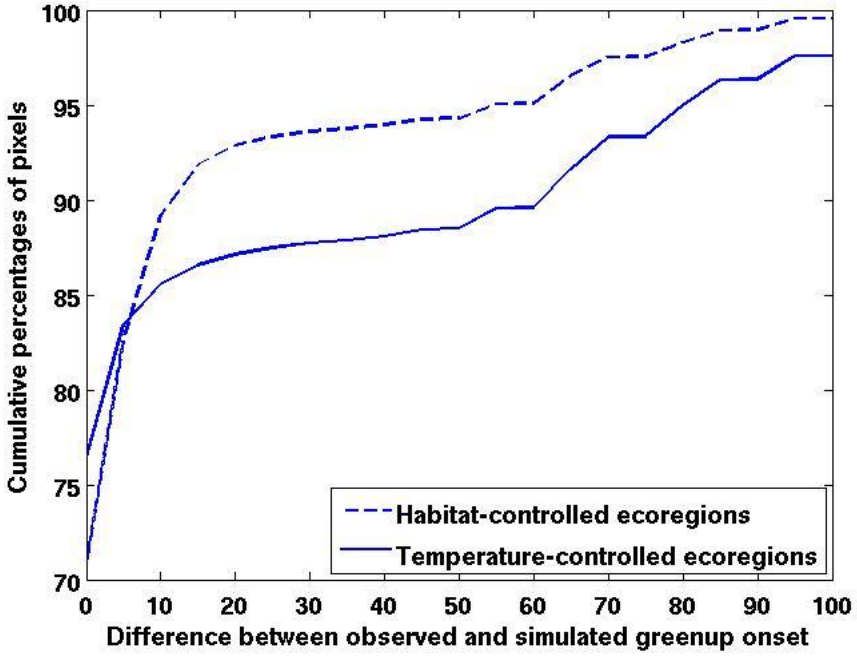

Fig. 6.10 Histogram of cumulated frequencies of absolute difference between satellite observed and model simulated greenup onset dates

6.5 Summary

The ecoregion dependent pattern is reflected by the identical interannual and spatial variability of greenup onset dates in each ecoregion. The interaction between latitude and elevation in each ecoregion results in the variability of temperature and further controls the vegetation phenological phases. The eight ecoregions can be divided into two groups according to the effect of environmental factors on greenup onset. The habitat-controlled group (AMF 50402, ARF 50403, CHF 50404, and OMF 50412), is sensitive to the habitat conditions (latitude and elevation). The temperature-controlled group (AHF 50401, NCF 50411, SMF 50413, and MACF 50517) is influenced mainly by the

temperature. The model 1 combining the latitude and elevation with LST is used to simulate greenup onset for habitat-controlled group. The model 2 based on GDD and CD is used to simulate greenup onset for temperature-controlled group. The models simulate greenup onset dates for each ecoregion realistically. The greenup onset dates for 90% of the habitat-controlled ecoregions and 80% of temperature-controlled ecoregions are simulated within 10 days of the satellite derived greenup onset.

In temperate and high latitudes, temperature is far less spatially heterogeneous than precipitation and the vegetation phenology is driven mainly by temperature. So the model used in this study based only on LST, can predict the vegetation greenup onset realistically. The accuracy of model simulated vegetation greenup onset is evaluated by comparing with satellite derived greenup onset dates. The uncertainty of the satellite observations is not considered in the comparison. Ecoregions with large error bars on satellite derived greenup onset dates have higher parameter uncertainties and hence larger uncertainties in the predicted greenup onset date. In the future, weights could be applied to the observations, determined by the uncertainty in the curve fitting procedure. If we assume that spatial and temporal variations are controlled by the same physical process, then we could use our ecoregion-based model to study interannual variability of phenology. Our phenological model can be viewed, within a given ecoregion, as the asymptotic (or long-term) response to climate change from one location to another one. Thus our model could be used to reproduce large temporal variability such as the decadal trends.

CHAPTER 7

CONCLUSIONS AND DISCUSSION

This dissertation utilized satellite remote sensing measurements to detect vegetation phenological phases and assessed the interannual and spatial variability of vegetation phenology of deciduous broadleaf forest in the eastern United States. An improved satellite-based approach for detecting vegetation phenology has been developed. Comparing the predicted results from satellite with ground measurements demonstrated the good performance of the improved approach. The proper vegetation indices for different phenological phases have been identified. Three important vegetation phenological phases: greenup onset date, dormancy onset date and growing length are determined by vegetation indices. After reviewing the series of satellite-derived vegetation phenology, the spatial variability of these phenological phases is quantified in latitude and elevation. Extensive interannual variability in vegetation phenology has been shown in DBF from 2001 to 2007. The climate regulation for the spatial and interannual variability in vegetation phenology has been expressed by the variation of annual mean LST along latitude and elevation. The LST based models have predicted the average timing of vegetation phenological phases in overall DBF scale. The effect of global warming on vegetation greenup onset is evaluated by the thermal-chilling model. Finally,

two types of ecoregion-based model for greenup onset are established and the results are compared with satellite observations.

The main achievements of this research included: 1) developing an improved approach for detecting vegetation phenological phases from satellite measurements and identifying proper vegetation indices for different phenological phases; 2) quantifying the spatial variability of vegetation phenology and climate regulation of phenological phases; 3) establishing two types of ecoregion-based model for vegetation greenup onset in eastern DBF.

7.1 CONCLUSIONS

7.1.1 Satellite-derived phenological phases

The improved approach for detecting phenological phases from satellite measurements utilizes the Fourier series to identify the single growth or senescence period. The advantage of this approach is more objective comparing with previous methods, since there is no need to set any parameters empirically. The field observations from the Harvard Forests and NOAA phenology network are used to validate satellite-derived phenology events. NDVI predicts more reasonable greenup onset dates than EVI. Whereas EVI-derived dormancy onset dates match the field observations better than NDVI, which correspond to a ground stage of 70% leaves drop in the fall within 2 days. So NDVI is suitable for greenup onset detection and EVI is more proper for dormancy onset detection. The spatial resolution of NBAR products is 1 km, the vegetation

phenological phases identified in this study are representative of canopy phenology, rather than individual species.

The satellite-derived vegetation phenology shows obvious spatial variability and interannual variability. When reviewing the series of satellite-derived vegetation phenology, a greenup wave is progressing northward in latitude and upward in elevation, and in reverse, a dormancy wave is progressing southward in latitude and downward in elevation. The presence of growing length is longer in the south and higher elevation. The rate of change is about 2 days per degree latitude or per 100-meter elevation for greenup onset. For dormancy onset, the rate of change is about 2 days per degree latitude and 1 day per 100-meter elevation. The interannual variability of greenup onset is evident at higher latitudes (45-50^{0}N), while the interannual variability of the dormancy onset is larger at middle (35-45^{0}N) and lower latitudes (30-35^{0}N). The extent of interannual variability of growing length is smaller than that of greenup onset and dormancy onset. There is a presence of slightly longer growing length in the seven years from 2001 to 2007, especially at higher latitudes, which is mainly contributed by the early greenup onset.

7.1.2 Climate regulation of vegetation phenology

The decreases of annual mean LST northward in latitude provide a potential reason for the latitude-dependent pattern of phenological events. Rate of change for annual mean LST is about 1.6 ^{o}C per degree in latitude lower than 42^{0}N. As the latitude higher than 42^{0}N, the latitude dependent pattern is not such obvious. In the elevation below 600 m, the annual mean LST decrease about 4 ^{0}C per 100 meters, while the annual mean LST

increase about 0.8 ^{0}C per 100 meters in elevation higher than 600 m. As the annual mean LST rise, the average timing of greenup onset begins earlier, the dormancy onset is delayed and the growing length is prolonged. The LST dependent pattern is more stable as the annual mean LST lower than 0 ^{o}C. While as the annual mean LST higher than 0 ^{o}C, the average timing of these three phenological events tends to fluctuate. The high goodness of fit (>0.8) indicates that the model based on annual mean LST predict the average timing of vegetation phenological events successfully. The greenup onset model suggests that the average greenup onset changes rapidly as the annual mean LST rise up from -20 ^{o}C to 0 ^{o}C. The average dormancy onset moves slowly as the annual mean LST lower than 0 ^{o}C, but shifts quickly as the annual mean LST higher than 0 ^{o}C. The growing length is more sensitive to annual mean LST than greenup onset and dormancy onset. There is always a quick shift of growing length as the annual mean LST rise from -60 ^{o}C to 30 ^{o}C. To investigate how global warming might influence dates of vegetation greenup onset in DBF over continental U.S., the thermal-chilling model is applied to satellite-derived greenup onset date. The results show that the thermal-chilling models can explain more than 80% of the variation in the GDD required for greenup onset. Global warming may advance forest greenup onset when the chilling requirements are far exceeded and may delay greenup onset when the chilling requirements are nearly exactly sufficient.

7.1.3 Ecoregion-based vegetation greenup onset model

The ecoregion dependent pattern is reflected by the identical interannual and spatial variability of greenup onset dates in each ecoregion. The interaction between latitude and

elevation in each ecoregion results in the variability of temperature and further controls the vegetation phenological phases. The eight ecoregions can be divided into two groups according to the effect of environmental factors on greenup onset. The habitat-controlled group (AMF 50402, ARF 50403, CHF 50404, and OMF 50412), is sensitive to the habitat conditions (latitude and elevation). The temperature-controlled group (AHF 50401, NCF 50411, SMF 50413, and MACF 50517) is influenced mainly by the temperature. The model 1 combining the latitude and elevation with LST is used to simulate greenup onset for habitat-controlled group. The model 2 based on GDD and CD is used to simulate greenup onset for temperature-controlled group. The models simulate greenup onset dates for each ecoregion realistically. The greenup onset dates for 90% of the habitat-controlled ecoregions and 80% of temperature-controlled ecoregions are simulated within 10 days of the satellite derived greenup onset.

In temperate and high latitudes, temperature is far less spatially heterogeneous than precipitation and the vegetation phenology is driven mainly by temperature. So the model used in this study based only on LST, can predict the vegetation greenup onset realistically. The accuracy of model simulated vegetation greenup onset is evaluated by comparing with satellite derived greenup onset dates. The uncertainty of the satellite observations is not considered in the comparison. Ecoregions with large error bars on satellite derived greenup onset dates have higher parameter uncertainties and hence larger uncertainties in the predicted greenup onset date. In the future, weights could be applied to the observations, determined by the uncertainty in the curve fitting procedure. If we assume that spatial and temporal variations are controlled by the same physical process,

then we could use our ecoregion-based model to study interannual variability of phenology.

7.2 Applications of this research

The improved approach for satellite-derived vegetation phenology presented in this work has several desirable properties. Since it treats each pixel individually without setting thresholds or empirical constants, the method is globally applicable. Further, it is capable of identifying phenological behavior characterized by multiple growth and senescence periods within a single year, which is common in croplands and semiarid regions. Finally, because the method is not tied to a specific calendar period (e.g., January to December), it provides the potential to monitor vegetation phenology in near real time.

In the context of global change processes, quantification of ecosystem-level response should provide a useful and important complement to species-level studies. Indeed, a key challenge confronting the global change community is better understanding how species-level responses to climate forcing aggregate to larger scales. The type of remote sensing-based analysis presented in this study, when linked to carefully designed field-based studies, provides a promising approach for tackling this issue.

This study is an initial step in constructing and validating a regional phenology model for DBF in eastern United States, which could be used as a phenology module in a satellite-based model of forest carbon cycling. Together with the meteorological and climatological data, this phenology model will be used to predict retrospective temporal and spatial variability of the greenup onset in temperate forests for better understanding

of the interactions between climatic variability and the terrestrial carbon cycle.

7.3 Limitations of this work

Validation is a key issue in remote sensing-based and model-based studies of phenology over large areas. While a variety of field programs for monitoring phenology have been initiated (e.g., Schwartz, 1999), these programs provide data that are typically species-specific and which are collected at scales that are not compatible with coarse resolution remote sensing observations. In 1-km resolution imagery, each pixel reflects the integrated response across landscapes with diverse species and phenological behavior. Although comparisons have been made in this work between ground observations and the remote sensing-based results, the results are far from satisfied and this type of activity is needed to more fully understand.

7.4 Future works

The accuracy of greenup and dormancy onset derived by satellite measurements is dependent on the temporal resolution of MODIS NBAR products. MCD43B4 reflectance represents that best characterization of the surface possible from the inputs available over a 16-day period. The compositing method likely contributed to the uncertainty of estimates of onset dates. For phenology studies aimed at detecting the effects of climate change, it may more meaningful if the MODIS product contained information on the dates from which the product was developed or weighted most heavily. In the further, nearly daily satellite products would be applied to detect vegetation phenology and the

uncertainty of the satellite-derived phenology results would be evaluated by the quality of satellite data.

Additional research is also needed to understand how we can compare the two sources (satellite and ground) of phenological data more effectively and realize their synergistic benefits. The satellite derived vegetation phenology is based on 1-km resolution data and each pixel reflects the canopy response with diverse species. The ground records usually measure vegetation phenology at individual species level. How to integrate the species level phenology to canopy level phenology is a key issue in validating remote sensing-based vegetation phenology. In the further, more detail information of ground records will be collected, such as the area of field plots, the composition and structure in vegetation community. The information together with phenophases of individual species will be integrated to reflect the canopy phenology and compared the results with satellite-derived phenology.

The MODIS LST product used in ecoregion-based model has a relatively low temporal resolution. The 8-day composite LST product may overestimate or underestimate the thermal and chilling conditions before the greenup onsets. In the further, the 8-day composite LST product would be instead of the daily LST product and the more accurate thermal and chilling requirements would be generated. Furthermore, more environmental factors, for instance, the soil moisture, and the photoperiod could be included to improve the performance of the model.

The relationship between vegetation phenology and the concentration of atmospheric carbon dioxide would be investigated in the further. The longer presence of green cover

would generate a cooling that mitigates warming by sequestering more CO_2 and increasing evapotranspiration. The analysis of net ecosystem exchange of CO_2 between forest ecosystem and the atmosphere will regulate seasonal and interannual fluctuations of carbon uptake.

REFERENCES

REFERENCES

Ahl, D.E., Gower, S.T., Burrows, S.N., Shabanov, N.V., Myneni, R.B., Knyazikhin, Y., 2006. Monitoring spring canopy phenology of a deciduous broadleaf forest using MODIS. Remote Sens. Environ. 104, 88–95.

Badeck, F-W., Bondeau, A., Bottcher, K., Doktor, D., Lucht, W., Schaber, J., Sitch, S., 2004. Responses of spring phenology to climate change. New Phytol. 162, 295 – 309.

Betancourt , J.L , Schwartz , M.D. , Breshears , D.D. , Cayan , D.R. , Dettinger , M.D. , Inouye , D.W. Post , E. and Reed , B. (2005) Implementing a U.S . National Phenology Network. EOS Trans.AGU 86 , 539 – 541 .

Bogaert, J., Zhou, L., Tucker, C.J., Myneni, R.B. Ceulemans, R., 2002. Evidence for a persistent and extensive greening trend in Eurasia inferred from satellite vegetation index data. J. Geophys. Res . 107, (D11) 10.1029/2001JD001075.

Botta, A., Viony, N., CIAIS, P., Friedlingstein, P., Monfray, P., 2000. A global prognostic scheme of leaf onset using satellite data. Glob Chang Biol. 6, 709-725.

Cannell, M.G.R. and Smith, R.I., 1983. Thermal Time, Chill Days and Prediction of Budburst in Picea sitchensis. Journal of Applied Ecology. 20, 951-963.

Cannell, M.G.R., Murray, M. B., Sheppard, L. J., 1985. Forest avoidance by selection for late budburst in Picea Sitchensis. Journal of Applied Ecology, 22, 931–941.

Cannell, M. G. R. and Smith, R. I., 1986. Climatic warming, spring budbursts, and forest damage on trees. Journal of Applied Ecology, 23, 177–191.

Chen, X., Hu, B., Yu, R., 2005. Spatial and temporal variation of phenological growing season and climate change impacts in temperature eastern China. Global Change Biol. 11, 1118 – 1130.

De Beurs, K.M. and Henebry, G.M., 2005. Land surface phenology and temperature variation in the international Geosphere-Bioshpere program high-latitude transects. Glob Chang Biol. 11, 779-790.

Delbart, N., Picard, G., Toan, T.L., Kegoat, L., Quegan, S., 2005. Spring phenology in Siberia in 1982–2004, observations by remote sensing, modeling, and impact on the terrestrial carbon budget. Geophys. Res. Abstr. 7, 01283.

Deng, F., Su, G., Liu, C., 2007. Seasonal variation of MODIS Vegetation Indexes and their statistical relationship with climate over the subtropic evergreen forest in Zhejiang, China. IEEE Geosci. Remote Sens. Lett. 4, 236 – 240.

Doubková, M. and Henebry, G.M., 2006. Synergistic use of AMSR-E and MODIS data for understanding grassland land surface phenology. IGARSS 2006, Denver, Colorado, July 30-August 4, 2006.

Duchemin, B., Goubier, J., Courrier, G., 1999. Monitoring phenological key stages and cycle duration of temperate deciduous forest ecosystems with NOAA/AVHRR data. Remote Sens. Environ., 67, 68–82.

Eidenshink, J.C., 1992. The 1990 Conterminous U.S. AVHRR Data Set. Photogramm. Eng. Rem. Sens. 58, 809 – 813.

Fischer, A., 1994. A model for the seasonal variations of vegetation indices in coarse resolution data and its inversion to extract crop parameters. Remote Sens. Environ., 48, 220-230.

Fisher, J.I. and Mustard, J.F., 2007. Cross-scalar satellite phenology from ground, Landsat, and MODIS data. Remote Sens. Environ. 109, 261 – 273.

Fisher, J. I., Richardson, A.D., Mustard, J. F., 2007. Phenology model from surface meteorology does not capture satellite-based green-up estimations. Global Change Biol. 13, 707 – 721.

Fitzjarrald, D. R., Acevedo, O.C., Moore, K. E., 2001. Climatic consequences of leaf presence in the eastern United States. Journal of Climate, 14, 598–614.

Friedl, M.A., Mclver, D.K., Hodges, J.C.F., Zhang, X.Y., Muchoney, D., Strahler, A.H., Woodcock, C.E., Gopal, S., Schneider, A., Cooper, A., Baccini, A., Gao, F., Schaaf, C.,

2002. Global land cover mapping from MODIS: algorithms and early results. Remote Sens. Environ. 83, 287-302.

Garber, M.P., 1983. Effects of chilling and photoperiod on dormancy release of container-grown loblolly pine seedlings. Canadian Journal of Forest Research, 13, 1265-1270.

GLOBE Task Team and others, eds., 1999. The Global Land One-kilometer Base Elevation (GLOBE) Digital Elevation Model, Version 1.0. National Oceanic and Atmospheric Administration, National Geophysical Data Center, 325 Broadway, Boulder, Colorado 80303, U.S.A. Digital data base on the World Wide Web (URL: http://www.ngdc.noaa.gov/mgg/topo/globe.html)

Goulden , M.L. , Munger , J.W. , Fan , S.M. , Daube , B.C. and Wofsy , S.C., 1996. Exchange of carbon dioxide by a deciduous forest: Response to interannual climate variability . Science 271 ,1576 – 1578 .

Haggerty, B.P. and Mazer, S. J., 2008 The Phenology Handbook. UCSB Phenology Stewardship Program.pp.1-21

Hari, P, Häkkinen, R., 1991. The utilization of old phenological time series of bud burst to compare models describing annual cycles of plants. Tree Physiology, 8, 281-287.

Häkkinen, R., 1994. Effect of climatic change on trees from cool and temperate regions: an ecophysiological approach to modeling of bud burst phenology. Canadian Journal of Botany, 73, 183-199.

Hicken, R.P. and Vittum, M.T., 1976. The importance of soil and air temperature in spring phenoclimatic modeling. Int. J. Biometeorol. 20, 200-206.

Hopkins, A.D., 1938. Bioclimatics; A science of life and climate relations. U.S. Dept, Agri. Misc. Publ. 280.

Huband, N. D. S. and Monteith, J. L., 1986. Radiative surface temperature and energy balance of a wheat canopy. Boundary-Layer Meteorology, 36, 1–17.

Huete, A.R., Liu, H.Q., Batchily, K., van Leeuwen, W., 1997. A comparison of vegetation indices over a global set of TM images for EOS-MODIS. Remote Sens. Environ. 59, 440 – 451.

Huete, A.R., 1988. A soil adjusted vegetation index (SAVI). Remote Sens. Environ. 25, 295-309.

Huete, A.R., Hua, G., Qi, J., Chehbouni, A., Van Leeuwem, W.J.D.G., 1992. Normalization of multidirectional red and NIR reflectances with the SA VI, Remote Sens. Environ., 40, 1-20.

Huete, A.R., Didan, K., Miura, T., Rodriguez, E. P., Gao. X., Ferreira, L. G., 2002. Overview of the radiometric and biophysical performance of the MODIS vegetation indices. Remote Sens. Environ. 83, 195-213.

Hunter A.F., Lechowicz M.J., 1992. Predicting the timing of budburst in temperate trees. Journal of Applied Ecology, 29, 597–604.

Justice, C.O., Vermote, E., Townshend, J.R.G., et al., 1997. The moderate resolution imaging spectroradiometer (MODIS): land remote sensing for global change research. IEEE Trans Geosci Remote Sens. 36, 172-181.

Kang, S., Running, S.W., Lim J., Zhao, M., Park, C. Loehman, R., 2003. A regional phenology model for detecting onset of greenness in temperate mixed forests, Korea: an application of MODIS leaf area index. Remote Sens. Environ. 86, 232-242.

Kathuroju, N., White, M.A., Symanzik, J., Schwartz, M.D., Powell, J.A. and Nemani, R., 2007. On the use of the Advanced Very High Resolution Radiometer for development of prognostic land surface phenology models. Ecol. Modell. 201, 144 – 156.

Kaufman, Y.J. and Tanre, D., 1992. Atmospherically resistant vegetation index (ARVI) for EOSMODIS. IEEE Trans. Geosci. Remote Sens. 30, 261 – 270.

Keeling, C.D., Chin, J.F.S., Whorf, T.P., 1996. Increased activity of northern vegetation inferred from atmospheric CO_2 measurements. Nature 382: 146-149.

Kikuzawa, K, 1995. Leaf phenology as an optimal strategy for carbon gain in plants. Canadian Journal of Botany, 73, 158-163.

Kim, Y. and Wang, G., 2005. Modeling seasonal vegetation variation and its validation against Moderate Resolution Imaging Spectroradiometer (MODIS) observations over North America. J Geophys Res. 110, D04106.

Kindermann J, Lüdeke M.K.B., Badeck F.W., Otto R. D., Klaudius, A., Hager, C. h. , Wiirth, G., Lang, T, Donges, S., Habermehl, S., Kohlmaier, G. H., 1993. Structure of a global carbon exchange model for the terrestrial biosphere: the Frankfurt Biosphere Model (FBIM). Water Air Soil Pollut 70, 675-684.

Kramer, K., 1994. Selecting a model to predict the onset of growth of Fagus sylvatica. Journal of Applied Ecology, 31, 172–181.

Linkosalo, T., 2000. Mutual regularity of spring phenology of some boreal tree species: predicting with other species and phenological models. Canadian Journal of Forest Research, 30, 667–673.

Lloyd, D., 1990. A pehnological classification of terrestrial vegetation cover using shortwave vegetation imagery. Int. J. Remote Sens. 11, 2269-2279.

Loveland, T.R., Merchant, J.W., Ohlen, D.O., Brown, J.F., 1991. Development of a land-cover characteristics database for the conterminous U.S . Photogramm. Eng. Rem. Sens. 57, 1453 – 1463.

MacDonald, G., 2002. Biogeography: Introduction to Space, Time, and Life, first ed. Wiley, New York.

Moulin S., Kergoat L., Viovy N., Dedieu G., 1997. Global Scale Assessment of vegetation phenology using NOAA/AVHRR satellite measurements. Journal of Climate, 10, 1154-1170.

Markon, C.J., Fleming, M.D., Binnian, E.F., 1995. Characteristic of vegetation phenology over the Alaskan landscape using AVHRR time-series data. Polar Record, 31, 179–190.

Menzel, A. and Fabian, P., 1999. Growing season extended in Europe. Nature 397, 659.

Moulin S, Kergoat L, Viovy N et al., 1997. Global-scale assessment of vegetation phenology using NOAA/AVHRR satellite measurements. Journal of Climate, 10, 1154–1170.

Murphy, R.E., Barnes, W.L., Lyapustin, A.I., Privette, J., Welsch, C., DeLuccia, F., Swenson, H.,Schueler, C.F., Ardanuy, P.E., Kealy, P.S.M., 2001. Using VIIRS to provide data continuity with MODIS. IEEE Geoscience and Remote Sensing Symposium 03, 1212 – 1214.

Murray, M. B., Cannell, G. R., Smith, R. I., 1989. Date of budburst of fifteen tree species in Britain following climatic warming. Journal of Applied Ecology, 26, 693-700.

Mynenl, R.B., Keeling, C.D., Tucker, C.J., Asrar, G., Nemanl, R.R., 1997. Increased plant growth in the northern high latitudes from 1981 to 1991. Nature. 386, 698-702.

Nizinski, J.J., and Sugier, B., 1998. A model of leaf budding and development for a mature quercus forest. Journal of Applied Ecology, 25, 643-653

Olson, D. M., Dinerstein, E., Wikramanayake, E. D. et al., 2001. Terrestrial ecoregions of the world: a new map of life on earth. Bioscience. 51, 933-938.

Peckham, S.D., Ahl, D.E., Serbin, S.P., Gower, S.T., 2008. Fire-induced changes in green-up and leaf maturity of the canaidan boreal forest. Remote Sens. Environ. 112, 3594-3603.

Peñuelas, J., Rutishauser, T., Filella, I., 2009. Phenology feedbacks on climate change. Science. 324, 887-888.

Reed, B.C., Brown, J.F., VanderZee, D., Loverland, T.R., Merchant, J.W., Ohlen, D.O., 1994. Measuring phenological variability from satellite imagery. J. Veg. Sci. 5, 703-714.

Reed, B. C., Schwartz, M. D., Xiao X., 2009. "Remote Sensing Phenology: Status and the Way Forward" Phenology of Ecosystem Processes. Ed. Asko Noormets. Springer New York, 2009. 231-246

Schaaf, C. B., F. Gao, A. H. Strahler, W. Lucht, X. Li, T. Tsang, N. C. Strugnell, X. Zhang, Y. Jin, J.-P. Muller, P. Lewis, M. Barnsley, P. Hobson, M. Disney, G. Roberts, M. Dunderdale, C. Doll, R. d'Entremont, B. Hu, S. Liang, and J. L. Privette, 2002, First Operational BRDF, Albedo and Nadir Reflectance Products from MODIS. Remote Sensing of Environment, 83, 135-148.

Sarvas R., 1974. Investigations on the annual cycle of development of forest tree autumn dormancy and winter dormancy. Communicationes Instituti Forestalis Fenniae, 84, 1–101.

Schwartz, M.D. and Reed, B.C., 1999. Surface phenology and satellite sensor-derived onset of greenness: an initial comparison. Int. J. Remote Sens. 20, 3451 – 3457.

Schwartz, M.D., Reiter, B., 2000. Changes in North American spring. Int. J. Climatol. 20: 929–932.

Schwartz, M.D., Reed, B.C., White M.A., 2002 Assessing satellite-derived start-of-season measures in the conterminous USA. Int. J. Climatol. 22, 1793-1805.

Schwartz, M.D., Caprio, J.M., 2003, North American First Leaf and First Bloom Lilac Phenology Data, IGBP PAGES/World Data Center for Paleoclimatology. Data Contribution Series # 2003-078. NOAA/NGDC Paleoclimatology Program, Boulder CO, USA.

Schwartz, M.D., Ahas, R., Aasa, A., 2006. Onset of spring starting earlier across the northern hemisphere. Glob Chang Biol. 12, 343-351.

Shabanov, N.V., Zhou, L., Knyazikhin, Y., Myneni, R.B., Tucker, C. J., 2002. Analysis of interannual changes in northern vegetation activity observed in AVHRR data from 1981 to 1994. IEEE Transactions on Geoscience and Remote Sensing. 40, 115-130.

Spano, D., Cesaraccio, C., Duce, P., Snyder, R.L., 1999. Phenological stage of natural species and their use as climate indicators. International Journal of Biometeorology, 42, 124–133.

Studer, S., Stöckli, R., Appenzeller, C., Vidale, P.L., 2007. A comparative study of satellite and ground-based phenology. Int. J. Biometeorol. 51, 405 – 414.

Stöckli, R., Rutishauser, T., Dragoni, D., O'keefe, J., Thornton, P.E., Jolly, M., Lu, L., Denning, A.S., 2008. Remote sensing data assimilation for a prognostic phenolgy model. J Geophys Res. 113, G04021.

Tateishi, R. and Ebata, M., 2004. Analysis of phenological change patterns using 1982–2000 Advanced Very High Resolution Radiometer (AVHRR) data. Int. J. Remote Sens. 25, 2287 – 2300.

Townshend, J.R.G., Justice, C.O., Skole, D., 1994. The 1 km resolution global data set, needs of the International Geosphere Biosphere Programme. Int. J. Remote Sens. 15, 3417 – 3441.

Tucker, C.J., Slayback, D.A., PinZon, J. E., Los, S.O., Myneni, R.B. Taylor, M.G., 2001. Higher northern latitude normalized difference vegetation index and growing season trends from 1982 to 1999. International Journal of Biometeorology, 45, 184-190.

Tucker, C.J., Pinzon , J.E., Brown , M.E., 2004. Global Inventory Modeling and Mapping studies, NA94apr15b.n11-VIg, 2.0, Global Land Cover Facility , University of Maryland, College Park , Maryland , 04/15/1994 .

Vegis, A., 1964, Dormancy in higher plants. Annual Review of Plant Physiology, 5, 185-222. Wan, Z., Zhang, Y., Zhang, Q., Li, Z. 2002 Validation of the land-surface temperature products retrieved from terra moderate resolution imaging spectroradiometer data. Remote Sensing of Environment, 83, 163-180.

Wang, J., Rich, P.M., Price, K.P. 2003. Temporal responses of NDVI to precipitation and temperature in the central Great Plains, USA. Int. J. Remote Sens. 24, 2345 – 2364.

White, M.A., Thornton, P.E., Running, S. W., 1997. A continental phenology model for monitoring vegetation responses to interannual climate variability. Global Biogeochem Cycles. 11, 217-234.

White, M.A., Running, S. W., Thornton, P.E., 1999. The impact of growing-season length variability on carbon assimilation and evapotranspiration over 88 years in the eastern US deciduous forest. Int J Biometeorol. 42, 139-145.

White, M.A., Nemani, R.R., Thornton, P.E., Running, S. W., 2002 Satellite evidence of phenological differences between urbanized and rural areas of the eastern United States deciduous broadleaf forest. Ecosystems. 5, 260-277.

Woodcock , C.E., Allen , R., Anderson, M., Belward, A., Bindschadler, R., Cohen, W., Gao, F., Goward, S.N., Helder, D., Helmer, E., Nemani, R., Oreopoulos, L., Schott, J., Thenkabail, P.S., Vermote, E.F., Vogelmann, J., Wulder, M.A. and Wynne, R., 2008. Free access to Landsat imagery. Science, 320, 1011.

Xiao, X., Zhang, J., Yan, H., Wu, W., Biradar, C. 2009. “Land Surface Phenology: Convergence of Satellite and CO 2 Eddy Flux Observation.” Phenology of Ecosystem Processes. Ed. Asko Noormets. Springer New York, 2009. 247-270.

Zhang, X., Friedl, M.A., Schaaf, C.B., Strahler, A.H., Hodges, J. C. F., Gao, F., Reed, B. C., Huete, A., 2003. Monitoring vegetation phenology using MODIS. Remote Sens. Environ. 84, 471-475.

Zhang, X., Friedl, M.A., Schaaf, C. B. Strahler, A.H., 2004. Climate controls on vegetation phenological patterns in northern mid- and high latitudes inferred from MODIS data. Glob Chang Biol. 10, 1133-1145.

Zhang, X., Friedl, M.A. and Schaaf, C.B., 2006. Global vegetation phenology from Moderate Resolution Imaging Spectroradiometer (MODIS). Evaluation of global patterns and comparison with in situ measurements. J. Geophys. Res. 111, G04017.

Zhou, L., Kaufmann, R. K., Tian, Y., Myneni, R.B., Tucker, C.J., 2003. Relation between interannual variations in satellite measures of northern forest greenness and climate between 1982 and 1999. J Geophys Res. 108, D14004.

CURRICULUM VITAE

Min Li received her Bachelor of Science in Urban & Rural Planning and Resource Management from East China Normal University, Shanghai, China in 2003 and Master of Science in Cartography and Geographical Information System from Beijing Normal University, Beijing, China in 2006. She joined George Mason University, Fairfax, VA, USA as a Ph.D. student and research assistant in 2006. Her research interest at the time of this dissertation included satellite remote sensing based approaches for detecting vegetation phenology, climate and environmental effects on the variability of phenological phases, ecoregion based models for estimating vegetation phenology on landscape level. Forest biomass estimation and wild land fire monitoring were also investigated during her Ph.D. study.